2007

The Development and Molecular Expression in Mammalian Cells of an HA-Tagged Plasmid Encoding for the Target Of Rapamycin (MTOR)

Kevin S. Dougherty
Wright State University

THE DEVELOPMENT AND MOLECULAR EXPRESSION IN MAMMALIAN CELLS OF AN HA-TAGGED PLASMID ENCODING FOR THE TARGET OF RAPAMYCIN (mTOR)

A thesis submitted in partial fulfillment
of the requirements for the degree of
Master of Science

By

KEVIN S. DOUGHERTY
B.S., Cedarville University, 2003

2007
Wright State University

WRIGHT STATE UNIVERSITY

SCHOOL OF GRADUATE STUDIES

November 30, 2007

I HEREBY RECOMMEND THAT THE THESIS PREPARED UNDER MY SUPERVISION BY Kevin S. Dougherty ENTITLED The Development and Molecular Expression in Mammalian Cells of an HA-Tagged Plasmid Encoding for the Target of Rapamycin (mTOR) BE ACCEPTED IN PARTIAL FULFILLMENT OF THE REQUIREMENTS FOR THE DEGREE OF Master of Science.

Dr. Julian Gomez-Cambronero
Julian Gomez-Cambronero, Ph.D.
Thesis Director

Dr. Timothy Cope
Timothy Cope, Ph.D.
Department Chair

Committee on Final Examination:

Dr. Julian Gomez-Cambronero
Julian Gomez-Cambronero, Ph.D.

Dr. David Cool
David Cool, Ph.D.

Dr. Larry Ream
Larry Ream, Ph.D.

Dr. Joseph Thomas
Joseph F. Thomas, Jr., Ph.D.
Dean, School of Graduate Studies

ABSTRACT

Dougherty, Kevin S. M.S., Department of Neuroscience, Cell Biology and Physiology, Wright State University, 2007. The Development and Molecular Expression in Mammalian Cells of an HA-Tagged Plasmid Encoding for the Target of Rapamycin (mTOR).

The protein kinase Mammalian Target of Rapamycin (mTOR) is a master controller of cell growth and proliferation due to its ability to integrate growth signals and regulate translation through 4E-BP1 and p70-S6K. We developed four phCMV2-HA-tagged plasmids to overexpress TOR in mammalian cells: Wild Type, D2357E (Kinase Dead), R2109A (PA Binding Deficient) and, S2035T (Rapamycin Resistant) each verified by restriction enzyme digestion and direct sequencing. Plasmid DNA was overexpressed in COS-7 cells and the 289 kDa protein detected in Western blots developed with anti-HA and anti-mTOR antibodies. Kinase activity of the overexpressed protein was detected by *in vitro* phosphorylation of 4E-BP1 and S6K. QRT-PCR detected a 200 fold increase in mTOR gene expression over mock transfected cells, but found no change in PLD2 gene expression. Immunoflourescence microscopy indicated that mTOR is perinuclear, concentrated in endosomal formations. This study provides the molecular biology tools for continuing investigation into the crosstalk between mTOR, S6K, PLD1 and PLD2.

TABLE OF CONTENTS

LIST OF FIGURES

Figure Title **Page**

LIST OF FIGURES (Continued)

LIST OF TABLES

Table Title **Page**

ACKNOWLEDGMENTS

I would like to thank my thesis advisor, Dr. Julian Gomez-Cambronero, for the opportunity to work in his lab. Many thanks also to Dr. Mauricio DiFulvio for teaching me about molecular biology research, your mentorship was crucial to my success in this project. Kathy Frondorf and Karen Henkels were always ready to help whenever you could, thank you. Thank you also to my committee members, Dr. David Cool and Dr. Larry Ream who provided their guidance on this project. Finally, thanks to my family, especially my Mom, you have always believed in me and supported me in whatever I do.

I. LITERATURE REVIEW

Discovery of mTOR

During a 1970's expedition to Easter Island, off the coast of Chile, South America, researchers discovered a strong antifungal metabolite produced by the soil bacteria *Streptomyces hygroscopicus*[1]. The newly discovered macrolytic lactone was named rapamycin after the island where it was found, which is called Rapa Nui in the local language[2]. Further study revealed immunosuppressive properties and the ability to inhibit mammalian cell growth while the macrolydes mechanism of action remained a mystery. The addition of rapamycin to cell cultures results in G1 arrest in a variety of cell types[3]. In 1980's the National Cancer Institute screening program demonstrated the anti-tumor activity of rapamycin[4]. These findings caused a flurry of research aimed at identifying the biochemical actions of rapamycin[5]. By 1991 the extraordinarily specific target of rampamycin was identified though mutations TORC1 and TORC2, which confer resistance to rapamycin, and aptly named Target of rapamycin (TOR)[6].

Advances in biochemistry lead to the cloning of the "mammalian target of rapamycin" (mTOR), also known in the literature as "FK506-binding protein" (FKBP12), "rapamycin-associated protein" (FRAP), "rapamycin and FKBP12 target" (RAFT1), "rapamycin target" (RAPT1), or "Sirolimus effector protein" (SEP) [7]. For the purposes of this thesis, we will use the first nomenclature. Every eukaryotic genome examined to date contains a mTOR gene[8]. The TOR protein is highly conserved from yeast to man, sharing about a 95% homology at the amino acid level,

suggesting that it plays a vital role in cellular function[9]. Genetically mTOR maps to the human chromosome 1p36.2[7].

Cellular Importance of mTOR

mTOR is known to sense mitogenic stimuli, extra cellular nutrient levels[10] and ATP[11]. It also regulates cell functions including actin reorganization of the cytoskeleton,[12] cell growth and proliferation,[13] cell survival,[14] transcription, translation initiation,[15] mRNA turnover, protein stability,[12] and repression of autophagocytosis (Figure 1). Dysregulation of the mTOR signaling pathway[16] is common in cancerous tumors including lung, bladder, renal, ovary, breast, prostate, gastric, pancreatic, and head and neck carcinomas[17]. Dysregulation of the mTOR pathway has also been observed in lymphomas, melanoma, glioma and several other brain diseases[18]. Unusually high mTORC1 activity is suspected as an underlying cause of these cancers[19].

mTOR has been shown to be essential in development of mouse embryos, causing severe birth defects to mouse knockout mutants[20]. Studies in *Drosophila melanogaster* and *Caenorhabditis elegans* have identified TOR as essential in embryonic development as well[21]. Disruptions of the mTOR gene in mice result in embryonic lethality with severe telencephalon malformation, termed the "flat-top" phenotype. Embryonic tissues requiring a rapid increase in cell proliferation, such as the telencephalon, limb buds and ventral body walls were malformed in the mTOR mutant genotype. This finding seems to implicate mTOR in sensing mitogenic signals and upregulating cell proliferation. Hentges' *et al.* showed no measurable

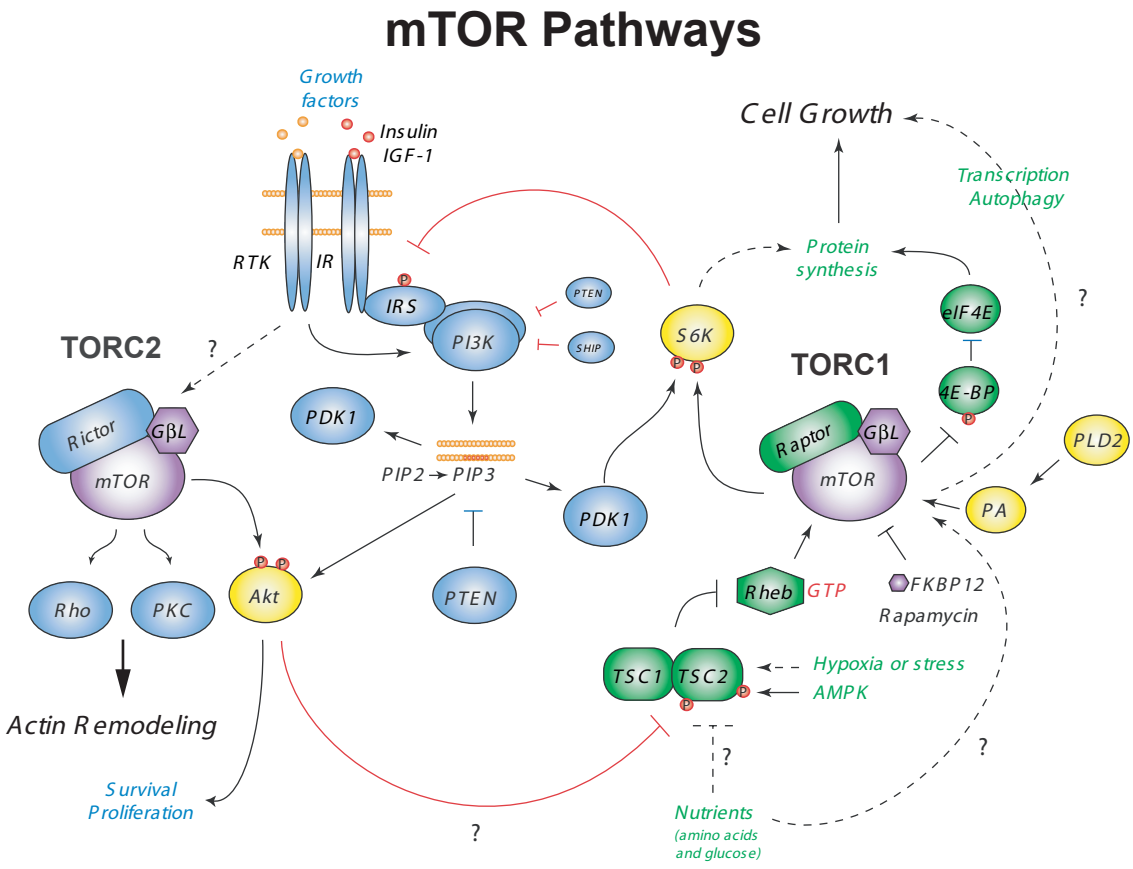

FIGURE 1:

mTOR plays a vital role in signaling cell growth, proliferation and survival. The signaling network consists of two major branches, TORC1 and TORC2. TORC1 responds to growth factors including insulin and insulin-like growth factors and controls several pathways that determine the mass of the cell. The TORC1 acts largely through the control of the PI3K pathway, phosphorylating downstream targets, S6K and 4E-BP1 to control protein synthesis. The TORC2 pathway is less well understood but has been implicated in cell survival and proliferation as well as control of the actin cytoskeleton, effectively regulating the shape of the cell. Main pathways are in black, with feedback loops depicted in red. Arrows indicate activation of the downstream molecule, while inhibition of the downstream molecule is indicated with a stopped line. Pathways which are yet unclear are indicated by dashed lines and question marks. Direct phosphorlyation is indicated with the letter 'p' in a red circle. Figure adapted from Guertin, 2005.

difference in cell size in the mTOR mutant mice compared to a wild type mouse[20]. This finding seemingly does not agree with previous reports that *Drosophilia* TOR mutants had a smaller average cell size than their wild type counterpart[22].

Characteristics of the "flat-top" phenotype include a failure to upregulate neuronal formation in the forebrain and inability to maintain gene expression in the prechordal region of the forebrain neuroectoderm[20]. "Flat-top" mouse embryos die at 12.5 days post coitus. The same lab showed no survival differences in TOR mutated embryo's versus wild type TOR embryo's treated with rapamycin[21]. After injecting rapamycin into wild type pregnant mice and observing effects similar to those in mTOR mutant mice they were able to assert that the malformed embryos were due to a disrupted mTOR pathway. This experiment reinforced the tetrogenic effects of rapamycin and demands its further study as an anticancer drug[16].

mTOR Structure

mTOR is a 289 kDa protein Serine/Threonine kinase which belongs to a family of phosphatidylinositol kinase-related kinases (PIKK)[23]. After TOR mutants TOR1-1 and TOR2-1were identified[24] a group of high molecular weight kinases including TOR, were identified that resembled the phosphoinositide 3-kinase family(PI3K). This new family which shared sequence homology and were found in all eukaryotic cells was given the name phosphoinositide 3-kinase related kinases (PIKK's)[25]. There are several subfamilies of PIKK's including TOR subfamily, *Atazia telangiectasia mutant,*[24] the ATM gene product and the DNA-dependent protein kinase. PIKK's are usually involved in functions critical to cell survival and

often regulate cellular responses to DNA damage, repair and recombination. PIKK's are also known to regulate cell cycle progression and cell checkpoints[26].

mTOR contains several conserved DNA sequences (Figure 2)[27]. It contains a C-terminal kinase domain similar to protein and lipid kinases that is critical for the function of this family of kinases[28]. mTOR also contains a unique domain at the extreme C-terminus end that are not seen in PI3 and PI4 Kinases[20].

The first 1200 amino acids of the mTOR sequence make up approximately 20 tandemly repeated motifs composed of Huntington, elongation factor 3, the A subunit of protein phosphatase 2A (PP2A), and TOR 1p (HEAT domains). The motif consists of patterns of approximately 40 amino acids in 3 repeating sequences, each containing the pattern of the hydrophobic; proline, aspartic acid, and arganine residues[7]. The HEAT domains modulate protein to protein interactions through an extended superhelical structure, but their exact function is yet unknown[12].

Carboxy-terminal to the HEAT domains is the short segment of amino acids, termed the FAT domain, unique to PI3K's. Found between amino acids 1382-1982 the FAT domain is always paired with the FATC domain at the extreme carboxy terminus of mTOR[29]. The FATC domain gains its name from its components including: rapamycin-associated protein (FRAP), ataxia telangiectasia mutated (ATM), and transformation/transcription domain-associated protein (TRAAP), and its position at the carboxy-terminus. While the FATC domain is unique to mTOR, researchers have suggested that the presence of the FAT and FATC domains serve to regulate kinase activity in mTOR[7]. Conservation of the FAT and FATC domains is

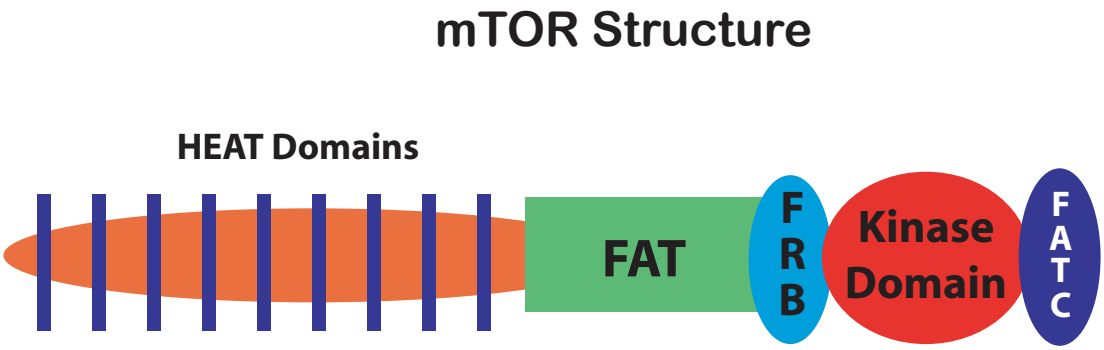

FIGURE 2:

A schematic representation of the structure of the mTOR protein. The first 1200 amino acids are patterns of approximately 40 amino acids in 3 repeating sequences. This domain modulates protein to protein interactions. The FAT domain is a 600 amino acid sequence that modulate the function of the kinase domain. Conservation of this domain is critical to mTOR kinase activity. The FRB domain is the location of the binding site for which PA and FKBP12 compete. The kinase domain is critical for cell cycle progression as mutations in this site lead to G1 cell cycle arrest. This domain is also responsible for phosphorylation of downstream components of the mTOR pathway. The FATC domain is always paired with the FAT domain and is equally critical for kinase activity.

critical as even the smallest change in amino acid sequence can cause mTOR to lose its kinase activity.

Carboxy-terminal to the FAT domain is the FKBP-12-rapamycin binding (FRB) domain, which binds the FKBP-12-rapamycin dimer. Mapped from 2025 to 3014[30], mutations in the FRB domain can confer rapamycin resistance to mTOR and have been exploited to allow a deeper understanding of the pathways with which mTOR is involved. The FRB domain also plays a role in the upstream regulation of mTOR. Studies have shown that FKBP12[31], which is known to bind the FRB domain, was competitive with phosphatidic acid (PA) for that site. The FRB domain contains a serine residue Ser2035 which is critically involved with the binding of the FRB region and the FKBP12-rapamycin complex. Mutations at this residue with any other amino acid containing a larger side chain than serine prevent the proper tertiary complex formation[32].

The mTOR kinase domain is carboxy-terminal to the FRB domain. The protein kinase domain resembles the catalytic domain of PI3K's and holds an affinity for serine and threonine residues[33]. The kinase domain in mTOR is essential for cell cycle progression that mTOR mediates. Mutations in the kinase domain lead to G1 cell cycle arrest[34]. This domain is also required for the phosphorylation of downstream components including S6 Kinase and 4E-BP1 and is interchangeable within the PI3K family[35]. mTOR does not have any known lipid kinase activity[36], although it does autophosphorylate[37].

mTOR is also thought to play a role in nuclear shuttling, which may have some regulatory effect on the downstream molecules, S6K and 4E-BP1. mTOR is

considered cytoplasmic, generally localized to intracellular membranes[38]. There is no known reason for mTOR's localization to intracellular membranes, however. Chen's lab has also shown data which suggests that the continuous movement of mTOR from the cytoplasm to nucleus has implications in S6 Kinase activation and phosphorylation[39]. Although mTOR has no conventional nuclear export or import signal, it is possible that it contains a novel transport sequence enabling it to move in and out of the nucleus[40]. The lack of a clear nuclear localization sequence is not uncommon in the ATM-related kinase family though, and may explain the apparent lack of sequence. Another proposed hypothesis is that mTOR translocates only after associating with an unknown transport vehicle containing a standard nuclear shuttling protein[39]. Ongoing research in different labs is aimed at confirming or disproving mTOR's need for such a shuttling vehicle.

Chen's lab performed a number of experiements to determine the effect of mTOR shuttling. Using leptomycin B (LMB), a specific inhibitor of the nuclear export receptor Crm1, the lab showed that the mTOR pathway was significantly inhibited in the presence of LMB[39]. LMB treatment led to an inhibition of 4E-BP1 phosphorylation and S6K activity. In other experiments with S6K2, Chen's lab concluded that: "It is thus likely that a balanced distribution of mTOR between the cytoplasm and nucleus, or an optimal shuttling rate of mTOR, may be essential for the maximal activation of downstream signaling[41]."

TORC1 and TORC2

mTOR exists as two different multiprotein complexes within the cell[42] (Figure 3). TOR complex 1 (TORC1) is composed of mLST8/GβL (mLST8 is also called G

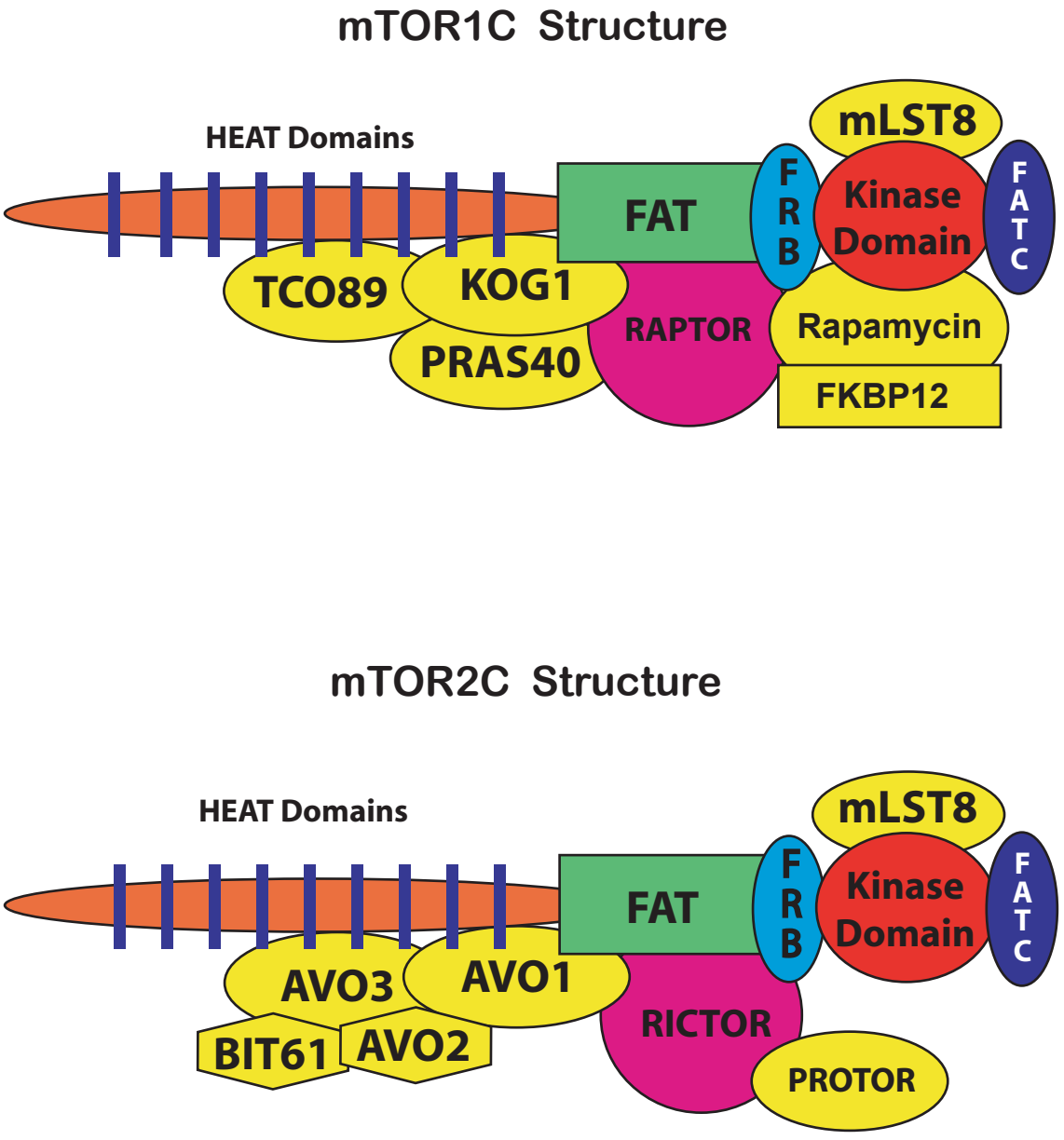

FIGURE 3:

Proteins associated with TORC1 and TORC2.

protein β-subunit-like protein) and Raptor (regulatory-associated protein of mTOR) and shows rapamycin sensitivity. To date, the function of mLST8/GβL is unknown, although it may serve as an activator molecule[43]. TORC1 controls many of the known pathways of the mTOR complex including phosphorylation of S6K1 and 4E-BP1. TORC1 is also responsible for transcription and translation initiation, thereby controlling the growth and proliferation of the cell[44]. TORC2 is composed of MLST8/GBL and RICTOR-PROTOR[45] (rapamycin-insensitive companion of mTOR and protein observed with RICTOR) complex, but shows no rapamycin sensitivity[42]. TORC2 is responsible for actin reorganization within the cell as well as phosphorylation of AKT at S473[44].

TORC1 and TORC2 respond differently to rapamycin. TORC1, complexed with GBL and raptor proteins, show sensitivity to rapamycin. Rapamycin and its receptor protein FKBP12 directly bind to and inhibit mTOR at the FRB domain. Although the mechanism is poorly understood[46], recent studies suggest that the rapamycin/FKBP12 complex competes with the activator molecule PA for mTOR binding sites. By interfering with the mTOR pathway, the effected cell is not able to proceed into the G1 phase of the cell cycle thereby unable to synthesize protein.

Upstream Regulators of mTOR

There are several known upstream regulators of mTOR. It is known that nutrient depravation or starvation conditions inhibit pathways that require mTOR[47], while insulin, insulin like receptors, and nutrients such as amino acids or glucose upregulate mTOR[48]. Protein synthesis is one of the most energy consuming tasks the

cell undertakes; therefore, it is easy to see why the cell strictly regulates these processes. Individual cells must constantly assess mitogenic and nutritional signals around them and determine if enough raw materials exist for growth or proliferation[49]. DNA and protein synthesis leading to an increase in individual cell size defines growth. An increase in the number of cells in a population is termed proliferation[50].

Eukaryotic cells have complex, and not yet fully understood mechanisms that regulate protein synthesis and breakdown. When cells sense a lack of raw materials including amino acids, oxygen, or growth factors cellular processes begin which prevent growth or proliferation[51]. In times of need, the cell may even catabolize translational machinery for the raw materials in order to maintain homeostasis. In a severe crisis, such as a lack of nutrients, cells initiate apoptotic pathways that eventually lead to the cells demise. In times of abundance however, TOR functions to upregulate translation, cell growth, and actin reorganization.

PI3K Pathway

Currently the best understood mTOR activation pathway is through PI3-Kinase (Figure 1). In this pathway, mTOR is activated through various extracellular growth factors including Insulin and Insulin-like growth factor-1 (IGF-1)[52]. Insulin and IGF-1 signal through integrins and chemokines through G-protein coupled receptors to the Insulin Receptor Substrate (IRS) in the plasma membrane of the cell. IRS then recruits PI3-Kinase to the cell membrane[49]. The newly recruited PI3-Kinase binds to phosphatidylinositol-4,5-phosphate (PIP2) in the cell membrane and converts

it to Phosphatidylinositol-3,4,5-phosphate (PIP3), a cell survival signal[53]. PIP3 recruits PDK1 and Protein Kinase B (Akt) to the membrane, binding the pleckstrin homology (PH) domain of Akt. This causes PIP3 to dimerize, exposing its active catalytic site[54]. PIP3 activates PDK1, which in turn phosphorylates and activates AKT[49].

AKT

AKT is of particular interest because of its important role in apoptosis inhibition. Phosphorylated AKT promotes cell proliferation through mTOR while inhibiting phosphorylation and activation of proteins such as the pro-apoptotic Bad protein[55]. Tumor suppressor genes phosphatase and tensin homolog (PTEN) and inositol polyphosphate-5-phosphatase D (SHIP) inhibit the phosphorylation of AKT by PI3K in a regulatory mechanism that prevents overgrowth[56]. However in some cancers, PTEN is found to be mutated and the lipid phosphatase that inhibits the PI3-kinase activity is not functional[57]. This dysregulated pathway then can not prevent the overexpression of cancerous cells, allowing cell proliferation regardless of nutrient status. Cancers with apoptotic resistant cells are commonly linked to PTEN mutations[7]. AKT may also directly phosphorylate mTOR or act as an inhibitor of Tuberous Sclerosis Proteins 1 and 2 (TSC1 and TSC2) by phosphorylation of TSC2[58].

Tuberous Sclerosis Complex (TSC1 and TSC2)

Distal to AKT in the activation pathway of mTOR is the Tuberous Sclerosis Complex. The TSC1/TSC2 complex is composed of the proteins hamartin (TSC1)

and tuberin (TSC2) which bind to mTOR *in vivo*, and also acts as a GTPase-activating protein of Rheb. TSC2 is an inhibitor of mTOR through Rheb, but when TSC2 is phosphorylated by AKT, its inhibitory effects are downregulated[7]. The precise mechanism through which the TSC1/TSC2 complex is inhibited is yet unclear, but some reports suggest it is through the dissociation of the TSC complex[59]. When the PI3K pathway looses the inhibitory effects of the TSC1/TSC2 complex, the cell shows an mTOR dependent increase in p70S6K activity. This increase in p70S6K activity provides the cell with a small level of resistance to amino acid depravation[59]. In nutrient poor environments, the TSC1/TSC2 complex inhibits the phosphorylation of p70S6K.

Recently studies have shown that the TSC1/TSC2 complex may also have a nutrient sensing path independent of the AKT pathway. In cell lines where the TSC1/TSC2 was mutated out, the expected p70S6K dephosphorylation response to nutrient depravation is not seen. This seems to suggest that the TSC1/TSC2 complex somehow signals nutrient levels to the cell, and that disturbing the TSC1/TSC2 complex serves to destroy that sensing pathway[10].

Rheb

Rheb is the last step in the PI3K pathway before mTOR. Rheb is a small G-protein activator of mTOR. TSC2 is a GAP (GTPase-activating protein) for Rheb. Non phosphorlyated TSC2 acts as a Rheb inhibitor by converting the active GTP-bound form of Rheb to the inactive GDP version. However, when the TSC1/TSC2

complex is inactivated through AKT phosphorlyation, Rheb transforms into its active GTP-bound protein and upregulates mTOR[60].

Recently, Rheb has been shown to bind directly to the kinase domain on mTOR, in a GTP-dependant manner[61]. Rheb's high GTP levels allow it to bind mTORC1, causing a conformational change in mTORC1[62]. This conformational change leads to the activation and phosphorylation of the two best known downstream targets: 4E-BP1 and p70 S6K. Gain of function Rheb mutants have been shown to be more active in promoting phosphorylation of 4E-BP1 and p70 S6K[63].

Most researchers would agree that Rheb binds mTOR but Rheb's mechanism of interaction to activate mTOR remains unclear. This is largely because it is difficult to detect direct interactions between Rheb and mTOR[64]. It is also unclear what role GTP plays in the pathway. Some labs have even suggested that Rheb and mTOR actually act in parallel pathways as opposed to the linear pathway presented here[9].

Phosphatidic Acid (PA)

Phosphatidic acid (PA) is a lipid second messenger used in several intracellular pathways and regulates an ever expanding list of signaling proteins. PA has been implicated as a mediator of mitogenic upregulation by hormones and growth factors[65]. The precise mechanism by which PA acts on mTOR is yet unknown, but some labs have reported that PA is a requirement for mTOR to phosphorylate S6K[65]. After serum stimulation, a rapid rise in PA levels is observed, and correlates with activation of mTOR signaling in human embryonic kidney (HEK) cells.

PA is most commonly a product of the enzymatic activity of phospholipase D (PLD), addressed later in this discussion[66]. PA is composed of a glycerol backbone with carbons 1 and 2 forming ester-links to fatty acids. The terminal carbon group links to a phosphate group, forming the negatively charged polar head group. There are at least three enzymes that are capable of PA generation: lysophosphatidic acid acyltransferase, and diacylglycerol kinase (DGK)[67] and PLD.

Diacylglycerol kinases (DGK) are a conserved family of lipid kinases that phosphorylate diacylglycerol (DAG) to produce PA. DAG is a second messenger whose cellular levels have been shown to increase transiently with extracellular fluxuations of growth factors and hormones. DAG is also activator of protein kinase C (PKC), and other GTPase-activating proteins including those in the Ras family of GTPases[68].

PA production by PLD can be suppressed by a reaction involving primary alcohols. In the transphosphatidylation reaction, an inert phosphatidyl-alcohol is produced instead of PA when reacting PLD2 with primary, but not tertiary alcohols. In this reaction, the primary alcohol replaces the water molecule and acts as the nucleophillic acceptor. The alcohol competes with the water to be the hydroxyl donor forming a phosphatidylalcohol. This is a commonly used reaction as an *in vitro* PLD activity assay[69]. The control experiment to rule out any effect of the alcohol not related to PLD is performed by using a tertiary alcohol instead of a primary alcohol that is not a substitute for PLD.

Several labs have shown that PA production through PLD is an essential event for mitogenic activation of mTOR . Cellular concentrations of PA are normally less

than 5% than that of phosphatidylcholine (PC), but during mitogenic activation the amount of PA within a cell increases, most likely due to PLD activation[70]. Using 0.3% 1-butanol, serum stimulated PA production can be effectively stopped[65]. Using the same transphosphatidylation reaction, 1-butanol was able to almost completely block the serum stimulated phosphorylation of S6K1 and 4E-BP1. The phosphorylation of serum stimulated activation of extracellular signal-regulated kinases (ERK1 and ERK2) was not affected by the presence of the 1-butanol. This experiment established the specificity of 1-butanol on PA production and implicates the involvement of PA in the phosphorylation of S6K and 4E-BP1[71]. From these findings, it can be asserted that PLD production of PA plays an essential role in the mTOR signaling pathway. The suppression of PA generated through PLD has been reported by a number of labs to inhibit the mTOR pathway in several cell phenotypes.

The lab led by Dr. Jie Chen has also shown evidence that PA binds to mTOR at the FKBP12-rapamycin-binding (FRB) domain. Small unilamellar vesicles (SUV's) containing purified FRB fragment bound to PA in very low concentrations[65]. This binding was specific for PA as other phospholipids were unable bind the FRB with such specificity. The FRB region is where the rapamycin-FKBP12 molecule binds mTOR as well. It is hypothesized that the competition between the rapamycin-FKBP12 complex and PA for the FRB site may be one of the regulating factors in mTOR activation[71]. Researchers previously suggested that the rapamycin-FKBP12 molecule induces a conformational change in the structure of mTOR[72]. However new data suggests the effects of rapamycin are realized through the competitive interaction between mTOR's FRB and PLD generated PA. Yet a third hypothesis suggests that

the pH locally around mTOR is reduced by PA generated PLD. mTOR is then pronated in a way that promotes its kinase activity, or allows for interaction with yet unknown promoter substrates[53].

Attempts at corroborating mTOR phosphorylation studies using exogenously provided PA have been inconclusive. Some labs have reported exogenously supplied PA was able to incorporate easily into cellular membranes and participate in cellular functions[73]. Others however, reported that signaling was disrupted in siRNA PLD2 knockdown cells, even with the presence of exogenously provided PA[74]. Recently there have been some questions about the validity of studies involving exogenously provided PA. It is difficult for PA to cross cellular membranes and reach appropriate sites to engage mTOR, and exogenously provided PA may activate mTOR as a result of another, yet unknown pathway[53].

The Role of mTOR in Hypoxia

During low oxygen conditions, mammalian cells immediately down-regulate energy consuming processes[75]. Translation is one of the first processes to be effected as the cell seeks to stave off the impending energy crisis. Hypoxia also upregulates HIF-1, a transcription factor which activates genes required for the cell's adaptation to the new environment[13]. Because it is yet unknown what pathways regulate HIF-1 in response to hypoxia, some have suggested mTOR as a potential mediator of the extracellular condtions[76]. However, other studies have shown that mTOR and S6K1 can respond to amino acid availability independently of the TSC1/2 pathway[77]. Hypoxia mimics rapamycin causing the dephosphorylation of mTOR and its

downstream effecter proteins, 4E-BP1 and S6-Kinase. These effects have been observed independently of the growth factors previously discussed in this review. These findings suggest yet another unresolved pathway that mTOR may use to effect the cell[78].

Downstream Molecules of mTOR/Raptor (TORC1)

Ribosomal S6 Kinase

The best characterized function of mTOR is translation regulation[72]. The S6K isoform, S6K-1 is a major ribosomal protein in mammalian cells, and responsible to phosphorylate the S6 ribosomal protein[79]. The ribosomal S6 subunit of the 40S ribosome selectively increases translation of some of the mRNA's containing the 5'-Terminal Oligopyramidine Tract (5'-TOP)[39]. mRNA's with a 5'-TOP often serve to encode ribosomal proteins and other transcription regulation proteins thereby upregulating transcription[80]. S6K is independent of mTOR[81] however, even low concentrations of rapamycin are thought to inhibit the phosphorylation activity of S6K[24]. While the actions of S6K are not well understood[48], S6K1 likely plays an important role in the regulation of cell cycle progression, cell growth and cell proliferation[82].

Structurally, the S6K protein is divided into four regions: the acidic NH_2 terminus, the catalytic domain, a linker region and a basic COOH- terminus containing an autoinhibitory pseudosubstrate domain[83]. Current data suggests that S6K remains in an inactive state with its acidic NH_2-terminus interacting with the basic COOH region, stabilizing the protein. This conformation allows the

pseudosubstrate region to autoinhibit the catalytic domain of S6K. After phosphorylation of several C-terminal sites, the S6K undergoes a conformational change and releases the pseudosubstrate, allowing the phosphorylation of T389 in the catalytic domain[82].

The mTOR and PI3K pathways can phosphorylate at least eight sites on S6K. These phosphorylation events are known to require several mediator molecules including PDK1, AKT, PKC, and the small G proteins Cdc42 and Rac1[82]. It is likely that there are other yet unknown mediator molecules. Only the phosphorylation of T229 on S6K's activation loop of the kinase domain has been described[84]. The remaining phosphorylation sites, while identified, remain less well understood. Two phosphorylation sites serine 371 and threonine 389 are known to be required for S6K activity[85]. Experiements show that mTOR can phosphorylate T389 directly *in vitro* while the kinase responsible for S371 is not yet known[33]. However, incubation with rapamycin causes dephosphorylation of threonine 229 and serine 404 suggesting mTOR's involvement with those residues as well.

Additionally, evidence now shows that mTOR phosphorylation is mediated by p70 S6 Kinase[52]. This feedback mechanism phosphorylates SER-2448 on mTOR, and does not appear to be controlled by the AKT pathway. This may be a negative feedback mechanism[86].

It has been shown that inhibition of mTOR signaling by rapamycin treatment leads to a dramatic decrease in rRNA gene transcription and pre-rRNA processing[87]. This includes the dephosphorylation of T389, the principle rapamycin-sensitive site, leading to the kinase inactivation of S6K[51]. This evidence suggests that mTOR

signaling is a vital link in sensing nutrient availability and regulating ribosome biogenesis on the basis of that information[88]. Inhibition of mTOR signaling has been shown to inhibit translation as well, but in a less dramatic fashion than its inhibition of transcription[89]. In mice, disruption of S6K1 leads to reduced animal size, suggesting a role for S6K1 in the control of cell size and growth. Amino acid depletion also causes S6K dephosphorylation, through the mTOR pathway, in a manner which is reversible by the replenishing of the addition of amino acids.

Ribosome synthesis is a hallmark indicator of cellular growth regulation. As nutrients become more readily available, cells upregulate ribosome synthesis, allowing for a rapid size increases and proliferation. As was previously discussed, this process is energy intensive and must be strictly regulated for survival purposes. HeLa cells, for example, produce about 7,500 ribosomes per minute, requiring the transcription of 150-200 rRNA genes and involving the synthesis of approximately 300,000 ribosomal proteins[47]. This tightly regulated process would be impossible except for the systematic interactions between nutrient sensing pathways and with coordinated support from assembly factors, ribonucleases, small nucleolar ribonucleoprotein particles and RNA helicases. This has been previously explained by Fingar *et al.* in their article on mTOR.

> "If the rate of cell growth is unable to keep up with the rapid rate of cell division, then cell proliferation cannot be sustained, since cells would progressively loose mass and size with each division cycle, resulting in inevitable cell death. Therefore, proliferating cells exhibit tight coordination between cell growth and cell cycle progression. In

addition, such coordination ensures that individual cells, and indeed organs and whole organisms, maintain a characteristic size." [83]

Recently a second S6 Kinase was discovered, S6K2[41]. S6K2 shows an 80% homology to S6K1 and is also phosphorylated in a rapamycin dependant manner. Unlike its cytosolic counterpart S6K1, however, S6K2 is nuclear, due to its C-terminal nuclear localization signal (NLS)[90]. Much less is known about S6K2 than S6K1, but current models suggest redundant functions. S6K1 is thought to play a more crucial role in growth control than S6K2[50].

The membrane-to-nucleus PI3K-mTOR pathway is beginning to reveal itself as more than just a linear pathway. Mounting evidence points to the hypothesis that the PI3K pathway operates under the nutrient sensing influence of mTOR only to a certain degree. Amino acid and energy sufficiency are mediated by mTOR primarily, while growth factors, hormones, and mitogens sufficiency are conveyed through the PI3K pathway and then to mTOR.

4E-BP1

Cells treated with mTOR inhibitor rapamcyin arrest at the G1/S boundary and mimic the physiological state of starved G0 cells[25]. mTOR kinases, in the presence of adequate amino acids, upregulate the signaling pathways by activating eukaryotic translation initiation factor 4 E (eIF-4E) protein synthesis, effectively inducting G1 progression[91]. The 12 kDa polypeptide 4E-BP1 is a strong repressor or eIF-4E, important for translation. By regulating energy use within the cell, mTOR serves as an effective gatekeeper.

In its inactive state when nutrients or growth factors are scarce, 4E-BP1 is hypophosphorylated and binds tightly to the 7-methylguanosine cap-binding protein eIF4E to inhibit eIF4E function[91]. Upon the return of adequate nutrients and growth factors, 4E-BP1 is phosphorylated and dissociates from eIF4E. eIF-4E is then able to specifically recognize and bind the 5'cap on a nuclear transcribed mRNA. Almost all nuclear transcribed mRNA contain a 5' cap structure; m7GpppN, (where 'm' stands for any methyl group and 'N' any nucleotide)[92]. eIF-4E is also available to bind the scaffolding protein eIF4G and assemble the translation initiation complex. While the translation initiation complex forms, eIF4G also interacts with eIF3, recruiting the 40S subunit to the 5' end of the mRNA[93]. Because the binding sites for 4E-BP1 and eIF4G overlap on eIF4E, their binding is competitive and mutually exclusive, ensuring 4E-BP1's ability to regulate eIF4E's activity.

Phosphorlyation and activation of 4E-BP1 is sensitive to mTOR inhibitors including rapamycin and other PI3K pathway inhibitors. Studies *in vitro* show that immunoprecipitated mTOR phosphorlyates threonine 37 and threonine 46 on 4E-BP1, suggesting mTOR as the active kinase *in vivo*[33]. These two sites are considered priming sites, as phosphorylation of serine 65 and threonine 70 must follow for eIF-4E to be released by 4E-BP1. The kinase for the phosphorylation of these sites is yet unknown, but mTOR may also act as the kinase there. In all, 4E-BP1 has seven known phosphorylation sites: Thr 37, Thr 46, Ser 65, Thr 70, Ser 83, Ser 101 and Ser 112[92]. As is expected then, inhibition of mTOR by rapamycin results in the hypophosphorylation of 4E-BP1.

TOR "Signaling Motif"

Both S6-Kinase and 4E-BP1 contain a TOR Signaling (TOS) motif, which may be recognized by the Raptor-mTOR complex. A functional TOS motif is required for mTOR to phosphorylate S6K1 and 4E-BP1 *in vivo*, as destroying this domain mimics rapamycin treatment of mTOR[94]. Studies show that an inactive TOS motif on 4E-BP1 is unable to bind mTOR and results in abnormally small cell growth and small cell size[95]. The mTOR/raptor/4E-BP1 complex will not properly form in the absence of a functional TOS motif. These experiments lead to the hypothesis that raptor interacts with mTOR to form a substrate presentation scaffold, and without the properly functioning regions, is ineffective at phosphorlyating downstream substrates[43].

The homology demonstrated in the TOS regions of S6K and 4E-BP1 is not unique, however, and is demonstrated in many other proteins[72]. This lack of specificitiy makes it difficult to identify sequences for which mTOR has a remarkable affinity. Also, phosphorylation sites are not conserved between the two molecules. This has lead some to propose that mTOR associated proteins may actually determine the substrate preference, leaving mTOR's kinase domain with no preference in substrate[33]. It is difficult then to prove with any certainty that S6K and 4E-BP1 are direct substrates of the mTOR-raptor complex.

Due to the nature of the many substrates that are apparently involved with the mTOR signaling path, there is mounting concern about the disruption of those proteins *in vitro*[83]. Recent studies show that mTOR and it associated proteins are easily disrupted with nonionic detergents. This may be one explanation for the

apparent disparity in kinase activity experiments and provide insight into why mTOR's *in vitro* kinase activity correlates poorly with the activation and phosphorylation of expected downstream targets *in vivo*[83].

Evidence continues to mount pointing to a possibility that there are one or more intermediate kinases that regulate the downstream molecules of mTOR. This kinase or may be regulated by or associate with mTOR in interactions that are yet unknown. This possibility should continue to drive research forward to elucidate the precise mechanism by which mTOR is regulated.

Clinical Applications

As was previously discussed, mTOR and its pathways are commonly overexpressed or mutated in cancer. Clinical studies on several prototype mTOR inhibitors, all rapamycin analogs, (CCI-779 [Wyeth], RAD001 [Novartis] and AP23573 [Ariad Pharmaceuticals] are currently taking place[16]. However, these drugs have only shown promise is a few cancers. The overall response to rapamycin treatments has been variable, with success often linked to certain cell types.

Several unexpected results of rapamycin-analog treatments have presented themselves. The first is the existence of a strong negative feedback loop from S6K to AKT[49]. This loop inhibits AKT when mTOR is activated which can promote cell survival and chemoresistance[48]. The very cancerous cells which the drug is attempting to eradicate may, in fact enter a survival mode, allowing them to survive and proliferate under stressful conditions such as nutrient or space deprivation. The second unexpected result of treatment is that prolonged rapamycin treatment has been

shown to lead to the inhibition of the mTORC2-RICTOR complex. This complex was previously thought to be insensitive to rapamycin. The cause for this finding is yet unknown, but it is speculated to be mediated through the AKT pathway.

The development of safe, effective pharmaceutical agents to counteract the dysregulation of the AKT/mTOR pathway in cancer should be a key focus of mTOR research right now. However, this goal will not be able to be reached until the complexity of the mTOR protein complex and the crosstalk between other signaling molecules are more fully realized. Defining the connection between the mTOR associated proteins and its kinase activity is an important challenge for the future.

II. HYPOTHESIS AND SPECIFIC AIMS

We hypothesize that mTOR can be overexpressed in a mammalian system and a complete study of this expression (protein activity and subcellular localization) can be pursued, taking advantage of an HA tag.

AIM 1:

Prepare an HA-tagged mTOR expression plasmid.

AIM 2:

Generate three HA-tagged mTOR mutated plasmids by site directed mutagenesis. Including:

PA binding deficient R2109A

Kinase Dead D2357E

Rapamycin Resistant S2035T

AIM 3:

Detect protein expression of plasmids by Western blotting; probe with anti-HA and anti-mTOR.

AIM 4:

Determine enzyme activity of overexpression plasmids (mock, HA-mTOR, Kinase Dead) using KLISA, Mass Spectrometry, or gamma ATP to detect phosphorylation of mTOR substrates.

Substrates 4E-BP1, S6K

Use Rapamycin, a known mTOR inhibitor as a negative control.

AIM 5:

Investigate the effects of mTOR transfection on gene expression and subcellular localization.

III. MATERIALS AND METHODS

Materials

COS-7 cells were purchased from American Type Culture Collection (ATCC) (Rockville, MD). mTOR, PLD1, PLD2 and, S6K Taqman gene expression assays purchased from Applied Biosystems (Foster City, CA). Protease Inhibitor cocktail set III, microcystin-LR and, K-LISA mTOR activity kit purchased from Calbiochem (San Diego, CA). Dulbecco's Modification of Eagle's Medium (DMEM) purchased from Cellgro (Herndon, VA). HA-Tag (6E2) Mouse mAb purchased from Cell Signaling Technology (Danvers, MA). TrichromRanger prestained molecular weight marker mix, 4-20% Precise Protein gels and, Scintiverse II scintillation cocktail obtained from Fischer Scientific (Chicago, IL). Enhanced chemiluminescence (ECL) Western blotting detection reagents purchased from GE Healthcare (Piscataway, NJ). phCMV2-HA vector (4.26 kb) purchased from Gene Therapy Systems (San Diego, CA). Various primers purchased from Integrated DNA Technologies Inc. (Coralville, IA). Lipofectamine, plus reagent, Opti-MEM reduced serum medium, Quant-iT Ribogreen RNA assay kit, dNTP's, SuperScriptII reverse transcriptase, random primers, single strand reverse transcriptase buffer, RNase out, Deoxyribonuclease I and, DTT purchased from Invitrogen (Carlsbad, CA). UltraClean Plasmid Prep Kit purchased from MOBIO Laboratories, Inc. (Carlsbad, CA). Quick Ligation Kit, Taq DNA Polymerase and ThermoPol Buffer, Restriction Enzymes and their buffers, Lambda DNA-HindIII Digest and, Antarctic Phosphatase, purchased from New England BioLabs Inc. (Ipswich, MA). Homo sapiens FK506 binding protein 12-rapamycin associated protein 1 (FRAP1) Human cDNA clone (also known as mTOR)

purchased from OriGene Technologies, Inc. (Rockville, MD). [^{32}P] γ–ATP (500 μci) purchased from Perkin Elmer (Waltham, MA). RNeasy minikit, Quiaquick gel purification kit and, QIAprep Spin Miniprep kit were purchased from Qiagen Inc. (Valencia, CA). 4E-BP1 (FL), HA-probe (Y11), α-myc-TRITC IgG antibody and, a-HA-FITC IgG antibody purchased from Santa Cruz Biotechnology, Inc. (Santa Cruz, CA). Monoclonal Anti-HA, Influenza Hemagglutinin Protein (HA-Tag) and, Influenza Hemagglutinin (HA) Peptide purchased from Sigma (St. Louis, MO). QuikChange XL Site-Directed Mutagenesis Kit, 96 well PCR plates, DH5α gold cells, and Brilliant II QPCR master mix purchased from Strategene (La Jolla, CA.). P70 S6 Kinase (T412E), active purchased from Upstate Biotechnology (Lake Placid, NY). ExoSAP-IT, DNA Ladder (1 KB), Agarose, molecular biology grade ultra pure water and, 10X TAE buffer purchased from USB Corporation (Cleveland, OH). Vectashield mounting media purchased from Vector Labs (Burlingame, CA). Ion exchange chromatography cellulose phosphate paper purchased from Whatman (Hillsboro, OR).

Methods

DH5a Transformation

This experiment was begun with a Homo sapiens FK506 binding protein 12-rapamycin associated protein 1 (FRAP1) Human cDNA clone (known for the purposes of this thesis as mTOR) purchased from OriGene Technologies, Inc. This DNA clone was the starting point of the thesis and the building block from which the four other plasmid constructs would come.

The filter containing the purchased, dried DNA clone was placed in a sterile eppendorf with 10 µl ultrapure water to achieve a final concentration of 100 ng/µl. DH5α cells (100 µl) were thawed on ice to which 50 ng of eluted plasmid was added. The cell-plasmid mixture was occasionally swirled and incubated on ice for 30 minutes. The mixture was then heat shocked for 45 seconds at 42° C, and chilled on ice for 2 minutes. Room temperature SOC media (900 ml) was added and the cells incubated at 37°C for 1 hour in a shaker at 230 RPM. After 1 hour 150 µl of the SOC-cell mixture was spread onto LB/Agar/Ampicillin solid media plates.

Individual colonies of the DH5α transformed with pCMV6-XL4-mTOR were selected and inoculated in 5 ml LB/Ampicillin. These were incubated at 37°C for 8 hours before mixing 850 µl of the bacterial culture and 150 µl glycerol to make glycerol stocks. Glycerol stocks were stored at -70°C.

DNA Preparation – Maxiprep

For maxiprep DNA preparation we used the UltraClean Plasmid Prep Kit purchased from MOBIO Laboratories, Inc. The manufacturer's instructions were

followed to obtain large quantities of DNA from cell cultures. One ml bacterial culture was added to 400 ml LB/Ampicillin and incubated in the shaker, overnight at 37°C. The next day the culture was prepared per the protocol provided with MOBIO's Plasmid Prep Kit. The cells were pelleted at 4500xg and resuspended in 5 ml Solution 1. The pellet was lysed by alkaline treatment by adding 10 ml Solution 2, and inverting 5 times. Thirty ml Solution 3 neutralized the mixture, after which it was inverted again 5 times. The cell mixture was centrifuged for 20 minutes at 4500xg, which allows for the separation of the DNA from the proteins. The pellet and floating protein and lipid mixture at top of the liquid were discarded. The filter column was centrifuged dry at 3600xg for 5 minutes. Then 2 ml of 65C ultrapure water was added to the column and centrifuged into a clean centrifuge column.

Restriction Enzyme Digestion

Five hundred ng of plasmid was incubated with 1 µl of the appropriate buffer, a minimum of 20 units of enzyme as required, and 1 µl of BSA as required. All restriction enzymes were obtained from New England BioLabs, and the manufacturer's instructions for digestion reactions were followed. One unit of enzyme is defined as the amount of enzyme required to digest 1 µg of λ DNA in 1 hour at 37°C in a total reaction volume of 50 µl. The total volume of the reaction was then taken to 10 µl and incubated at 37°C for a minimum of 2 hours. After incubation, 2 ml gel loading buffer was added to each digestion and the mixture was loaded into a 1% agarose gel. The gel was run at 100V for approximately 40 minutes, until the marker bands were clearly separated. Images of the gels were captured

under ultraviolet light with Kodak's Gel Logic 200 image system using Capture GL Molecular Imaging Software version 4.0.1.

Mutagenesis

Mutagenesis was performed as outlined in Stragagene's QuikChange XL Site-Directed Mutagenesis Kit. Fifty ng of purified plasmid was added to 5 µl 10X mutagenic buffer. Sense and antisense mutagenic primers (0.65 µl) were then added. Primers were designed at www.idtdna.com and purchased from that same company (Tables 1, 2). The primers were stored at a stock concentration of 200 ng/µl in TE, pH 7.5. One µl dNTP's, three µl QuikSolution, and ultrapure water to 49 µl were added. Next 1 µl Pfu Turbo polymerase was added, the mixture mixed and centrifuged. The mutagenesis reaction was placed in the PCR machine and cycled. After the PCR reaction was complete, 1 µl Dpn I was added and allowed to react for 1 hour at 37°C. This mutagenic, Dpn I-treated PCR reaction was then used to transform XL10 cells.

XL-10 Cell Transformation

To transform the mutagenesis reaction, 45 ul XL10 competent cells were added to 2 µl β-Mercaptoethanol and incubated on ice for 10 minutes. Next, 2 µl of the Dpn I-treated mutagenesis reaction was added, and incubated for 30 minutes on ice. The mixture was then heat shocked at 42°C for 30 seconds after which it was placed on ice for 2 minutes. NZY^+ media (450 µl) was preheated to 43°C and added to the reaction. This mixture was incubated for 37°C for one hour in the shaker at

Primer	Mutagenic Primer Sequence
mTOR (Mfe/Hind) Sense	5’ – GAGGCCTTGGCCGAAGCCGCGCCAATTGCAGG GCAAGCTTCTTGGAACCGGACCTGCCGCCGC -3’
mTOR (Mfe/Hind) Antisense	5” – GGCGGCGGCAGGTCCGGTTCCAAGAAGCTTGC CCTGCAATTGGCGCGGCTTCGGCCAAGGCCTC– 3’

TABLE 1:

Mutagenic primers were designed to introduce two point mutations into pCMV6-XL4-mTOR to introduce two new restriction sites, HindIII and MfeI to the plasmid. These sites allowed for removal of the mTOR insert and ligation into the phCMV2-HA vector. The sequence underlined and in red above is the *HindIII* point mutation. The sequence underlined and in blue represents the *MfeI* mutation. After mutation, digestion with *HindIII* and the *NotI*, a site which was already present in the mTOR sequence, released the mTOR insert from the pCMV6 backbone and allowed for purification of the sequence. The sticky ends created by digestion with *HindIII* and *NotI* of mTOR correspond to the same sticky ends created in the phCMV2-HA plasmid with the same digestion. These complementary sticky ends provided ideal ligation conditions.

Primer	Mutagenic Primer Sequence
mTOR D2357E Sense	5’ - GATCCTGCACATTGAATTCGGGGACTGCTTTG - 3’
mTOR D2357E Anti-sense	5’ – CAAAGCAGTCCCCGAATTCAATGTGCAGGATC – 3’
mTOR R2109A Sense	5’ – CTCTATTATCATGTGGTCGCGAGAATCTCAAAGCAGC – 3’
mTOR R2109A Anti-sense	5’ – GCTGCTTTGAGATTCTCGCGAACACATGATAATAGAG – 3’
mTOR S2035T Sense	5’ – GCCTGGAAGAGGCAACACGTTTGTACTTTG– 3’
mTOR S2035T Anti-sense	5’ – CAAAGTACAAACGTGTTGCCTCTTCCAGGC– 3’

TABLE 2:

Mutagenic primers were designed to introduce two point mutations into phCMV2-HAmTOR-WT to introduce new restriction sites to the plasmid. These sites allowed for the detection of the mutation by restriction enzyme digestion after cells are transformed. The sequences underlined and in red represent the mutation sites. The D2357E plasmid contains an EcoRI mutation, the R2109A plasmid contains an NruI mutation and the S2035T contains an AflIII mutation.

230 RPM. After incubation, 200 µl of the transformation reaction was plated on LB/Agar/Ampicillin solid media plates and incubated overnight at 37°C.

DNA Preperation - Miniprep

For DNA miniprep we used Qiagen's QIAprep Spin Miniprep Kit and followed the manufacturer's detailed instructions. Briefly, the 3 ml cultures of transformed XL-10 or DH5α cells were pelleted at 4000x g for 10 minutes and the supernatant removed. The pellet was resuspended in 250 µl buffer P1 and transferred to labeled 1.5 ml eppendorf tubes per the instructions provided in Qiagen's Plasmid miniprep kit. Buffer P2 (250 µl) was added, and the tube inverted 6 times. Buffer N (350 µl) was added, and the contents of the tube centrifuged at 18,000x g for 10 minutes. The supernatant was passed through the Miniprep columns by centerfuging at 18,000x g for 2 minutes, flow through being discarded. Column filters were washed with 750 µl buffer PE and centrifuged to dry. Filters were eluted with 50 µl buffer EB into clean eppendorf tubes.

DH5a Transformation with pCMV6-mTOR

DH5α cells were transformed with pCMV6-mTOR plasmid. The procedure follows a similar protocol to the one described for the transformation of pCMV6-XL4-mTOR plasmid. Fifty ng of plasmid was used to transform 100 µl competent DH5α cells. Individual colonies were selected from the solid agar/ampicillin plates and 5 ml cultures of LB/ampicillin were inoculated and grown for 5 hours at 37°C.

The two most confluent cultures after 5 hours were used to prepare the 200 ml LB/ampicillin broth for maxiprep.

Purification of mTOR Insert

Five μg of pCMV6-mTOR and 50 Units of *HindIII* were combined with the appropriate buffers and incubated at 37°C for 6 hours. After inactivation of *HindIII* for 20 minutes at 65°C, 50 Units of *NotI* was added with the appropriate buffer. This mixture was incubated overnight at 37°C. Gel purification of the mTOR insert proceeded per Qiagen's QIAquick Gel Extraction protocol.

Digestion and Dephosphorylation of phCMV2-HA

Five μg of the phCMV2-HA vector was combined with 50 Units of *HindIII* and the appropriate buffers. This mixture was incubated for 6 hours at 37°C. After heat inactivation of *HindIII* for 20 minutes at 65°C, 50 Units of *NotI* were added with appropriate buffers and the mixture was incubated overnight at 37°C. The phCMV2-HA vector, with *HindIII* and *NotI* sticky ends was dephosphorylated with Antarctic Phosphatase.

Ligation of $^{Hind\ III}$phCMV2-HA$^{Not\ I}$ and $^{Hind\ III}$mTOR$^{Not\ I}$

Fifty ng of dephosphorylated $^{Hind\ III}$phCMV2-HA$^{Not\ I}$ vector was combined with a 3-fold molar excess of purified $^{Hind\ III}$mTOR$^{Not\ I}$ insert. Ten μl of 2X ligation buffer was added, followed by 1 μl of T4 DNA Ligase. The mixture was centrifuged and incubated at room temperature for 5 minutes. The ligation reaction was chilled

on ice and then used to transform DH5α cells. Transformation of DH5α cells with the phCMV2-HAmTOR-WT plasmid proceeded as outlined previously with adjustments made for the ligation mixture. Five µl ligation mixture was added to 100 µl XL-10 cells and mixed by gently pipetting up and down. The transformation reactions were plated on LB/agar/Kanamycin solid media plates. These plates were incubated overnight at 37°C.

Generation of the phCMV2-HAmTOR-WT Plasmid

Primers were ordered from www.IDTDNA.com to allow sequencing around the ligation site of the phCMV2-HAmTOR-WT plasmid (Table 3). PCR primers were stored in stock concentrations of 100 pmol/µl. Each PCR reaction contained 15 µl PCR buffer, 1 µl dNTP's, 1 µl $MgSO_4$, 1 µl primer set, 42 µl water, 0.25 µl Taq Polymerase DNA and, approximately 10 pg plasmid. The sense/antisense "535 primer set" were used in one reaction and a second reaction contained the sense/antisense "716 primer set." Ten µl of PCR sample was added to 4 µl of ExoSAPit and mixed. The reaction was incubated at 37°C for 15 minutes followed by 80°C for 15 minutes.

Cell Transfection and Lysate Preparation

Plasmid transfection to mammalian COS-7 cells was carried out under standard transfection conditions, using Invitrogen's Lipofectamine and Plus reagents as vehicles for the plasmids to enter the COS-7 cells. Six well plates were used, wells with cell confluency from 50% to 80%. Each well received 600 µl of cold Opti-mem,

Primer	Primer Sequence
HAmTOR-535 sense	5’ – AATGGGCGTGGATAGCGGTTTGAC-3’
HAmTOR-535 antisense	5’ – CTAGATGTGGTGGCAGCGGTGGTG – 3’
HAmTOR-716 sense	5’ – GCAAATGGGCGGTAGGCGTGTA – 3’
HAmTOR-716 antisense	5’ – ACTGGGTCATTGGAGGGGAGGAGGTTC – 3’

TABLE 3:

PCR Primers were designed against phCMV2-HAmTOR-WT to enable sequencing of the ligation site near the HA tag. The 535 primer set gave fragment 535 bp in length, and the 716 primer set gave a 716 bp fragment when run on a 2% agarose gel.

5 µl of Lipofectamine and 5 µl of Plus reagent along with the proper amount of plasmid. After a 48 hour incubation at 37°C, with controlled humidity and 5% CO_2, the cells were harvested. Cell lysates were taken from COS-7 cells transfected with each of the 4 plasmids.

Lysates were obtained using a lysis buffer modified from Kim *et al.*[10]; 50 mM Tris HCL, 100 mM NaCl, 10% Glycerol, 1% Tween 20, 1 mM EDTA, 25 mM NaF, 50 mM B-Glycerolphosphate, 1:200 Sigma Phosphatase Inhibitor Cocktail I, 1:200 Calbiochem Protease Inhibitor Cocktail Set III. This buffer was named KLISA Lysis Buffer (KLB). Cells were scraped from their wells, and rinsed with lysis buffer before being sonicated for 10 seconds. After sonication, the fragments were pelleted via centrifugation for 2 minutes at 14,000 RPM. Protein concentration was determined using the BioRad Protein Assay Kit, with the plates read by an Amersham BioTrack II plate reader.

Western Blotting

SDS-PAGE gels were run using Pierce 4-20% Precise Protein gels and TrichromeRanger Prestained Molecular Marker. Gels were run at 70 Volts for approximately 90 minutes. The proteins embedded in the SDS-PAGE gels were transferred to PVDF membranes during a 70 mA, 1.5 hour transfer. The PVDF containing the proteins were dried overnight and Western Blotting was performed the next day. Western Blotting was performed with 1:750 anti-mTOR and 1:5000 anti-rabbit IgG and Horseradish Peroxdase. Additional experiments used 1:1000 anti-HA Primary antibody and 1:5000 anti-mouse IgG. Amersham's ECL Reagents were used

to wash the PVDF's and then in a dark room, mounted to X-Ray film in a cassette. Film was developed 24 to 48 hours later.

Kinase Assay

A recipe for a 2X mTOR Kinase Assay buffer was found published by Kim *et. al.* [39]. Kim's Kinase Buffer is composed of; 50 mM Hepes-KOH (pH 7.4), 100 mM KCL, 40% glycerol, 20 mM $MgCl_2$, 8 mM $MnCl_2$, 2 mM DTT, 100 μm ATP.

Using 19 μl of 2X Kim Kinase Assay Buffer, 20 μl COS-7 cell lysate and 1 μl of either p70 S6 Kinase (T412E), or 4E-BP1, the cell lysates were tested for kinase activity. The mass spectrometer used SAX2 Protein Chips by Ciphergen. 1 μl SPA supernatanent was loaded on top of each of the samples and allowed to dry. The chips were then run in the mass spectrometer and the data analyzed for peaks indicating phosphorylated proteins.

A second, different, kinase assay used COS-7 cell lysates that were immunoprecipitated with anti-mTOR antibodies to concentrate the mTOR. This assay consisted of 140 μl cell lysate, 100 μl LB2, 8 μl HA-agarose beads were combined and incubated at 4°C in a rotator for 2 hours. After 2 hours the beads were washed with cold LiCL and NaCl and resuspended in Lysis Buffer. Kim's 2X Kinase buffer was modified to create a 4X buffer, while the glycerol concentration was reduced to 20%.

For the [^{32}P] γ–ATP kinase assay, 12.5 ml Kim's 4X buffer, 1 μci [^{32}P] γ–ATP, 23.8 μl H_20, 12.5 μl immunoprecipitated HA-agarose bead suspension, and either 1 μl S6K or 1 μl 4E-BP1 were incubated for 25 minutes at 37°C. After

incubation, the reactions were boiled for 7 minutes, with strong vortexing every 2 minutes. Fifty µl of the supernatant was loaded into the Pierce 4-20% Precise Protein gel. Gel was run at 70 V for approximately 100 minutes, or until the wavefront was run off the gel. After the proteins were transferred to a PVDF membrane, the PVDF was loaded into a film cassette with X-ray film and stored overnight at -70°C. X-Ray films were exposed for a period of 24 hours up to two weeks.

Real Time PCR

COS-7 cells were transfected with pc-DNA-myc-PLD2, and phCMV2-HAmTOR-WT plasmids under conditions described previously. Cell lysate was obtained by scraping the wells and rinsing the lysate with TBS. Using the Qiagen RNeasy Minikit, RNA was extracted from the cell lysate. The obtained RNA was subject to DNase treatment, following the protocol provided with Invitrogen's DNAase I kit. Next, an aliquot of the RNA was removed for quantification purposes. A 6.3 µl aliquot of RNA was quantified against an RNA standard using Molecular Probes Ribogreen RNA Quantitation Kit. Then an equal quantity of RNA from each sample of DNA treated RNA was then reverse transcribed to cDNA. The cDNA was then stored at -70°C.

The RT-PCR is set up such that each transfection condition is probed with each of the probes designed against mTOR, S6K, PLD1 and PLD2. A Master Mix of 25 µl Stratagene Brilliant III Supermix, 1 µl of the respective probe/primer set, 3 µl Glucuronidase housekeeping gene probe/primer set, and 16 µl H_20 was prepared for

the RT-PCR reaction. The cDNA from each condition was added and the RT-PCR reaction run per the protocol provided with the supermix.

Immunoflourescence Microscopy

COS-7 transfected cells were fixed on glass coverslips by adding 1 ml 4% paraformaldehyde to each cover slip. After a 10 minute incubation period at room temperature the paraformaldehyde was aspirated and cells permeabilized with 1 ml 0.5% Triton X-100 in PBS. Permeabilized cells were incubated on at room temperature for another 10 minutes. Cells were then blocked with 1 ml 10% fetal bovine serum in 0.1% Triton X-100 in PBS. Cells were incubated at room temperature for 4 hours. Cells were probed by adding 1 ml of 1:1000 anti-HA FITC antibody conjugate in blocking buffer solution. The 6-well plate was then covered and stored in the dark at 4°C overnight. Any excess antibody was aspirated from the coverslips, and then the coverslips were washed with 1 ml PBS. Probing with 1:1000 TRITC Phalloidin dye followed. After aspiration of anti-TRITC, 1 ml 1:2000 DAPI dye in PBS was used to stain nuclei. Coverslips were incubated at room temperature for 5 minutes in the dark. DAPI was aspirated and coverslips washed 3X with PBS. Coverslips were rinsed with ddH_20 and allowed to air dry. Coverslips were mounted, cell side down onto a glass microscope slide with a drop of Vectashield mounting media between the coverslip and slide.

An Olympus Fluoview Laser scanning confocal microscope with a 60X objective was used to view the slides. Images were captured and analyzed using MetaView v.6.0 software from Universal Imaging Co.

IV. RESULTS

Aim 1: Prepare an mTOR Expression Plasmid.

This lab has previously carried out studies using siRNA's and Real Time PCR. In her thesis, Farnaz Tabatabaian, M.S., developed a cell model of differentiated HL-60 cells and transfected them with siRNA's using an Amaxa electroporator [96]. She was able to quantitate gene expression levels of PLD1, PLD2, mTOR and S6K. Using siRNA technology, Tabatabaian sought to determine the impact of PLD gene silencing and its impact on mTOR and S6K levels. These studies provided insight into protein expression and gene regulation within several different cell lines however, they lacked investigation into mTOR and its effect on cell lines. This was largely because the lab had no way to over-express the mTOR protein kinase. The development of such a molecular tool was one of the aims of the present thesis and provides a method to specifically investigate the role mTOR plays in the cell (Figure 4).

pCMV6-XL4-mTOR

An mTOR expression plasmid construct was readily obtainable from commercial sources. For this thesis we purchased a Homo sapiens FK506 binding protein 12-rapamycin associated protein 1 (FRAP1) Human cDNA clone (also known as mTOR) from OriGene Technologies, Inc. (Rockville, MD). This plasmid was 13, 394 base pairs and contained an mTOR open reading frame of 8.7 kilobases linked to a 4.7 kilobase pCMV6-XL4 backbone (Figure 5). This plasmid was named pCMV6-XL4-mTOR. However, the backbone of the plasmid did not contain any sequences

HA-Tagged mTOR Plasmid Generation Process

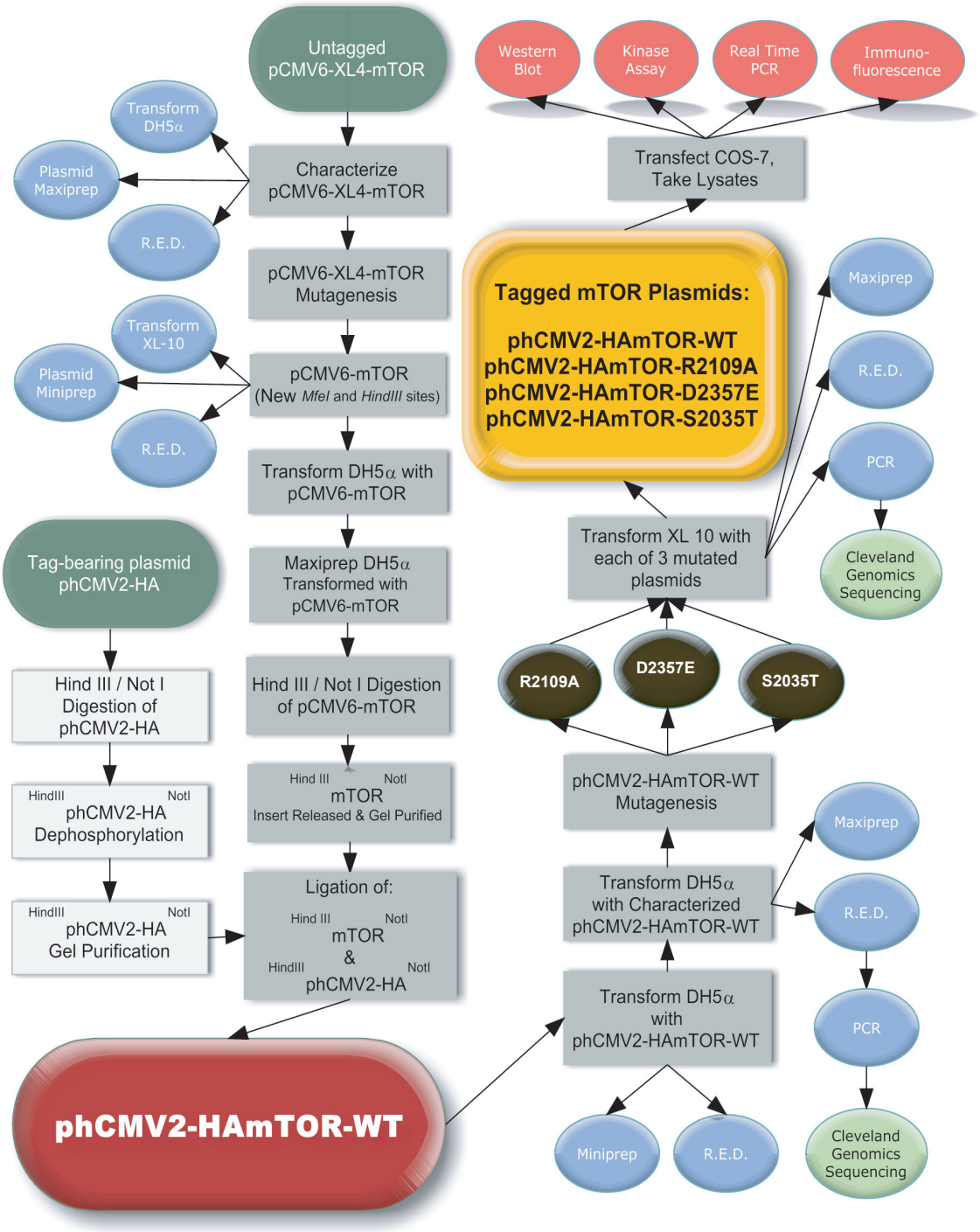

FIGURE 4:

Scheme outlining steps taken to develop an HA-tagged mTOR construct for this thesis.

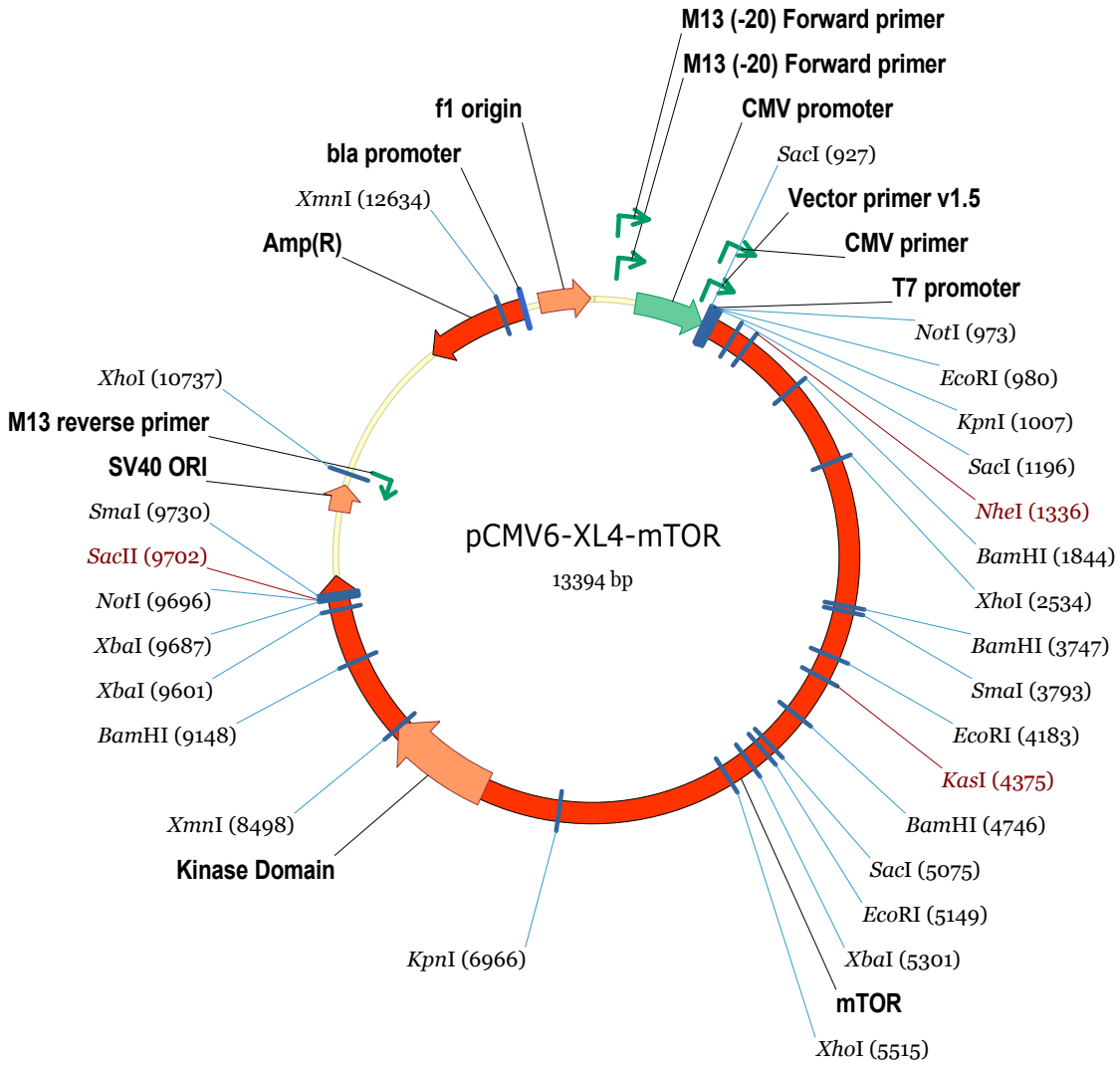

FIGURE 5:

Scheme showing a Vector Map of 13,394 bp pCMV6-XL4-mTOR.

for a tag. A tagged protein as a result of overexpression of the plasmid in mammalian cells is needed for protein detection and kinase activity studies. Thus, it was first necessary to subclone the mTOR open reading frame into a plasmid that would enable detection of the mTOR tagged protein. For this purpose, we chose the phCMV2-HA vector that bears the Hemaglutinin epitope tag or "HA tag". The mTOR insert was removed, mutated and spliced into a phCMV2-HA vector. The new vector, with the HA tag allowed for easier identification of the transfected mTOR.

To establish a baseline purity and concentration the pCMV6-XL4-mTOR was transformed into DH5α cells. The DH5α cell line is known for its high rate of transfection efficiency and high plasmid yield and therefore served as a suitable agent. Using colonies obtained from the pCMV6-XL4-mTOR transfection, cultures were inoculated for miniprep. Miniprep colonies were screened by restriction enzyme digestion for the presence of an insert of the correct length and proper restriction sites. One colony which had the indications of the proper plasmid insert was used to inoculate a culture for maxiprep. Using a plasmid prep kit, purified DNA was extracted from the cell culture. The plasmid obtained from maxiprep was quantified and qualified by a 1% agarose gel and spectrophotometry.

Restriction enzyme digestions were performed on the pCMV6-XL4-mTOR plasmid obtained from the maxiprep. Using the supplied vector map, enzymes were chosen which would cut the plasmid in pieces large enough to discern if there were any irregularities between the plasmid which was ordered and that which was

received. All gel bands that were predicted by the vector map were seen on the 1% agarose gel (Figure 6).

Mutagenesis

Mutagenic primers were designed to introduce new restriction sites into the phCMV6-XL4-mTOR plasmid (Table 1). These mutations allowed the restriction enzyme removal of the mTOR insert from this plasmid and placement into the pCMV6 plasmid containing the HA tag. Through mutation, the PCR primers added an additional *MfeI* site and an additional *HindIII* site near the promoter region of mTOR (Figure 7). These additional sites were used to identify the mutated plasmid during restriction enzyme digestions as well as allow for ligation into the new vector (Figure 8). The newly mutated plasmid was named pCMV6-mTOR.

pCMV6-mTOR

XL-10 cells from Stratagene were used when transforming the mutagenic plasmid due to their efficiency in transforming unmethylated plasmids. Next, 26 individual colonies of XL-10 cells transformed with pCMV6-mTOR were selected from the plates grown overnight (Figure 9). Colonies that showed adequate growth in liquid broth overnight were selected for miniprep. Restriction enzyme digestion performed on each of the 26 cultures to verify the *MfeI* and *HindIII* sites, indicating the presence of the mutated plasmid. Additional restriction enzyme digestions were performed with other carefully chosen pairs of enzymes on miniprep clone number

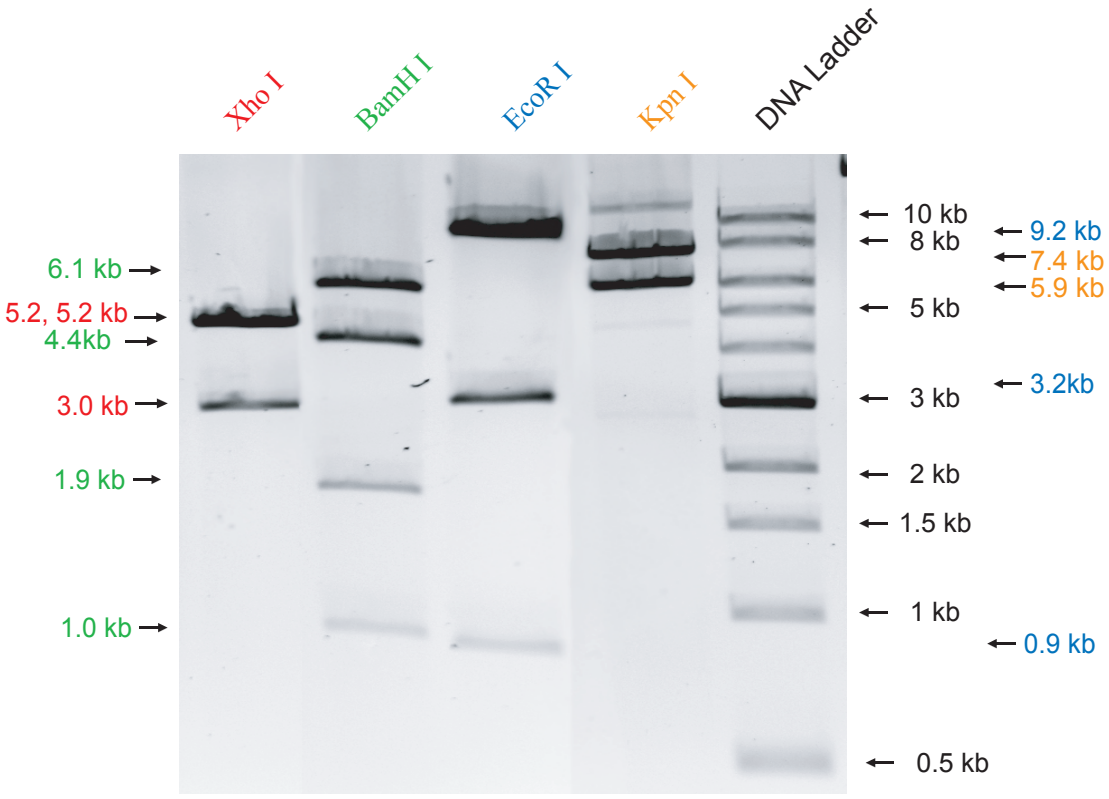

Restriction Enzyme Digestion of pCMV6-Xl4-mTOR

FIGURE 6:

Restriction enzyme digestion of pCMV6-XL4-mTOR plasmid purified by maxiprep from DH5a cells. Lane 1 shows expected banding at 5.2 (two bands), and 3.0 kb with XhoI digestion. Lane 2 is a BamHI digestion with bands at 1.0, 1.9, 4.4, and 6.1 kb. Lane 3 digestion shows expected banding at 9.2, 3.2, and 0.9 kb with EcoRI. Lane 4 is a KpnI digestion showing the expected banding at 5.9 and 7.4 kb. Lane 5 is 1 Kb DNA Ladder for reference. Each digestion revealed the expected banding indicating the DH5a cells were able to be transformed and could produce an intact, pCMV6-XL4-mTOR plasmid. The sum of the fragment lengths in each column equal the total length of the 13.3 kb pCMV6-XL4-mTOR plasmid. Digestion results were predicted using NEBcutter V2.0 software avaliable at www.neb.com, and the vector map provided by the manufacturer of the plasmid.

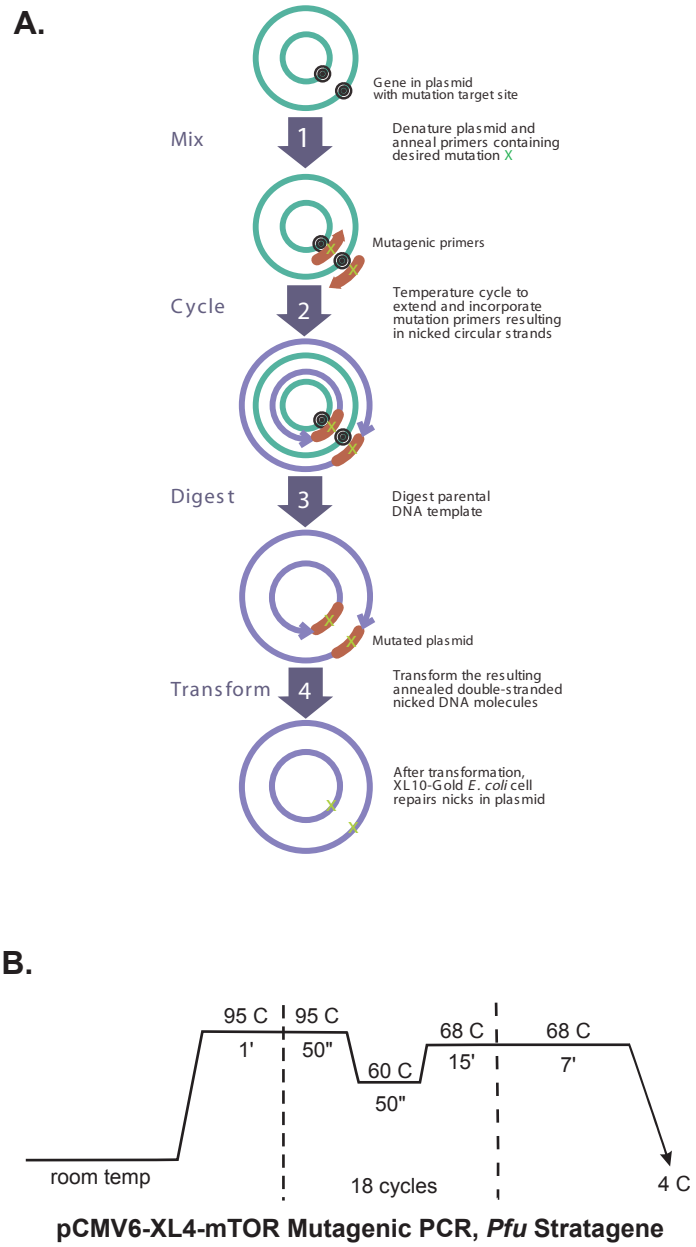

FIGURE 7:

A. Scheme outlining 1-Day Mutagenesis method used to mutaganize pCMV6-XL4-mTOR to pCMV6-mTOR.

B. PCR map outlining Mutagenic PCR reaction used in mutagenesis of pCMV6-XL4-mTOR to pCMV6-mTOR.

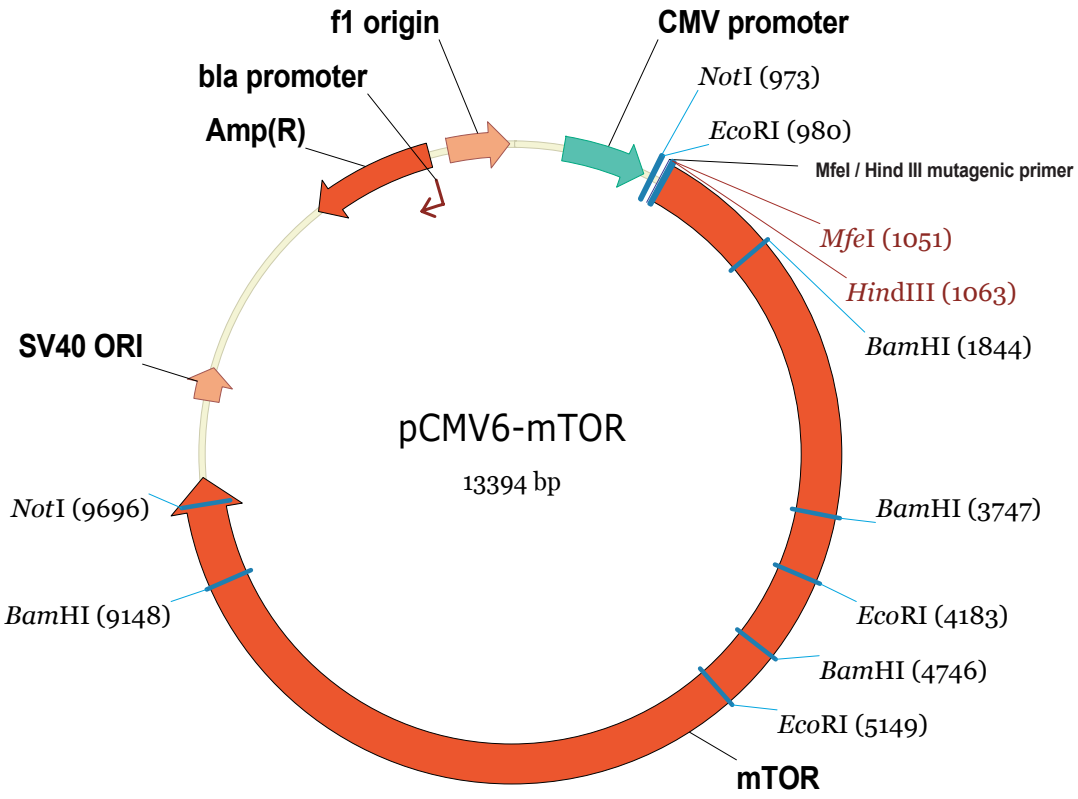

FIGURE 8:

Scheme showing a Vector Map of 13,394 bp pCMV6-mTOR.

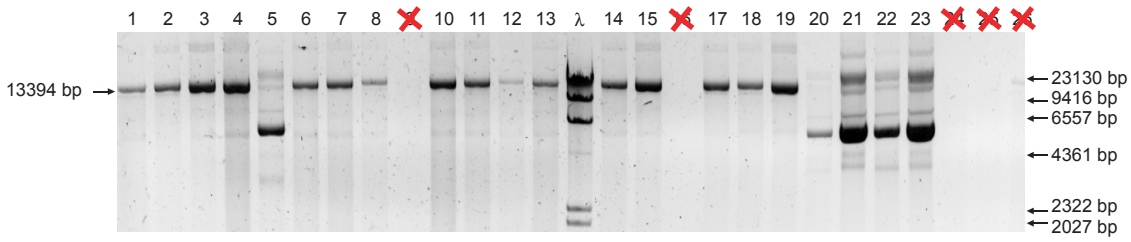

Restriction Enzyme Digestion

FIGURE 9:

Twenty six colonies of pCMV6-mTOR transformed XL-10 cells were selected for miniprep. Purified DNA was run on a 1% agarose gel to screen for colonies containing a 13.4 kb plasmid. These colonies will be subject to a restriction digest to screen for the proper *HindIII* mutation. Colonies 9, 16, 24, 25 and, 26 had no plasmid DNA and were excluded from the restriction enzyme digestion. Colonies 5, 20, 21, 22 and 23 were suspected to contain a pCMV6-mTOR fragment but would be included in the restriction digestions because they contain at least some plasmid DNA.

three to verify sequences of proper length (Figure 10). This step will prevent using a plasmid that has an unsuspected deletion.

Using the pCMV6-mTOR plasmid from the miniprep of clone number 3, DH5α cells were transformed. A robust colony of DH5α cells was again selected and a maxiprep was performed to obtain a large quantity of pure pCMV6-mTOR. After maxiprep, the plasmid concentration and integrity of the pCMV6-mTOR plasmid were verified. A 1% agarose gel revealed a distinct band at approximately 13 kb indicating the presence of proper length DNA (Figure 11). The spectrophotometer confirmed the DNA concentration estimate made from the gel, of 300 ng/μl and a DNA purity of 1.994 ($A_{260/280}$).

The mTOR insert was next removed from pCMV6-mTOR and purified to be used in ligation. This was accomplished through a *HindIII*/*NotI* double enzyme digestion of pCMV6-mTOR. The addition of the Hind III site in the promoter region of the mTOR insert and the presence of a *NotI* site allowed removal of the mTOR insert from the pCMV6 backbone with a simple double digestion. All restriction sites were mapped using Invitrogen's Vector NTI software. The resulting 8633 bp ^{HindIII}mTOR^{NotI} fragment was visualized on a 1% agarose gel (Figure 12).

Ligation of $^{Hind\ III}$phCMV2-HA$^{Not\ I}$ and $^{Hind\ III}$mTOR$^{Not\ I}$

The phCMV2-HA vector with mTOR ligated into allowed for easier tracking of transfected mTOR for both immunoprecipitation and western blotting because of the HA tag present in the vector. This lab has used the phCMV2-HA vector extensively and has had much success with it.

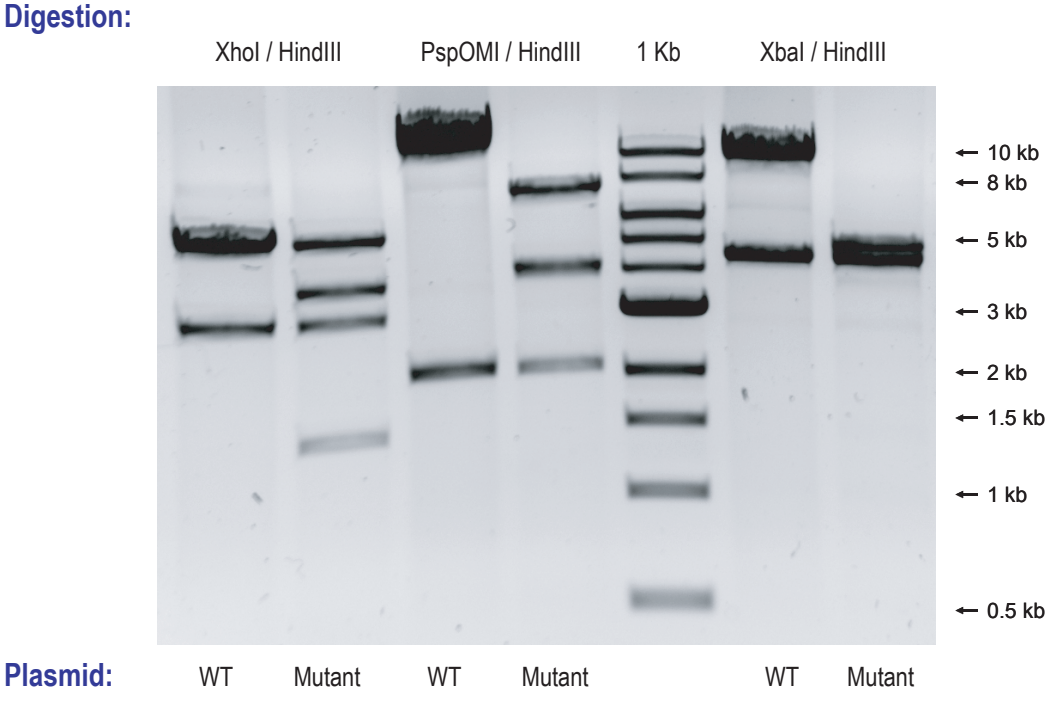

FIGURE 10:

Restriction enzyme digestion of pCMV6-XL4-mTOR and pCMV6-mTOR. The pCMV6-XL4-mTOR was mutated by the addition of a *HindIII* restriction site to give the pCMV6-mTOR plasmid. Each pCMV6-XL4-mTOR plasmid is digested with the noted enzymes and run next to the mutated pCMV6-mTOR plasmid digested with the same enzymes. *XhoI/HindIII* double digestion of pCMV6-XL4-mTOR gives the expected bands at 5.2, 5.2 and 3.0 kb while digestion with the mutant pCMV6-mTOR gives 5.2, 3.7, 3.0 and 1.5 kb bands. The *PspOMI/HindIII* digestion of the pCMV6-XL4-mTOR plasmid gives the expected bands at 11.1, 2.0, and 0.2 kb. With the addition of the *HindIII* site in the mutant plasmid, the bands as expected are 7.2, 3.9, 2.1, and 0.2 kb. *XbaI/HindIII* double digestion also reveals the presence of the additional *HindIII* site in the mutant as the W.T. bands are 9.0, 4.3, and 0.1 kb while the mutant has bands at 4.7, 4.3, 4.3, 0.1 kb.

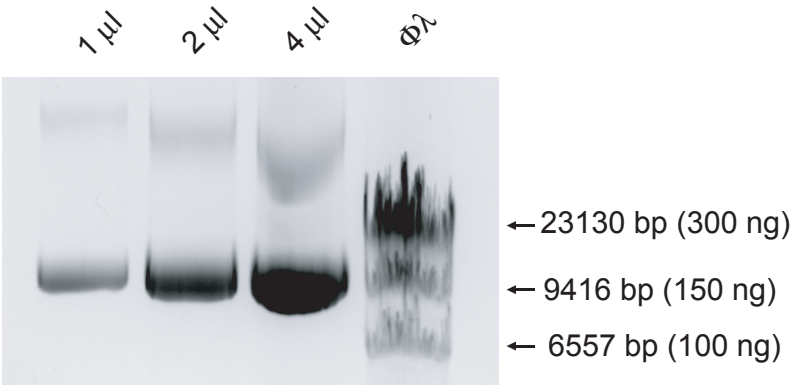

Verification of Plasmid Integrity

FIGURE 11:

Verification of pCMV6-mTOR plasmid maxiprep integrity. DH5α cells were transformed with pCMV6-mTOR and a maxiprep was performed. Concentration of pCMV6-mTOR purified plasmid was estimated at 300 ng/µl using λ DNA as a reference. Each lane contains the indicated amount of purified plasmid. For confirmation the plasmid prep (1:10 dillution) was also quantitated by spectrophotometry at O.D. 260/280:

Concentration = 323 ng/µl

DNA Purity ($A_{260/280}$) = 1.994

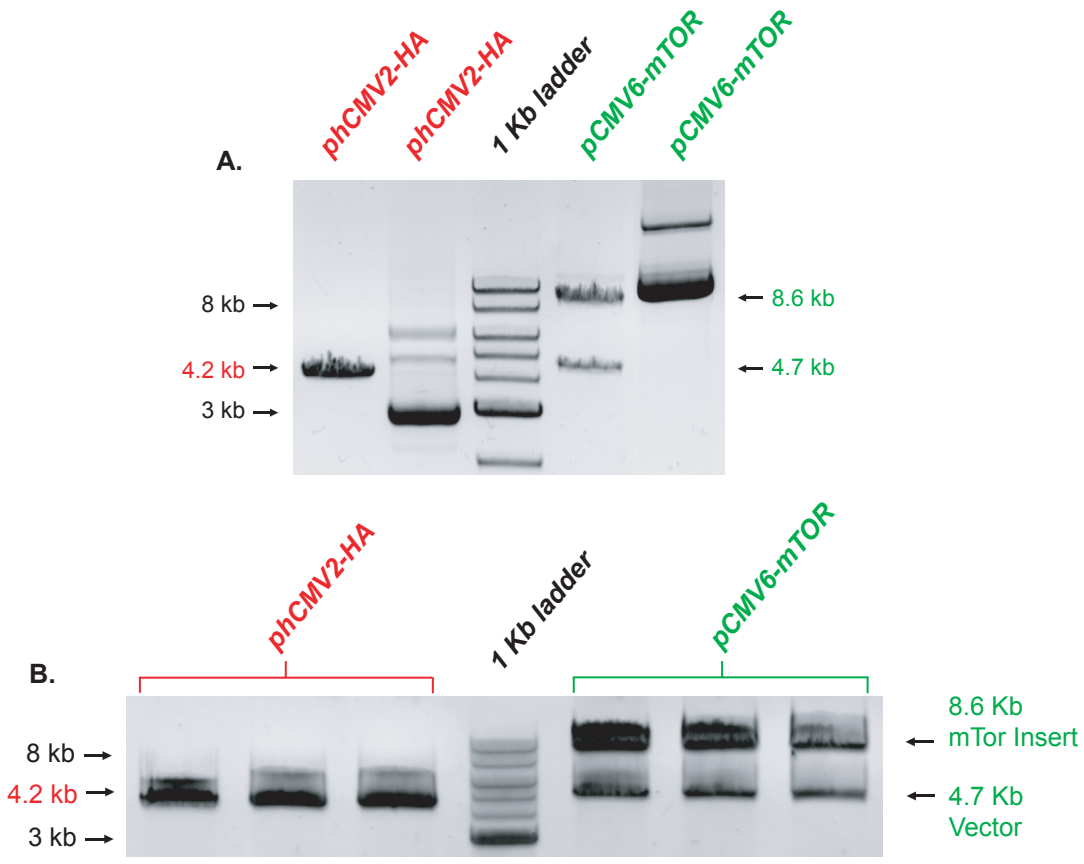

FIGURE 12:

A. Restriction enzyme digestion of mutated plasmid, pCMV6-mTOR and HA-tagged vector. phCMV2-HA vector digested with *HindIII* and *NotI* gave a 4.2 kb band on the gel. These restriction sites are within 60 base pairs of one another resulting a 4.2 kb band and a small band that was run off the gel. The *HindIII* and *NotI* digestion of pCMV6-mTOR gives the mTOR band at 8.6 kb and the pCMV6 vector band at 4.7 kb. Both undigested plasmids also show the relaxed, coiled and supercoiled states.

B. After dephosphorylation of phCMV2-HA vector, gel purfication was performed on pCMV6-mTOR and phCMV2-HA, both double digested with *HindIII* and *NotI*. The double digestion created complementary sticky ends on both the vector and insert, facilitating their ligation. The 4.7 phCMV6 vector was discarded, while the 8.6 mTOR insert and the 4.2 kb phCMV2-HA vector were collected from the gel.

The phCMV2-HA vector was digested with *HindIII* and *NotI*, sites which were conveniently present in the vector (Figure 12). The resulting digested vector was then dephosphorylated to prevent reannealing of the vector onto itself, reducing the possibility of a looped section of plasmid DNA. After dephosphorylation, the 4.2 kb ^{HindIII}phCMV2-HA^{NotI} vector was agarose gel purified alongside the 8633 bp ^{HindIII}mTOR^{NotI} insert. The phCMV2-HA vector and mTOR inserts were excised from the gel, and after concentration determination, could be ligated because of complementary sticky ends.

Next, the dephosphorylated $^{Hind\ III}$phCMV2-HA$^{Not\ I}$ vector was combined with a 3-fold molar excess of purified $^{Hind\ III}$mTOR$^{Not\ I}$ insert. The newly formed plasmid, named phCMV2-HAmTOR-WT contained a Kanamycin resistant gene which was used in colony selection and a HA tag which allowed for the tracking of transfected mTOR (Figure 13). Transformation into DH5α cells immediately followed the ligation procedure.

Characterization of the phCMV2-HAmTOR-WT Plasmid

Nine robust colonies of DH5α cells transformed with the ligation reaction were selected from solid media for miniprep. A miniprep was performed and a 1% agarose gel confirmed the presence or absence of the undigested plasmid. Colonies which contained any amount of plasmid were subjected to a double enzyme digestion to determine the presence of a proper length fragment and the correct orientation of the mTOR insert into the vector (Figure 14). The phCMV2-HAmTOR-WT double digestion with *HindIII* and *EcoRV* yields bands of 11.3 kb and 1.5 kb in a properly

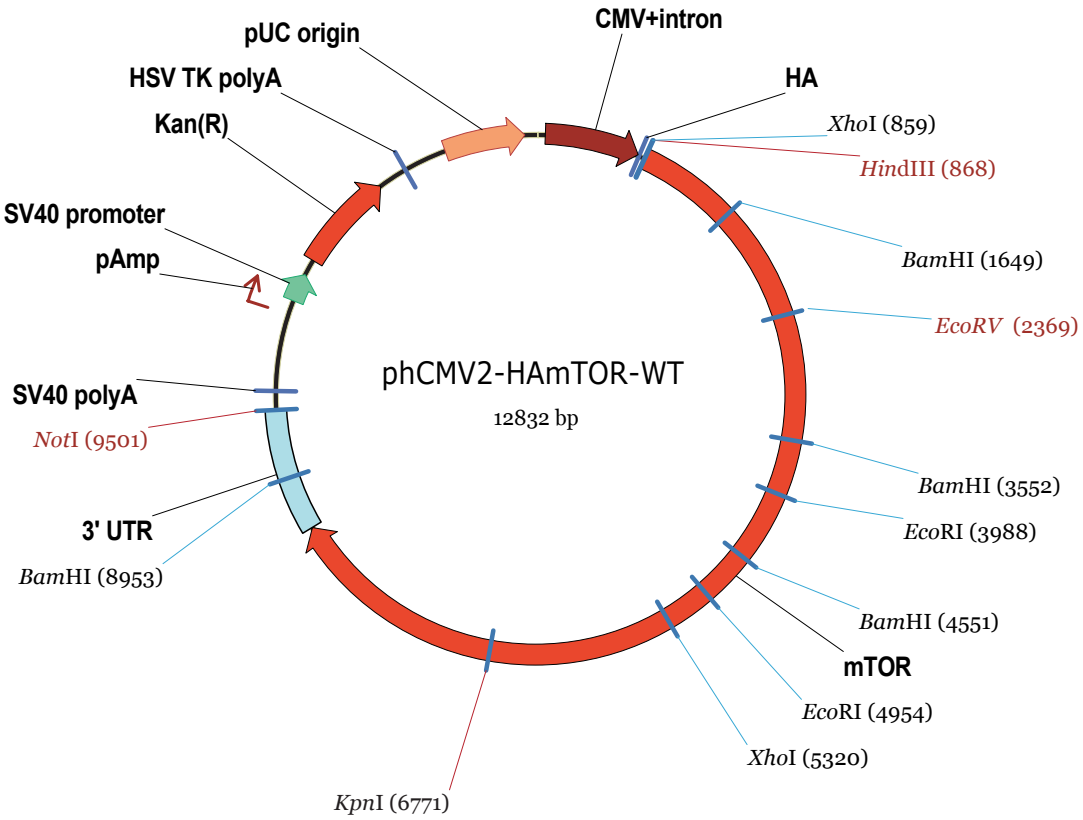

FIGURE 13:

Scheme showing vector map of phCMV2-HAmTOR-WT designed using Vector NTI software.

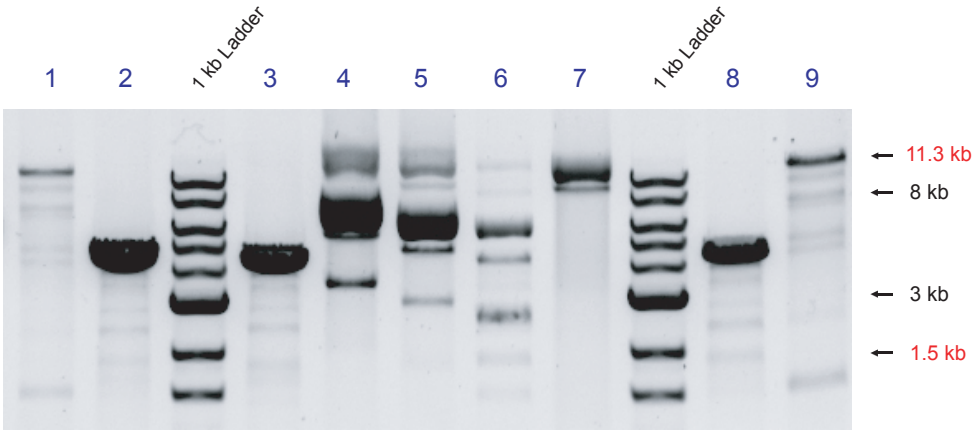

FIGURE 14:

Double Restriction enzyme digestion of nine colonies of DH5α cells transformed with phCMV2-HAmTOR-WT. Enzymes *HindIII* and *EcoRV* were chosen for the double digestion because *HindIII* is present only in the properly mutated mTOR insert. The *EcoRV* restriction site serves as a way to check the orientation of the insert into the vector. A 1.5 kb band along with an 11.3 kb band indicated a proper length, properly oriented plasmid. Therefore, colonies 1 and 9, which have the expected bands at 11.3 and 1.5 kb, were presumed to contain ligated plasmid and were further examined. Colonies 2, 3 and, 8 were only linearized, indicating they did not contain one of the restriction sites. The remaining colonies have other unexpected bands, indicating the ligation was not successful in those colonies. All colonies except number 1 and 9 were discarded.

oriented phCMV2-HAmTOR-WT plasmid. Only colonies one and nine contained the proper bands on the gel and colonies with bands of any other length were discarded.

Purified phCMV2-HAmTOR-WT plasmid from colony nine was selected to transform DH5α cells. It was determined by the gel that this colony contained a proper length and properly oriented plasmid. This colony also had a higher concentration of plasmid than colony number one, the only other colony which had a properly oriented and proper length plasmid. This additional transformation step provides extra assurance that the final plasmid is produced exactly as expected. A maxiprep was performed on the transformed DH5α cells and purified phCMV2-HAmTOR-WT was obtained. Concentration and purity were determined with a spectrophotometer as well as on a 1% agarose gel. (Figure 15). DNA concentration was determined to be 400 ng/µl and DNA purity 1.8 ($A_{260/280}$). Again, restriction enzyme digestions were performed to confirm the presence of a proper length plasmid. Digestions with *XmnI*, *BspEI*, *BamHI*, *EcoRI/NotI*, *HindIII/KpnI* and *Fsp/MfeI* were performed, each reaction verifying the phCMV2-HAmTOR-WT plasmid (Figure 16).

To further increase the assurance that the generated plasmid is what was desired, PCR primers were designed against phCMV2-HAmTOR-WT. Two sets of PCR primers, each targeting a mutation site of the phCMV2-HAmTOR-WT plasmid were designed online at www.idtdna.com. The lyophilized powder primers were purchased from Integrated DNA Technologies, Incorporated (Table 3). After PCR the DNA fragments were run on a 2% agarose gel to confirm purity and proper length. The remaining volume of PCR mixture was purified and sent for sequencing.

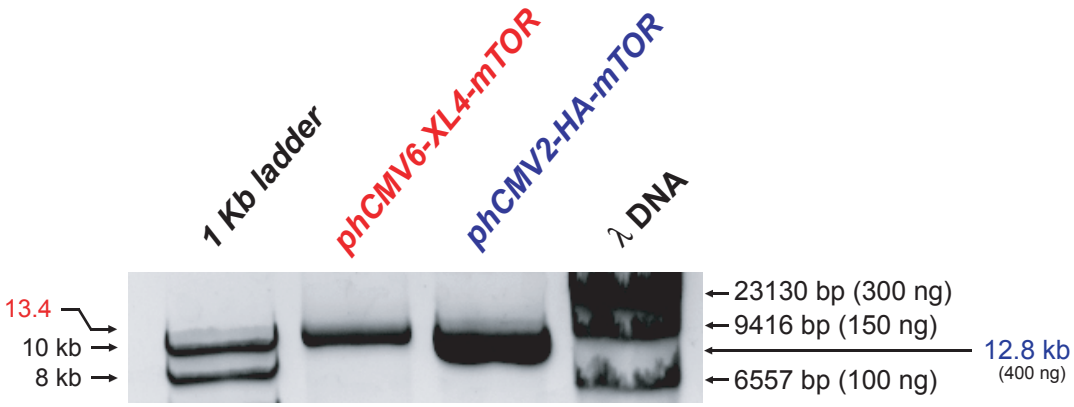

FIGURE 15:

An agarose gel was used to check the concentration of the 12.8 kb phCMV2-HAmTOR-WT plasmid after maxiprep. The 13.4 kb phCMV6-XL4-mTOR was run as a reference, its concentration was previously established at 150 ng/μl. phCMV2-HAmTOR-WT concentration was estimated at 400 ng/μl. This estimate was verified by spectrophotometry. Purity was 1.8 ($A_{260/280}$).

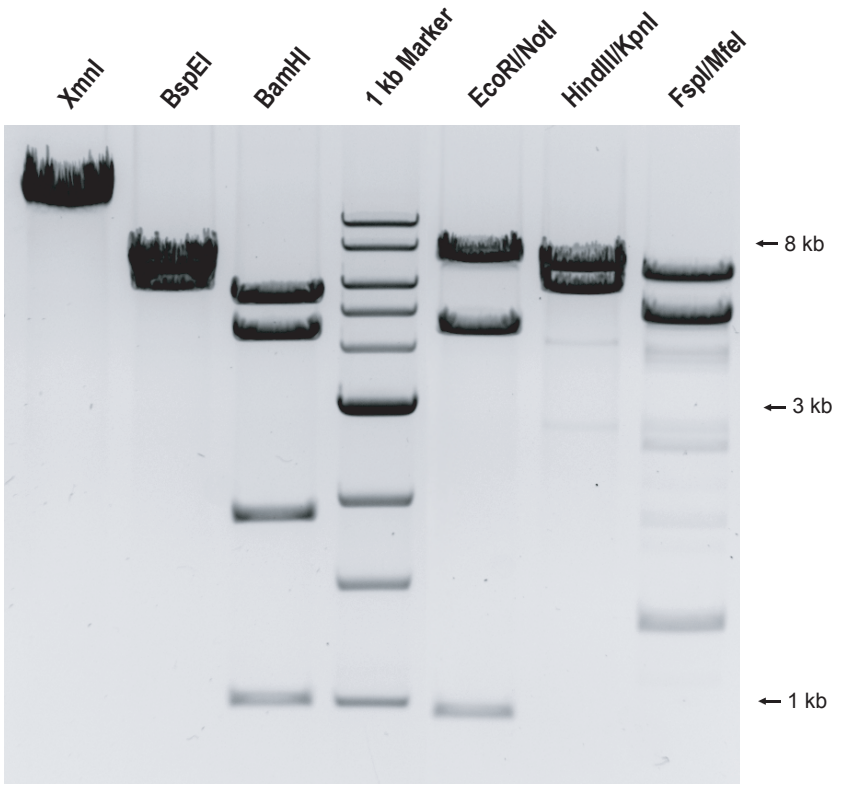

Restriction Enzyme Digestion

FIGURE 16:

Restriction enzyme digestions of phCMV2-HAmTOR-WT. Digestions confirmed the proper orientation and size of plasmid. *XmnI* cuts the plasmid only once and results in a linearized band at 12.8 kb. *BspEI* cuts the plasmid at two sites and results in 6.0 and 6.8 kb bands. *BamHI* digestion results in 4 cuts with bands at 5.5, 4.4, 1.9 and 1.0 kb. The double digestion of *EcoRI* and *NotI* results in three bands at 7.3, 4.5 and 1.0 kb. The double digestion of *HindIII* and *KpnI* result in two bands, found at 6.9 and 5.9 kb. *FspI* and *MfeI* double digestion result in 3 bands, found at 6.5, 4.9 and 1.3 kb. The faint banding seen in the *FspI/MfeI* lane is likely undigested plasmid as a result of incomplete digestion in that reaction. Each of the digestions confirms the presence of the phCMV2-HAmTOR-WT plasmid in proper orientation and proper length.

Concentration was estimated and the PCR reactions were sent to Cleveland Genomics for sequencing. Sequencing confirmed the presence of the point mutations and thus the successful generation of the HA-tagged mTOR construct, phCMV2-HAmTOR-WT.

Aim 2: Generate Mutated mTOR Plasmids by Site Directed Mutagenesis

The newly generated phCMV2-HAmTOR-WT was further mutated to provide additional valuable molecular tools for the laboratory. Using the same mutagenic procedures as described in the methods section, point mutations added additional restriction sites to the phCMV2-HAmTOR-WT construct and gave it different characteristics.

Previously Jie Chen's lab described a kinase dead mutant produced by mutating the Aspartic Acid (D) at position 2357 to a Glutamic acid (E)[28]. This mutant gained an additional *EcoRI* site at that location, and was named phCMV2-HAmTOR-D2357E (Table 4). When analyzed on a gel, a restriction enzyme digestion of phCMV2-HAmTOR-D2357E with *EcoRI* would have 3 bands: 8.9, 3.0 and, 1.0 kb. Using New England Biolabs' NebCutter, at www.neb.com, only 2 bands at 11.9 and 1.0 kb would be seen with a similar digestion of phCMV2-HAmTOR-WT.

In 2001 Chen's lab described a different mTOR mutant, this time a PA deficient mutant that had its 2109 position Arginine mutated to an Alanine[65]. This mutant gained an *NruI* restriction site and was named phCMV2-HAmTOR-R2109A.

Plasmid	phCMV2-HAmTOR-WT	phCMV2-HAmTOR-D2357E	phCMV2-HAmTOR-R2109A	phCMV2-HAmTOR-S2035T
Mutation Present	None	Kinase Dead	PA deficient	Rapamycin Resistant
Restriction Site Added	N/A	*EcoRI*	*NruI*	*Afl3*
A.A. prior to mutation	N/A	Aspartic Acid	Arganine	Serine
A.A. after mutation	N/A	Glutamic Acid	Alanine	Threonine
Mutation Position	N/A	2357	2109	2035
Stock Concentration	400 ng/µl	250 ng/µl	200 ng/µl	300 ng/µl
Purity (260/280)	1.8	1.83	1.81	1.69

TABLE 4:

Table indicates the mutations present in the three HAmTOR construct mutants. Also indicates the sites added, the amino acid that was present prior to and after mutation, the mutation position and the stock concentration and purity of the construct. For the purposes of this table, the phCMV2-HAmTOR-WT is considered the parental plasmid, and therefore no mutations are listed.

The parental phCMV2-HAmTOR-WT plasmid construct does not contain an *NruI* restriction site, therefore a restriction digestion of phCMV2-HAmTOR-WT with *NruI* results in a linearized plasmid(Table 4).

The earliest described mTOR mutant came from Brown *et. al*., where the authors described the mutation of Serine at 2035 to a Threonine, creating a rapamycin resistant mutant[37]. This mutant gained an additional *AflIII* restriction site and was named phCMV2-HAmTOR-S2035T (Table 4). The phCMV2-HAmTOR-WT construct contains only three *AflIII* sites, and were seen at 6.0, 5.9 kb and, 882 bp. The phCMV2-HAmTOR-S2035T construct contains four sites which give observed bands at 6.0, 5.8, 1.0 kb and, 112 bp.

The well planned mutation of these plasmids with the addition of a new restriction site provided the advantage of being able to easily identify the mutants. A simple restriction enzyme digestion was all that was necessary to confirm that the successful mutation. However, the mutants were subject to PCR to ensure the integrity of the plasmid.

The three mutants described were prepared and sequenced in a fashion similar to the methods used to prepare the phCMV2-HAmTOR-WT plasmid. Using phCMV2-HAmTOR-WT as the parental plasmid, PCR primers were carefully designed at www.idtdna.com to direct point mutations at the chosen sites (Table 2). These three separate point mutations conferred the desired additional restriction sites into the DNA. The mutagenesis reactions were then used to transform XL-10 cells, and those colonies provided the material for a miniprep analysis. After minipreps of

the three mutant plasmids, restriction enzyme digestions were designed to test for the presence of the new restriction sites, indicating a successful mutagenesis (Figure 17).

The mutant plasmids were also subject to PCR and sequencing at Cleveland Genomics. Cleveland Genomics sequencing revealed the successful point mutations of each of the plasmids, without any unexpected mutations in the DNA. With the sequence of each of the three mutated plasmids confirmed, and after positively identifying the additional restriction sites on the restriction enzyme digestion gel we were able to conclude with certainty that our plasmids could be produced as planned.

Aim 3: Detect Protein Expression of Plasmids by Western Blotting; Probed with Anti-HA and Anti-mTOR.

COS-7 cells were used for protein expression experiments because they are capable of expressing large quantities of protein and are easily cultured, even in sub-optimal conditions. The COS-7 cell line is from African green monkey kidney cells, and have a fibroblast morphology. They are adherent to glass and plastic and retain complete permissiveness for lytic growth of the SV40 viral DNA, a circular DNA virus of Rhesus Monkey origin. Each of the 4 plasmids generated in this thesis contain SV40.

COS-7 cells were cultured in T-75 flasks and maintained in 90% DMEM, 10% FBS. For transfection, the cells were split into 6-well plates (Figure 18). Multiple products are available commercially for the transfection of adherent cells including: lipofectin, lipofectamine 2000, Superfect, FuGENE HD and

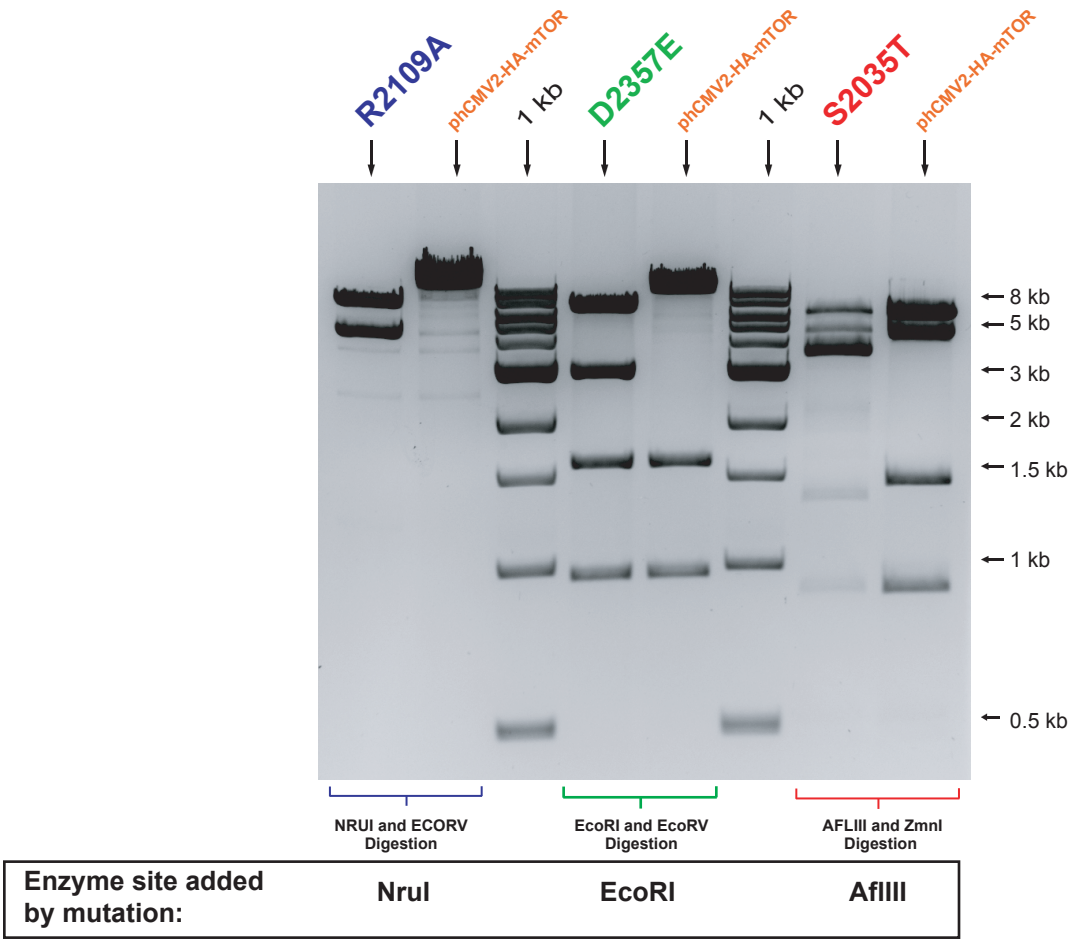

FIGURE 17:

The digestion of the phCMV2-HAmTOR-R2109A construct, with its additional *NruI* restriction site gives two bands, 8.0, 4.8 kb as opposed to the WT plasmid which is linearized (12.8 kb) by the single cut of the *EcorV* enzyme. The digestion of the phCMV2-HA-mTOR-D2357E construct shows the addition of an *EcoRI* site by the presence of the expected four band pattern shown: 7.2, 2.9, 1.6 and, 0.9 kb. The phCMV2-HAmTOR-WT plasmid was cut only three times, giving expected banding pattern of 10.2, 1.6 and, 0.9 kb. The digestion of the phCMV2-HA-mTOR-S2035T plasmid gives the banding pattern 6.0, 4.5, 1.3, 0.9 and, 0.1 kb due to the presence of an additional *AflIII* site. The 113 bp band was run off the gel, but it is clear that the additional *AflIII* site is present due to the change from the phCMV2-HAmTOR-WT band of 1.4 kb to the mutant phCMV2-HAmTOR-S205T which shows a 1.3 kb band. The phCMV2-HAmTOR-WT plasmid banding shows the expected pattern of 6.0, 4.4, 1.4 and, 0.9. All banding patterns were predicted with NEBcutter 2.0 at www.neb.com.

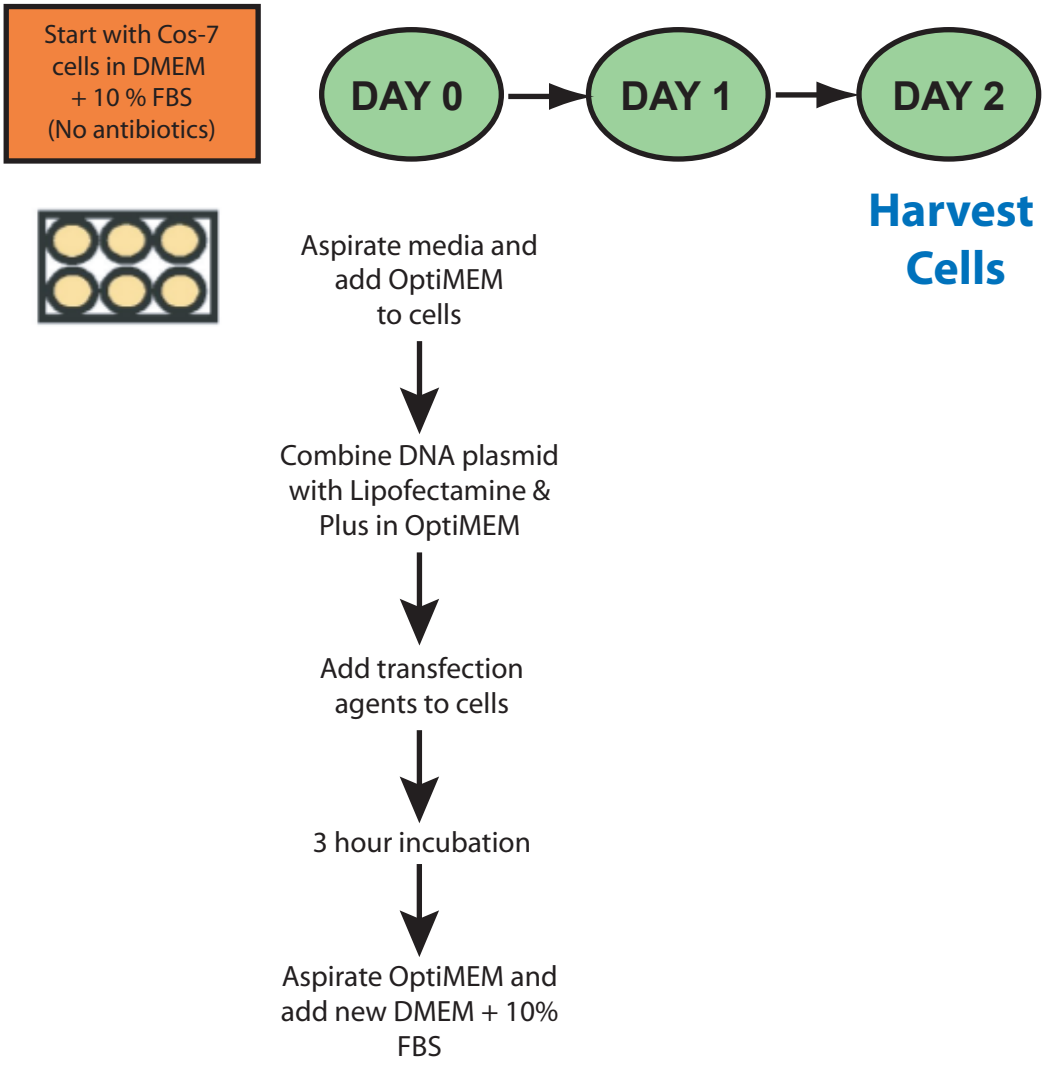

FIGURE 18:

Scheme outlining protocol for transfecting COS-7 cells using Lipofectamine and PLUS reagents to allow for the overexpression of HA-tagged mTOR.

Lipofectamine-Plus combination. The combination of Lipofectamine and Plus was chosen because the lab had previous success with those agents.

Dose response experiments were carried out to establish the amount of each plasmid that was required for an effective transfection of the COS-7 cells. For these experiments each of the four plasmids were transfected in different plates. The phCMV2-HAmTOR-WT plate had wells with increasing amounts of plasmid as follows: 0.0, 0.5, 1.0, 1.5, 2.0 and, 3.0 μg. Each of the mutant plasmids were also transfected in their own plate with an increasing amount of plasmid identical to the phCMV2-HAmTOR-WT plate. The transfection reactions were allowed to precede for three hours after which time the cells were washed and incubated for another 48 hours in DMEM + 10% FBS media. Cell lysates were harvested using lysis buffer described in methods and a cell scraper to remove the adherent cells from the plastic culture wells.

Additionally, time course experiments were performed to determine the optimal time for harvest of transfected COS-7 cells (Figure 19). Transfections were performed with the phCMV2-HAmTOR-WT plasmid and compared with mock transfections. Lysates were harvested at 0 hours (immediately after 3 hour transfection incubation), 15, 24, 48 and 72 hours. The lysates obtained after a 72 hour incubation had the highest concentration of total protein. An increase in total protein has been interpreted as an indicator of cell growth. While these two can not be absolutely conclusively linked, thymidine experiments in our lab have given evidence to conclude an increase in protein concentration is linked to cell growth.

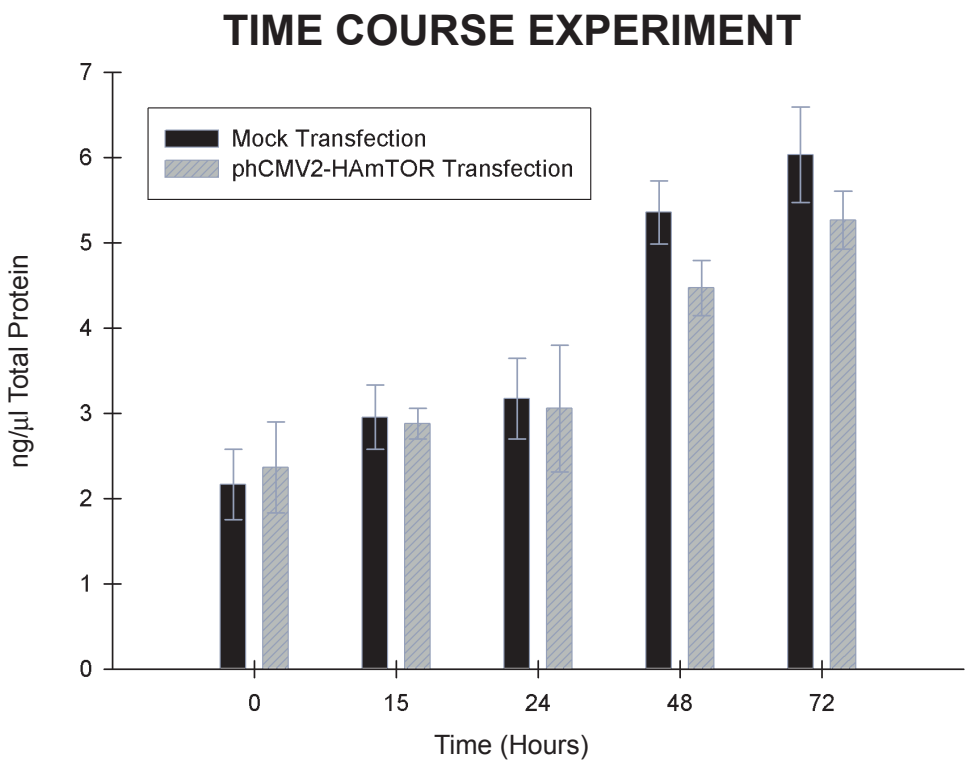

FIGURE 19:

COS-7 cells were transfected with either phCMV2-HAmTOR-WT or subject to a mock transfection. The cell lysates were then harvested at 0, 15, 24, 48 or, 72 hours. The zero hour lysate was taken immediately after the 3 hour transfection incubation. The black bars represent a mock transfection, the gray bars represent transfection with the phCMV2-HAmTOR-WT plasmid DNA. An increase in total protein has been interpreted as an indicator of cell growth. This interpretation has been verified in our laboratory through thymidine incorporation experiments. Cell lysates taken at 72 hours had a moderate percentage of dead cells, and a noted morphology change. Cell viability studies conducted by our lab have routinely shown a rapid decrease in cell viability 48 hours post-transfection. For this reason, lysates for this thesis were taken at 48 hours post transfection.

There was a higher cell death rate in the cultures allowed to incubate for 72 hours. Also, by 72 hours post transfection there was a noted morphology change in some of the cells in the culture. As a result, we determined that by 48 hours the cells had produced an adequate amount of protein for our experiments and had a consistent morphology.

Protein concentration determination was carried out using a commercially available protein assay solution. This concentration determination provided the necessary information to normalize the samples for SDS PAGE and Western Blot. After the samples were normalized to a standard quantity of protein, SDS-PAGE gels were run. The embedded proteins were transferred to a PVDF membrane and a Western blot was performed (Figure 20). Western blots consistently showed transfection with 2 μg of plasmid as optimal for maximum protein expression (Figure 21). Using 2 μg of plasmid DNA resulted in a four fold increase in protein expression over mock transfections.

AIM 4: Determine Enzyme Activity of Overexpression Plasmids using KLISA, Mass Spectrometry, or [^{32}P] γ-ATP to detect phosphorylation of mTOR substrates.

We used a commercially available mTOR kinase assay to determine kinase activity of the overexpressed HA-mTOR (Figure 22). While there are a small number of articles which report some data while using a commercially available kit, this lab enjoyed little success with the product. Various experimental conditions were used, and various data interpretation techniques were employed in an effort to elucidate

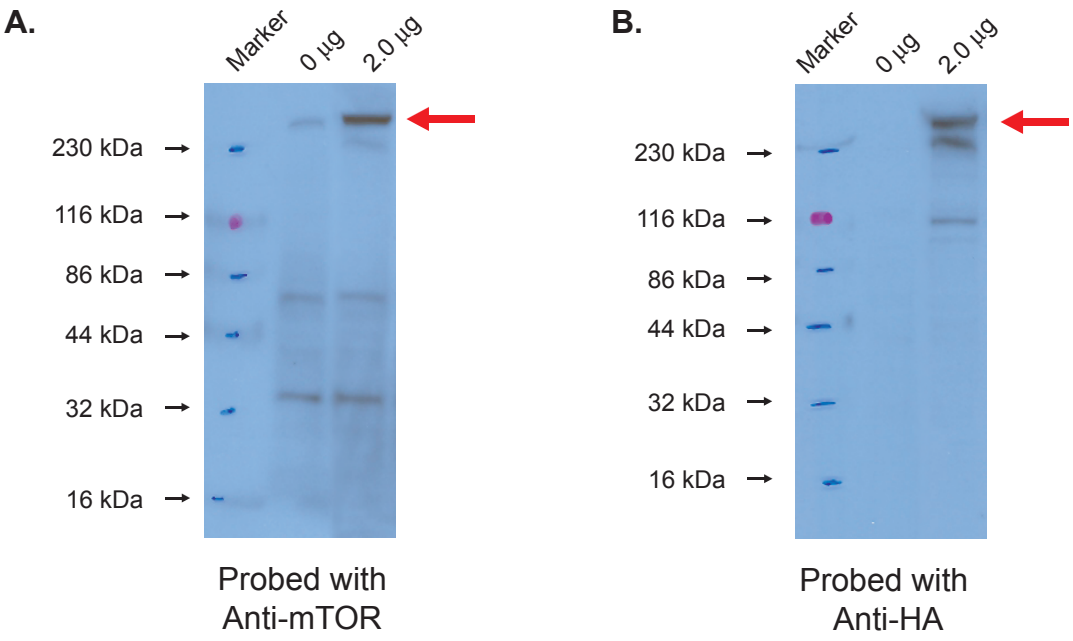

FIGURE 20:

A. Western Blots were probed with anti-mTOR and developed on X-ray film using the Kodak ECL method. This experiment used cell lysates transfected with 2 µg of phCMV2-HAmTOR-D2357E plasmid DNA or a mock transfection. Sonicates were taken and 600 ng total protein was loaded into each lane of the gel. The PVDF was probed with the primary antibody Anti-HA and the secondary antibody, Anti-mouse. In the mock transfection lane, a faint band representing endogenous mTOR can be observed at 289 kDa, noted by the red arrow. The endogenous and exogenous mTOR is represented by the darker band at 289 kDa in the lane with lysate from cells transfected with phCMV2-HAmTOR-D2357E.

B. Probing the blots with Anti-HA, we were able to visualize the exogenous mTOR only. Thus in the mock transfected lane, there was no band because there was not any HA tag in that lysate. In the 2 µg transfected lane, the band representing the transfected HA-mTOR can be visualized, again noted by the red arrow. In subsequent experiments the Anti-HA probe was used in order to detect only exogenous mTOR.

Western Blots Probed with Anti-HA

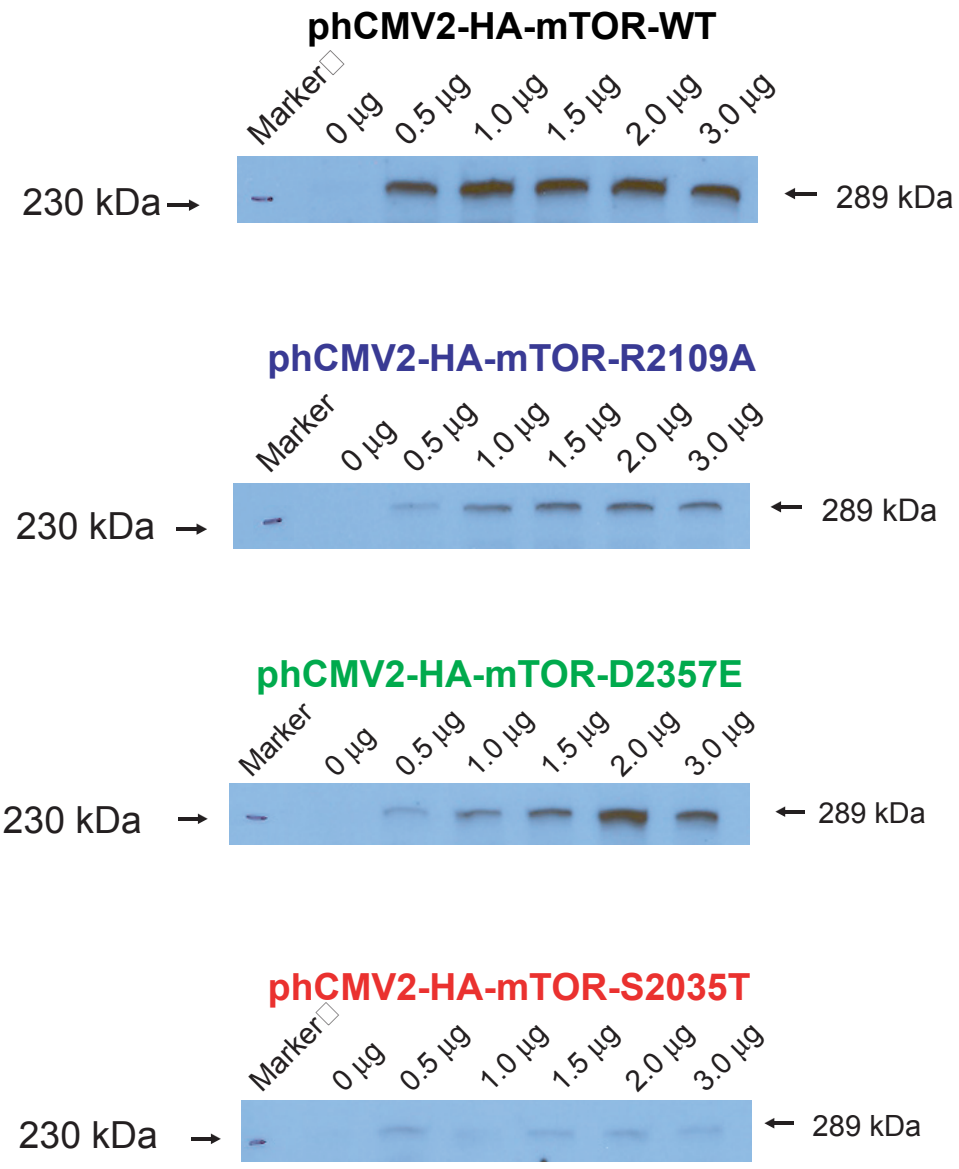

FIGURE 21:

Lysates were used for Western Blot analysis to determine protein expression of each of the constructs. The films above depict the transfection of the noted amount and type of plasmid DNA. The gels were probed with Anti-HA and Anti-mouse HRP. The indicated 289 kDa band represents the HAmTOR present in each condition.

mTOR ELISA Based Assay

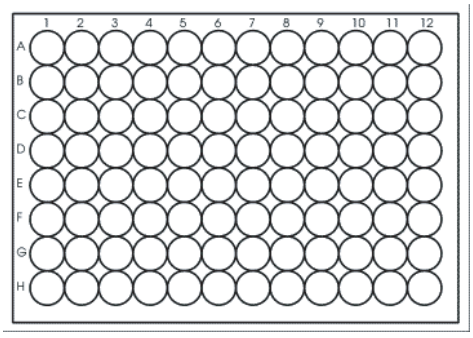

Glutathione-Coated 96 well plate

1. Obtained COS-7 Lysates

2. Supplied mTOR substrate binds to solid support of Glutathione-coated 96 well plate

3. Incubated 50 ml mTOR lysate with 50 ml supplied Kinase Assay buffer and ATP in 96 well plate

4. Active mTOR was phosphorylated p70S6K at Thr389

5. Phosphorylated substrate was detected with Anti-p70S6K-T389 antibody followed by HRP-Antibody Conjugate and TMB substrate

6. Absorbance was read at 450 nm in Biotrak II Visable Plate Reader

FIGURE 22:

The commercially available mTOR activity Kit is an enzyme linked Immunosorbent assay (ELISA). It relies on the phosphorylation of p70S6K-GST fusion protein as its indicator of mTOR activity. The phosphorylation is detected by Anti-p70S6K-T389 antibody followed by detection with HRP-antibody conjugate and TMB substrate. The relative activity of the mTOR was determined by the absorbance at 450 nm as determined by a Biotrak II Visable Plate Reader. The manufacturer's protocol was followed for all steps of the assay.

reproducible data while using the kit. A calibration was performed using the supplied mTOR standard and different types of water to ensure the pH of the samples did not effect the kit (Figure 23). Calibrations revealed data that modeled the manufacturers standard curves, but with absorbance values that trended much lower than the manufacturers data.

The data we obtained with the KLISA mTOR kit revealed a 2.6 fold increase in mTOR activity of the 1 μg W.T. plasmid transfected cells over mock transfections. Transfections with 2 μg of the W.T. plasmid revealed a five fold increase in mTOR activity. However this data was not reliably reproducible and measured absorbances often varied widely (Figure 24).

A literature review was conducted and revealed that other labs previously had difficulty with the commercially available mTOR kits. Several kinase assay recipes were found, and a suitable one was modified for use. The 2X Kim Kinase Buffer was used in combination with a Mass Spectrometer to obtain kinase activity data from the COS-7 cell lysates transfected with each of the 4 created plasmids. COS-7 lysates were incubated with 2X Kim Kinase Buffer and prepared on a spectrometer protein chip. The phosphorylated proteins should have been discernable from the non-phosphorylated proteins by the 80 Dalton increase in molecular weight.

The cell lysate and Kinase assay buffer were incubated with active and inactive versions of p70S6 Kinase as well as 4E-BP1. As discussed earlier, both are known downstream phosphorylation targets of mTOR. A calibration with Bovine Serum Albumin (BSA) was performed to determine the sensitivity of such an experiment (Figure 25). Unfortunately it was soon suspected that the amount of

mTOR KLISA Kit Calibration

A.

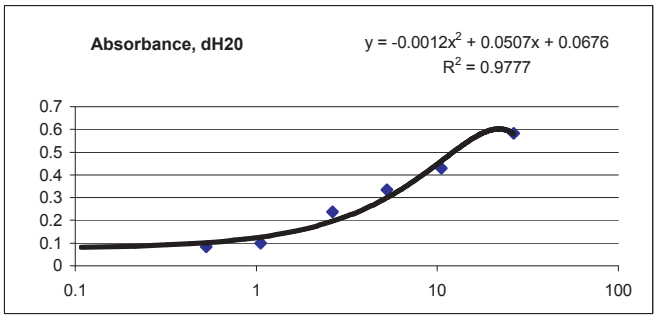

B.

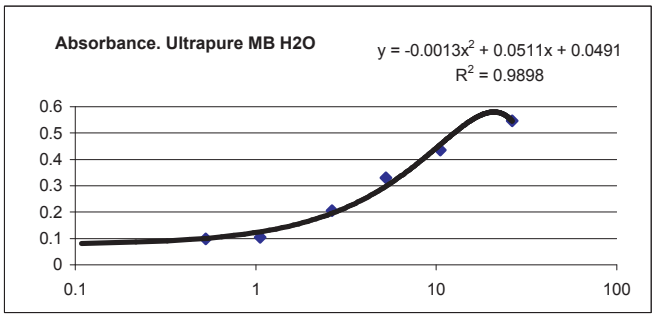

C.

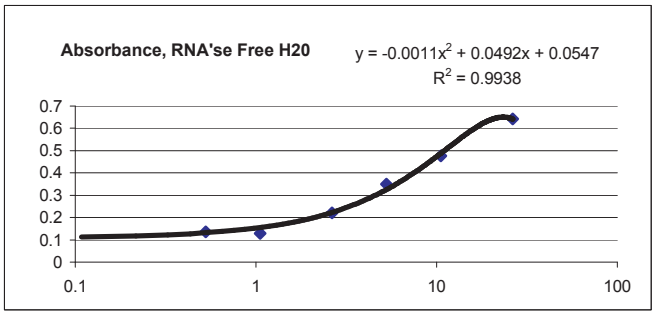

FIGURE 23:

mTOR KLISA kit calibrations. Each of graphs represents a calibration of the KLISA kit, using different types of water with the mTOR standard supplied with the kit. A dilution series was made up using 0.0, 0.5, 1.0, 2.5, 5.0, 10.0, 25.0 and 50.0 ml of mTOR standard, the specified type of water was used to bring the total reaction mixture to 50 ml. The Y-axis lists measured absorbance, the X-axis represents the amount (in ml) of water present in the sample. Each of the graphs was fit with a polynomial regression line with the lowest R2 value of 0.97.

A. Water from distilled water tap on the lab bench.

B. Molecular Biology Grade, Ultrapure RNA'se free water supplied from USB.

C. RNA'se free water supplied from Qiagen.

A.

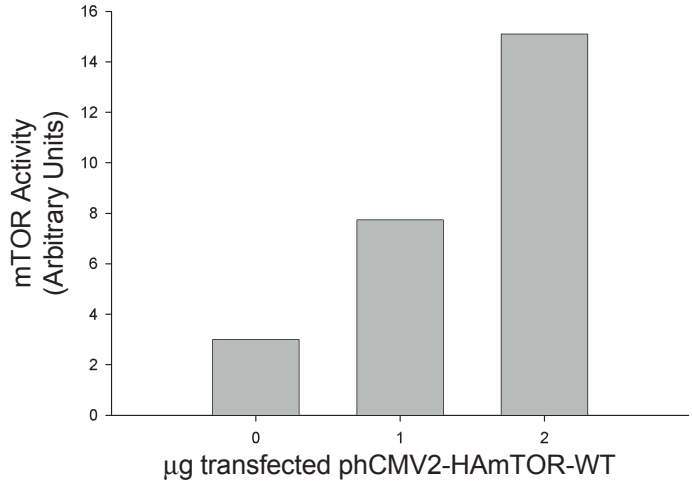

B.

Lysate #	COS7 Transfection	Abs 450	Units	ng/rxn	U/ng
1	Mock 0.0	0.161	12.636	4.203	2.988
2	1.0 μg WT	0.165	16.273	4.229	7.741
3	2.0 μg WT	0.182	31.727	2.102	15.093

FIGURE 24:

Kinase activity as determined by mTOR KLISA kit.

A. The graph shows μg of phCMV2-HAmTOR-WT used for the transfection on the X-axis. The Y-axis is the units of mTOR activity. Units of mTOR activity were defined arbitrarily, by comparing the experimental values to those obtained from the supplied mTOR standard.

B. The chart defines the paramaters used to construct the graph. Lysate number was assigned for tracking purposes. COS-7 transfection details the amount of plasmid DNA used to transfect the condition. Abs 450 is the raw data obtained from the visable plate reader. Units is a relative measurement of mTOR activity compared to a μl quantity of mTOR standard supplied with the kit. This relative number takes into account the amount of DNA in each sample and the corresponding amount of mTOR actvity. The standard curve generated an equation of Y = 0.0011x + 0.1471. This equation was used to obtain the Units value for the chart. The amount of protein per condition is listed as ng/rxn. The value of Units/nanogram is listed last and shows the mTOR activity per nanogram of total protien.

MASS SPECTROMETRY

BSA Calibration

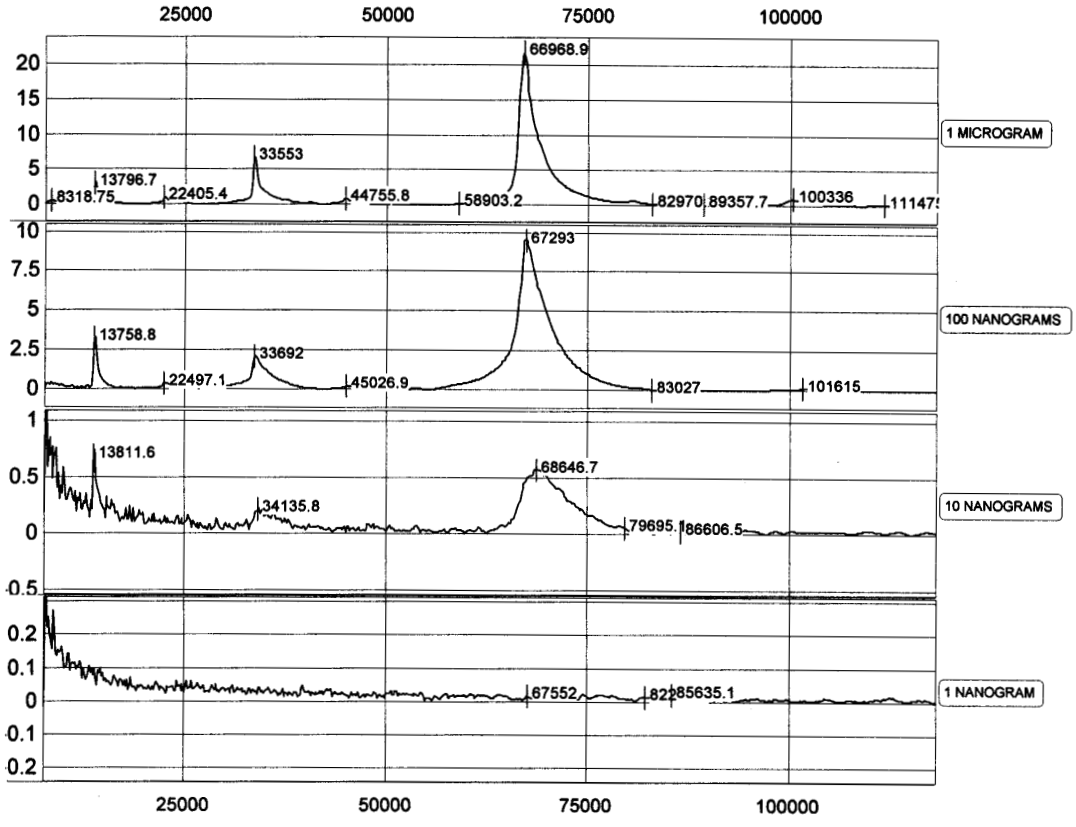

FIGURE 25:

A Bovine Serum Albumin (BSA) calibration was performed to insure the mass spectrometer was functioning properly and could detect proteins at different concentrations. BSA, a 66 kDa protein could be easily detected above the 10 ng quantity, but detection below that quantity was poor. The chart shows the peaks seen when a protein chip was run with the quantity of protein noted on the right side of the chart.

glycerol in the kinase mixture was too great, inhibiting the detection of the small quantities of protein. The chip which the kinase assay was run on often did not dry out enough for the mass spectrometer to read it. Therefore, the chips often sat in a 37°C oven overnight or in some cases, over the weekend in an attempt to dry them.

After the chips were dried, the spectrometer revealed no peaks that could be reasonably linked to this experiment (Figure 26). Therefore, no conclusive results could be obtained. The expected shift could not be visualized, and in some cases, no protein could be detected. Various adjustments to Kim's Kinase buffer were unable alleviate the difficulties encountered with this method of kinase assay.

A third kinase assay was developed using radiolabeled [^{32}P]γ–ATP (Figure 27). This assay was adapted from Kim *et. al.* and designed to avoid some of the difficulties the previous assays posed[10]. COS-7 cell lysates were taken as described in Methods, and an immunoprecipitation was performed with HA-agarose beads in an effort to concentrate the transfected mTOR. This assay used the 4X Kim Kinase Buffer and the immunoprecipitation reactions were incubated with either p70 S6 Kinase or 4E-BP1 protein. Experiments with p70 S6 Kinase (T412E), an active kinase, revealed a large amount of autophosphorylation.

The ability of p70 S6K to autophosphorylate covered the phosphorylation that was expected by mTOR (Figure 28). The kinase reaction using 4E-BP1 enjoyed more success, in part because 4E-BP1 does not have any autophosphorylation abilities (Figure 29). This assay shows the ability of mTOR to incorporate [^{32}P]γ–ATP into 4E-BP1. Lysates from COS-7 cells were used for the 4E-BP1 kinase reactions. These kinase reactions were run on SDS-PAGE gels and transferred to

MASS SPECTROMETRY KINASE ASSAY

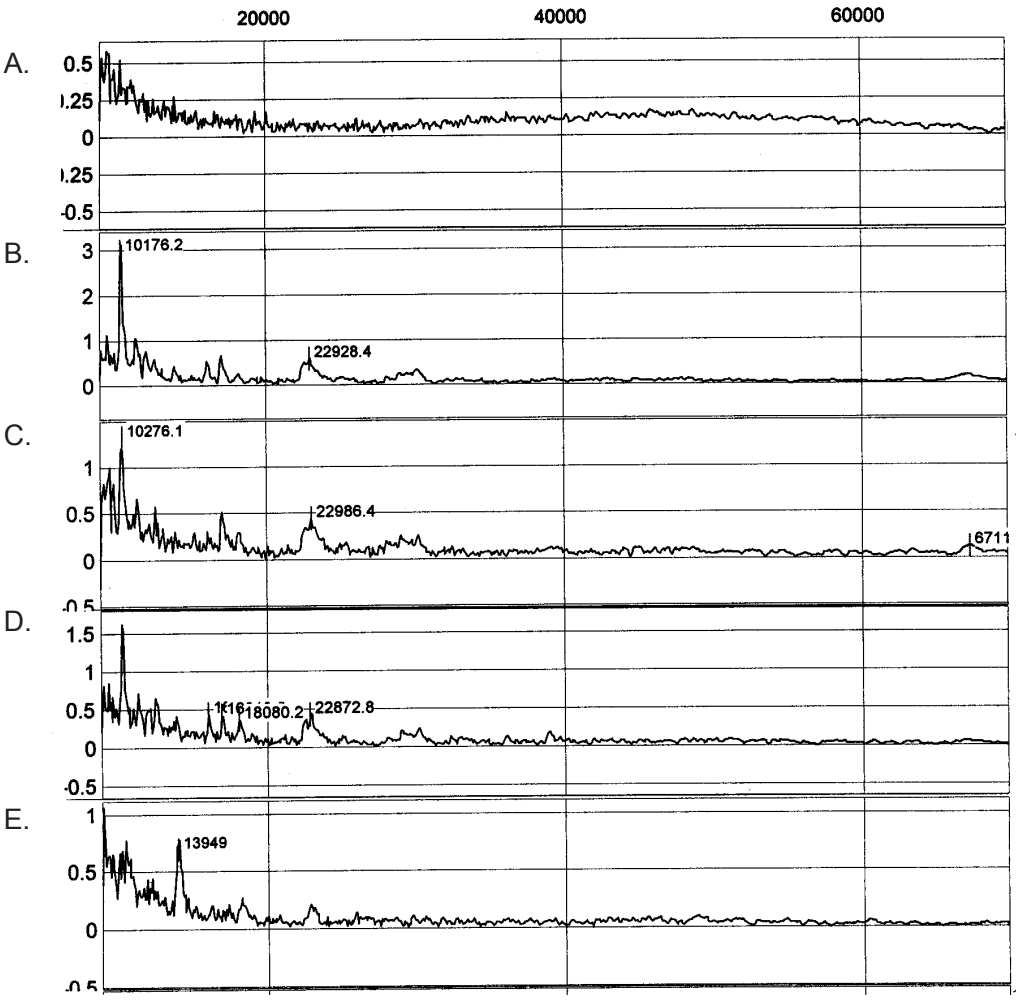

FIGURE 26:

The mass spectrometry kinase reaction did not reveal any discernable peaks.

A. Kinase reaction with no 4E-BP1, to get a baseline.

B. 4E-BP1 and [^{32}P]γ -ATP incubated with lysate from mock transfection.

C. 4E-BP1 and [^{32}P]γ -ATP incubated with lysate from transfection with phCMV2-HAmTOR-WT.

D. 4E-BP1 and [^{32}P]γ -ATP incubated with lysate from transfection with phCMV2-HAmTOR-D2357E.

E. 4E-BP1 and [^{32}P]γ -ATP incubated with mTOR standard that was supplied with commercially available mTOR kinase assay kit.

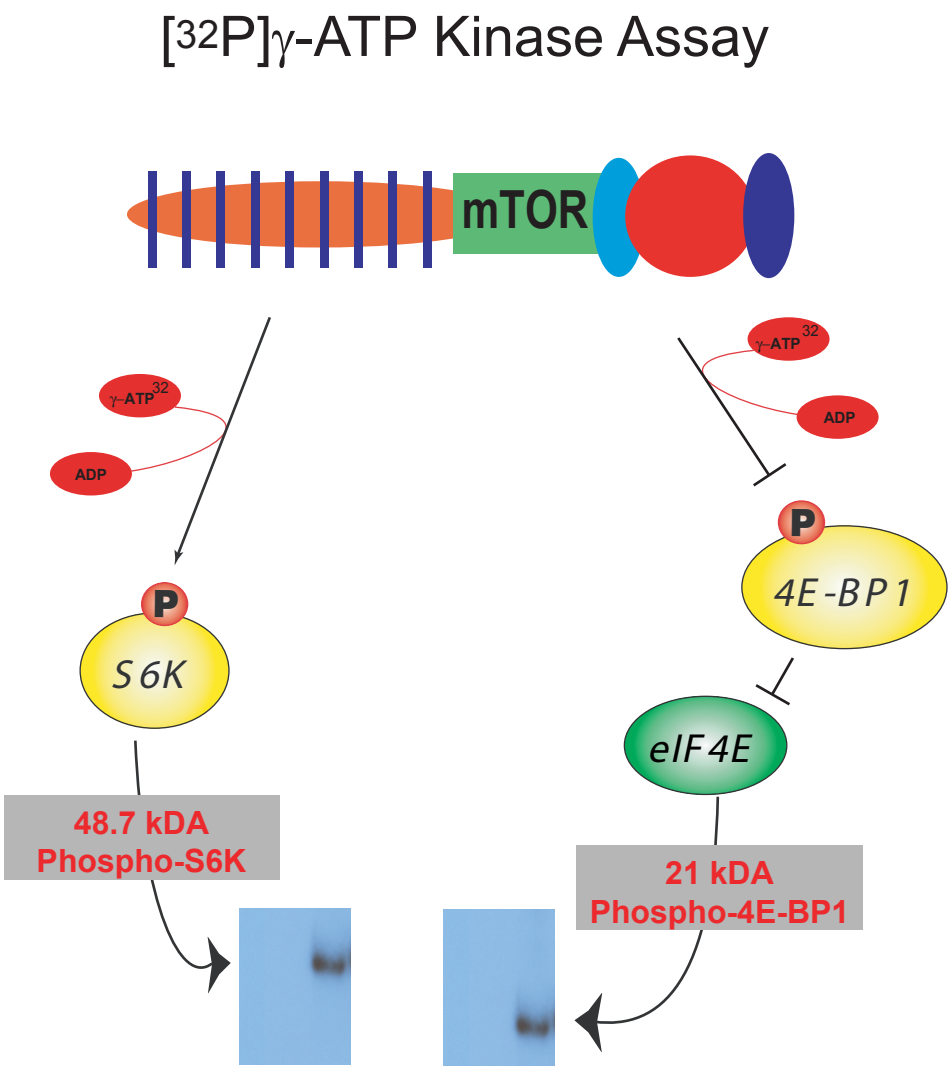

FIGURE 27:

An mTOR kinase assay was developed using [^{32}P]γ-ATP to detect phosphorylation of the known substrates, p70 S6K and 4E-EBP. Lysates of COS-7 cells transfected with the HA-mTOR plasmids were incubated with 5 μci of [^{32}P]γ -ATP and one of the substrates. The kinase reaction was incubated for 20 minutes and then run on an SDS-PAGE gel. The proteins in the gel were transfered to a PVDF membrane which was then exposed to X-ray film.

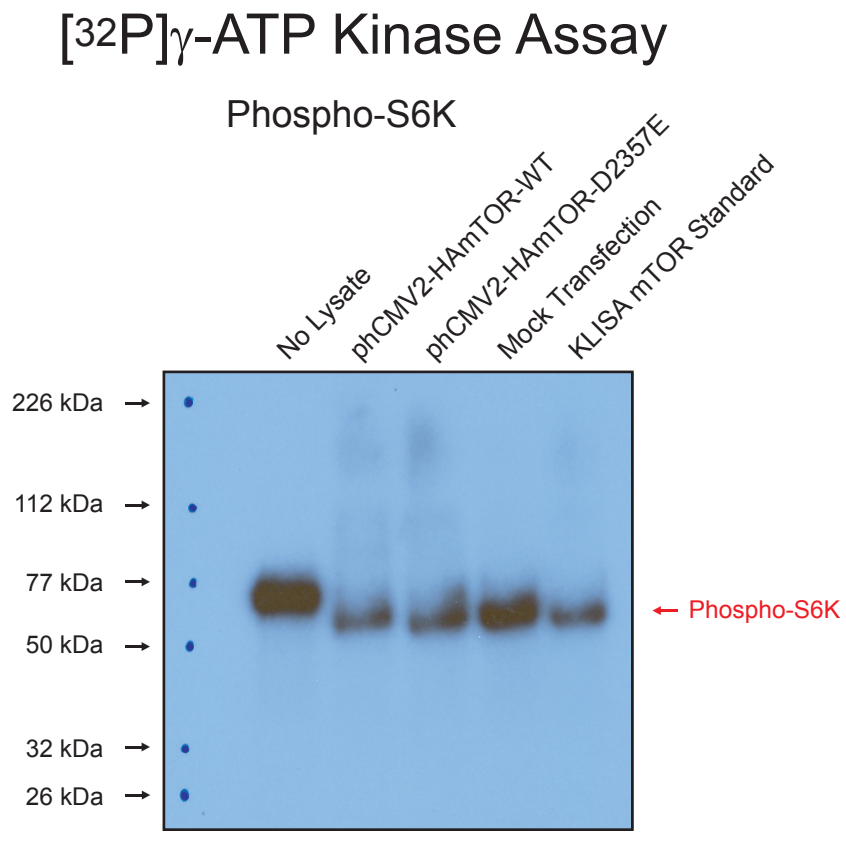

FIGURE 28:

X-ray film shows kinase assay using [^{32}P]γ-ATP. COS-7 cells were transfected as indicated and lysates used in kinase assay. This assay used p70 S6 Kinase (T412E) active, as the substrate. mTOR is known to phosphorylate the 48.7 kDA downstream target, p70 S6k. We were expecting mTOR to encorporate the [^{32}P]γ-ATP into the p70 S6K and the degree of phosphorylation would be detected by the intensity of the band on the film. However in this experiment, all the lanes, including the mock transfection and the lane with no lysate showed phosphorylation. We now hypothesize that the active p70 S6K autophosphorylated and covered any mTOR phosphorylation of the kinase. When the experiment was repeated with heat denatured p70 S6K to render the kinase inactive, no phosphorylation of any type was observed.

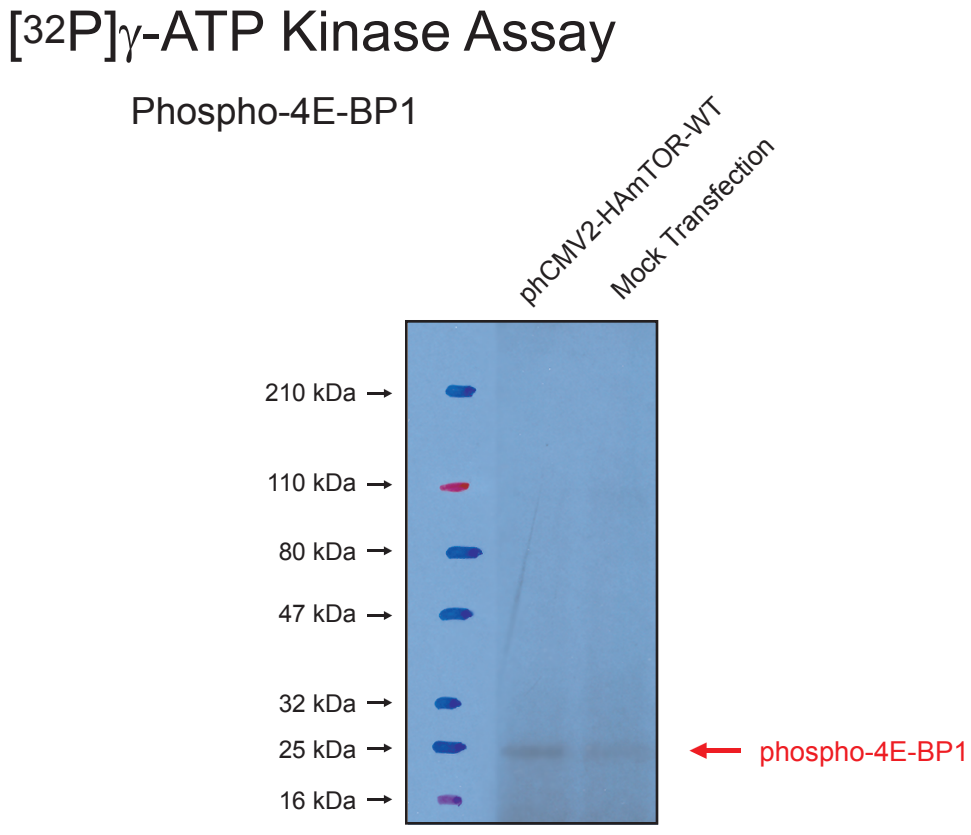

FIGURE 29:

X-ray film showing kinase assay using [^{32}P]γ-ATP. This assay used protein 4E-BP1 as the substrate. mTOR is known to phosphorylate the 21 kDA downstream target, 4E-BP1. This protein is not able to autophosphorylate and provided a more accurate picture of the kinase activity of mTOR. The first lane is lysate taken from COS-7 cells transfected with phCMV2-HAmTOR-WT. The second lane is lysate taken from a mock transfection. The mock transfection shows some mTOR activity because of the endogenous mTOR present.

PVDF membranes. These membranes with the proteins, and incorporated [^{32}P]γ–ATP were then exposed to X-ray film (Figure 30). Once the film was developed, ImageGauge V.4.0 software was used to quantify the band strength of the phosphorylated protein (Figure 31).

The ImageGuage software revealed a 13 fold increase in phosphorylation of 4E-BP1 with the phCMV2-HAmTOR-WT plasmid over a mock transfection. Additionally the Kinase Dead mutant, phCMV2-HAmTOR-D2357E had a 4 fold increase in phosphorylation. The two other plasmids, phCMV2-HAmTOR-R2109A and phCMV2-HAmTOR-S2035T showed still larger increases in phosphorylation of 4E-BP1 when overexpressed in COS-7 cells.

This third kinase assay had the most success of the three assays. Phosphorylation of the two substrates could be detected, but phosphorylation levels varied. Several changes were made in the technique used to incubate the kinase mixture, and the amount of [^{32}P]γ–ATP used in the reaction was varied. The difficulty of obtaining mTOR kinase data does not come completely as a surprise however.

Researchers hypothesize that because of the large mulitmeric structure of mTOR, that the processing of mTOR for kinase assay can interrupt these interactions[10]. The roles that these additional proteins play is largely unknown, but suspected to mediate kinase activity and mTOR function. Ongoing studies to establish more firmly the *in vivo* protein to protein interactions is essential to the understanding of mTOR. Until then, reliable kinase data may be unattainable.

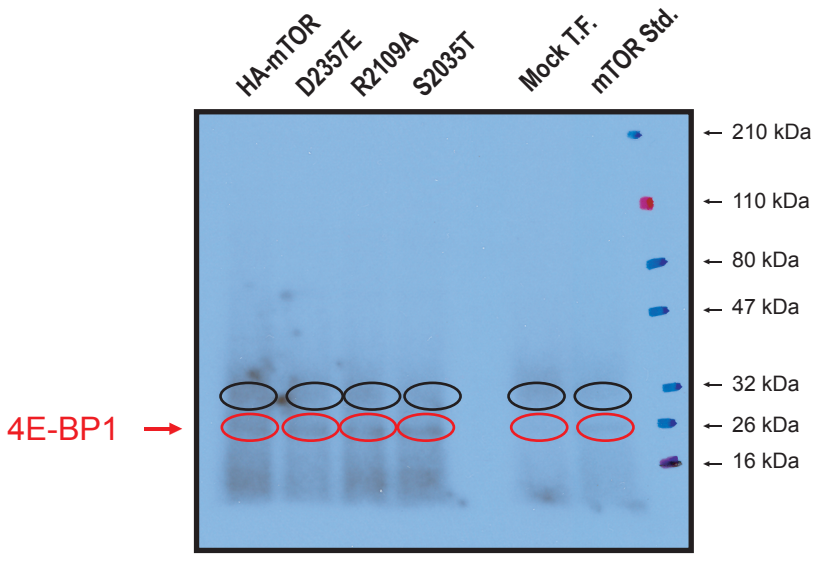

FIGURE 30:

The kinase reaction using 4E-BP1 and [^{32}P]γ-ATP was analyzed using Fuji ImageGauge V.4.0. A reference area was obtained for each band and is noted as a black oval on the gel. The relative density of this oval was measured with the software. An oval of the same area, in red, was then used to measure the relative density of the 21 kDa 4E-BP1 phosphorylated band. The reference density was then subtracted from the band density to obtain a relative density indicating the amount of phosphorylated 4E-BP1 present in the sample.

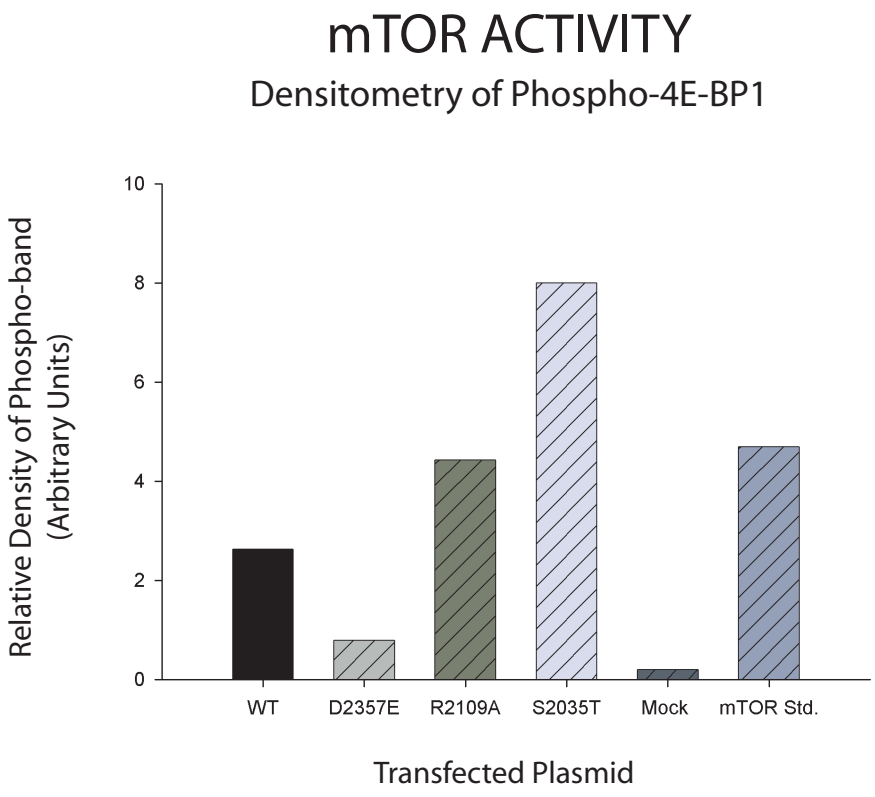

FIGURE 31:

Relative Density for each sample from the previous figure. The mTOR standard was supplied with the mTOR KLISA kit and was run to determine if the standard contained any active mTOR. Its relative value should be considered alone and not compared to that of the other samples. Transfection with 2 μg of phCMV2-HAmTOR-WT yielded a relative density of 2.63. Transfection with D2357E gave a relative density of 0.79. Transfection with R2019A gave a relative density of 4.43. Transfection with S2035T gave a relative density of 8.00. A mock transfection yielded a density of 0.20. The mTOR standard resulted in a relative density of 4.7.

AIM 5: Investigate the effects of mTOR Transfection on Gene Expression and Sub-cellular Localization

Gene Expression

Real Time PCR is a tool which has a high sensitivity to small amounts of DNA and is generally more accurate than traditional PCR. This tool allowed investigation into the molecular workings of the cell. Using the computer generated Ct values the gene fold of a mock transfection could be compared to that of cells transfected with plasmid DNA. Gene fold is a relative measurement of the greater number of copies cDNA are produced during a PCR reaction.

RT-PCR relies on the fluorescence of a probe attached to a primer designed against a gene of interest (Figure 32). Taqman gene expression probes were obtained for these experiments from Applied Biosystems, Foster CA. These probes were designed against the sequence of interest: mTOR, S6K and PLD2. The probe is bound just downstream of the primers, near the target sequence. When the polymerase reaches the 5' end of the probe, the fluorophore, attached at the 5' end of the probe is released. Once the flourophore is released, it is free of the inhibitory effects of the 3' quencher molecule. It is this separation that causes the fluorescence which is subsequently detected by the Real Time PCR machine. The intensity of fluorescence is increased as the number of DNA template increases, and more flourophore's are released.

Lysate from COS-7 cells transfected with plasmid DNA were obtained and RNA was extracted from the lysates with a Qiagen RNeasy Kit. RNA was quantified

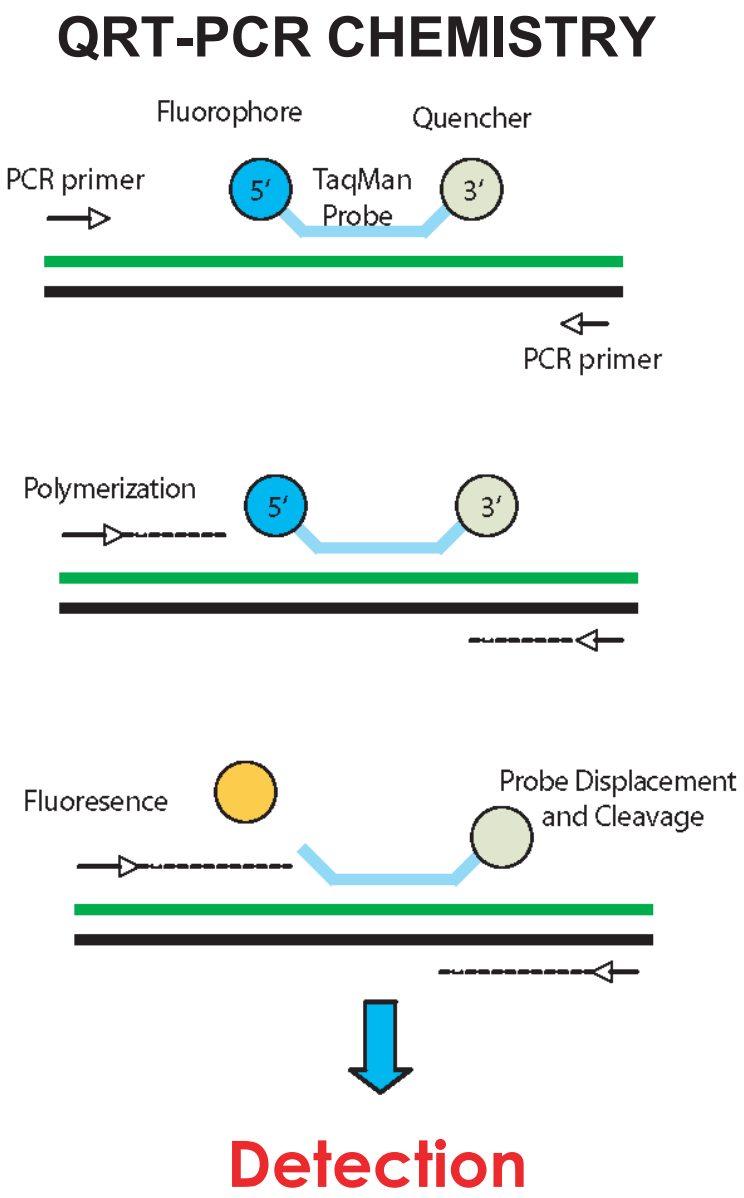

FIGURE 32:

Scheme outlines Real Time PCR chemistry using the Taqman probes. Taqman DNA polymerase moves in a 5' direction toward the Taqman probe. The exonuclease activity of the polymerase causes the release of the flourescent dye into the solution. With the release of the dye the quencher can no longer mask the signal of the flouophore. The increase in flourescence is detected during the exponential phase of the PCR reaction. Obtaining data at the exponential phase of the PCR reaction is a more accurate and reproducible method of obtaining gene fold data.

against an RNA standard using Molecular Probe's Ribogreen RNA Quantitation Kit. An equal amount of RNA from each condition was reverse transcribed to cDNA. After cDNA was obtained, RT-PCR could be carried out. For this thesis each of the transfection conditions from which the cDNA was obtained were incubated with the mTOR PCR probe. This allowed the detection of mTOR in all the transfection conditions (Figure 33).

Using the Ct value which was calculated by the PCR computer, the gene fold could be calculated for each of the experimental conditions. The fluorescence of the mTOR probe is compared against the fluorescence of a housekeeping gene, in this case glucuronidase. This ΔCt value was then compared against the mock transfection to normalize the data. This ΔΔCt value is then used in the equation $y=2^{(-\Delta\Delta Ct)}$ where y is the gene fold[97]. This calculation gives a relative value of the amount of mTOR cDNA present in the sample.

Our data shows that transfection with the mTOR plasmid DNA constructs does in fact significantly increase the gene fold of a sample (Figure 34). We detected a 170 fold increase in mTOR gene expression using our phCMV2-HAmTOR-WT plasmid. Additionally, the kinase dead phCMV2-HAmTOR-D3457E plasmid showed a 160 fold increase in gene expression. The Myc-PLD2 plasmid, when lysates were probed for mTOR gene expression, showed only negligible change.

Immunoflourescence Microscopy

Immunoflourescense images were obtained to visualize the localization of the transfected mTOR (Figure 35). These images were obtained after transfecting COS-7

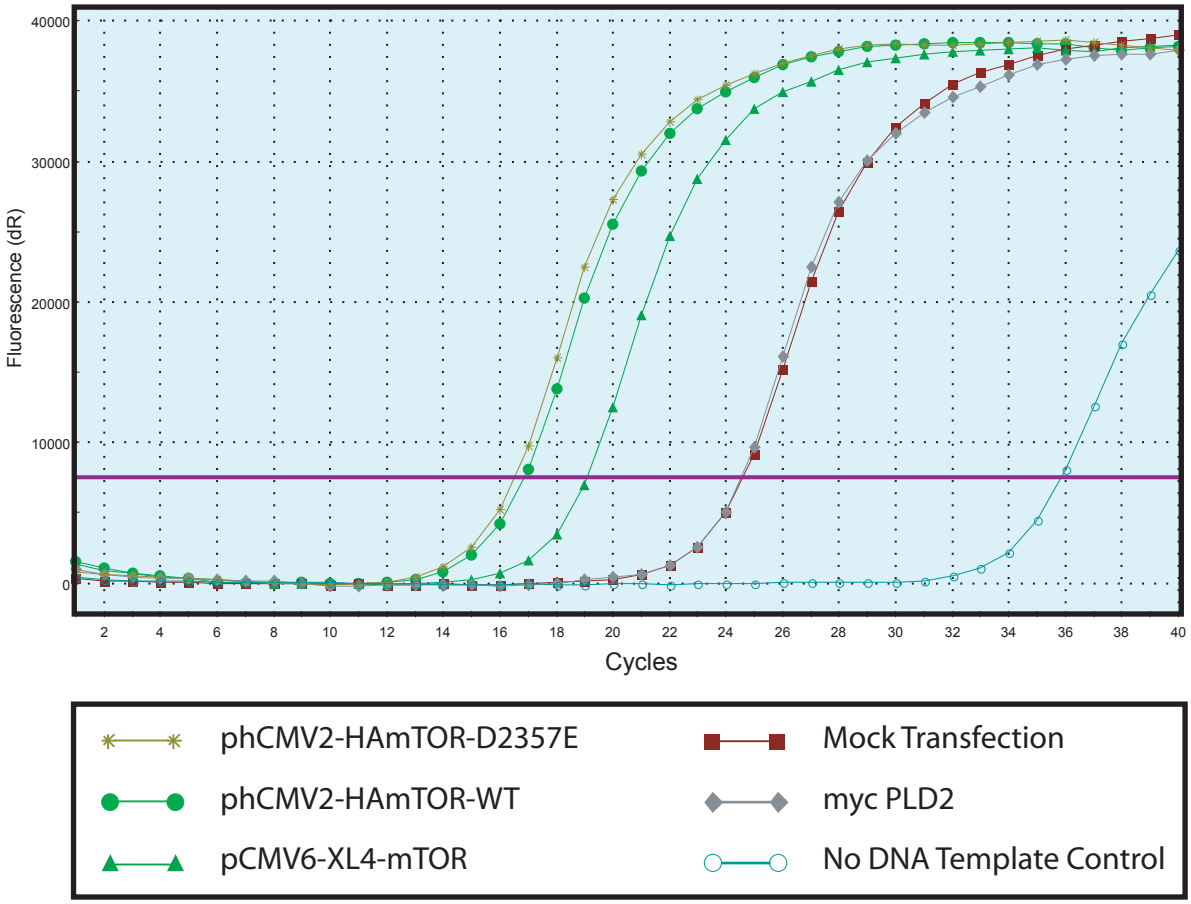

FIGURE 33:

Real Time PCR was used to determine the increase in gene fold after transfection with a DNA plasmid. The graph shows a typical readout from the RT-PCR machine. The purple horizontal line represents the Ct value, calculated by the RT-PCR machine. A smaller Ct value represents a higher cDNA expression, and thus larger gene fold. All conditions were probed with the mTOR probe. Thus the relative amount of mTOR in each sample was examined. The lysates transfected with phCMV2-HAmTOR-D2357E, phCMV2-HAmTOR-WT and, pCMV6-XL4-mTOR each have a relatively high mTOR gene fold, as would be expected. The mock transfection and myc PLD2 have lower mTOR levels as they are only expressing basal mTOR. The no DNA template control is run to ensure the validity of the data and shows no amplification until the end of the PCR reaction.

GENE FOLD ANALYSIS

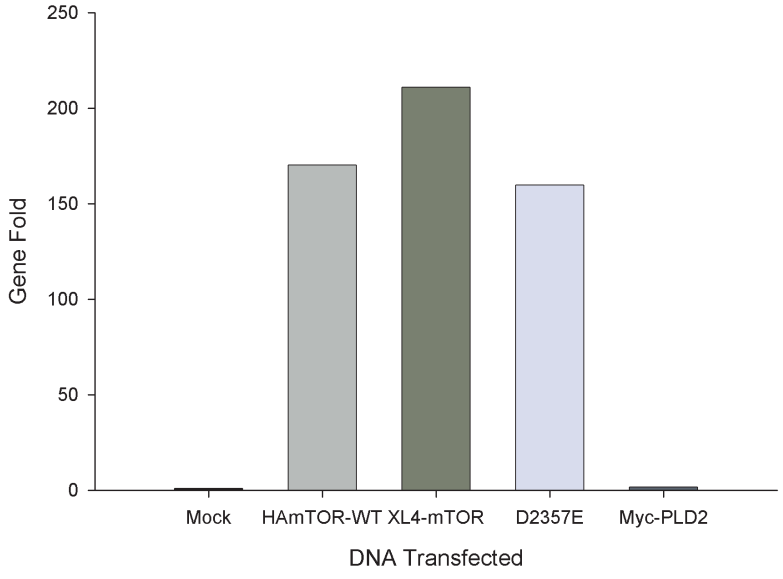

Transfection Condition	Mock T.F.	HAmTOR WT	pCMV6-XL4-mTOR	phCMV2-HAmTOR-D2357E	Myc-PLD2
mTOR(FAM)	22.01	14.49	18.09	14.12	22
Gluc (TexRed)	23.07	22.96	26.87	22.5	23.66
ΔCt	-1.06	-8.47	-8.78	-8.38	-1.66
ΔΔCT	0	-7.41	-7.72	-7.32	-0.6
2^(-ΔΔCT) "Gene Fold"	**1.0**	**170.1**	**210.8**	**159.8**	**1.5**

FIGURE 34:

Using the ΔΔCt value, gene fold for each of the transfection conditions can be calculated. The ΔCt value is calculated by subtracting the Ct value of the gene of interest from the Ct value of a housekeeping gene, glucuronidase. This ΔCt value is then subtracted from the mock transfection to normalize the samples to obtain a ΔΔCt value. Finally the ΔΔCt value is used in the equation $2^{-\Delta\Delta Ct}$ to obtain gene fold. This data shows a 170 times increase of the mTOR gene in the phCMV2-HAmTOR-WT transfected lysates compared to the mock transfection. The pCMV6-XL4-mTOR plasmid showed a 210 times increase in mTOR gene expression. Similarly phCMV2-HAmTOR-D2357E showed a 160 times increase. The lyastes from Myc-PLD2 transfected cells showed no increase in mTOR gene expression.

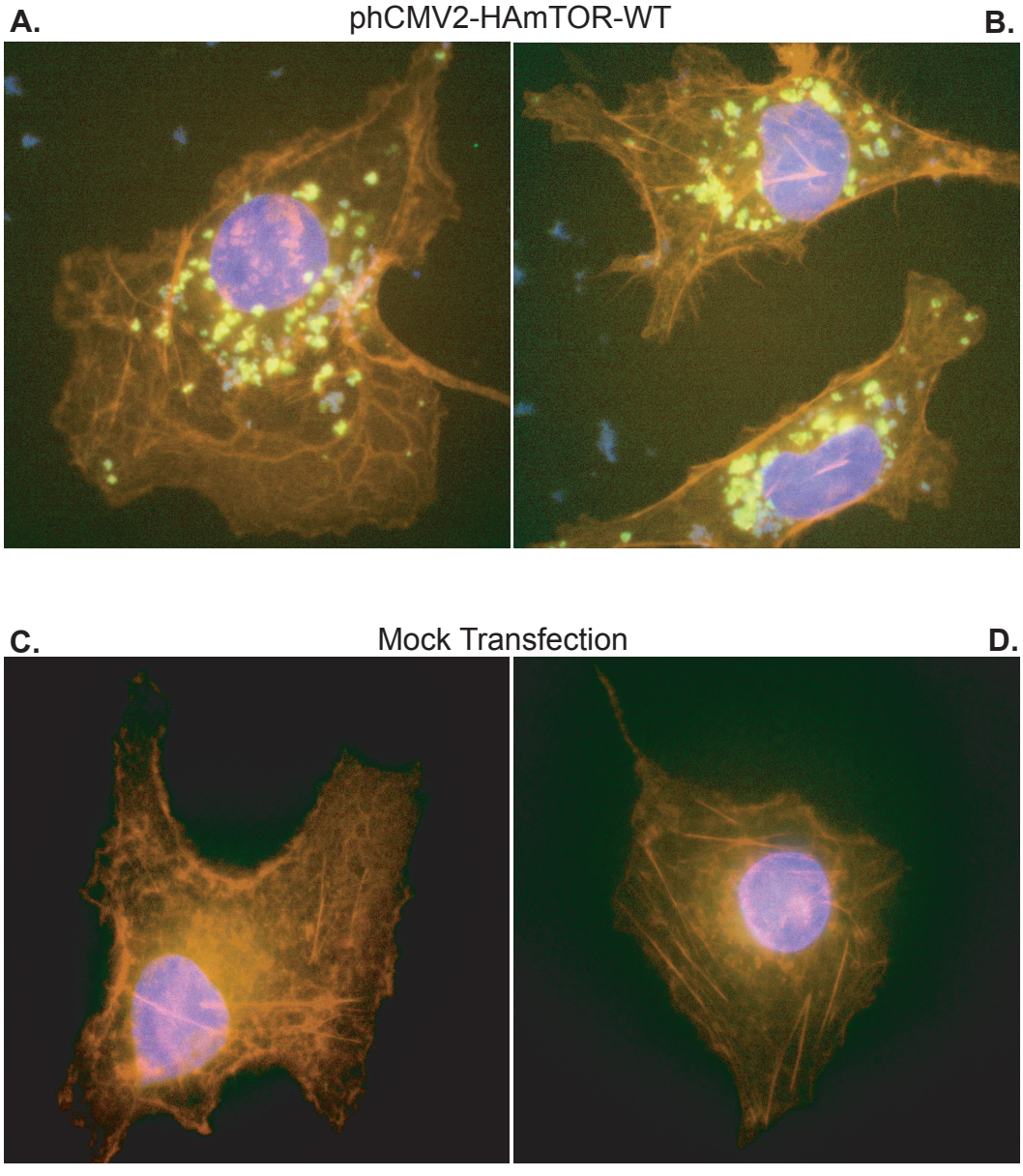

FIGURE 35:

COS-7 Cells transfected with phCMV2-HA-mTOR-WT (A and B) or a Mock Transfection (C and D). The polymerized Actin in the cell is stained red with Phalloidin TRITC dye containing a Rhodamine tag. The DNA is stained blue by a DAPI dye. The flourescent green color is the transfected mTOR, tagged by the anti-HA FITC antibody conjugate. The mTOR has a perinuclear distribution, and none was observed in the nucleus or around the plasma membrane. The punctuate dots of mTOR are likely endosomal vesicles.

cells with phCMV2-HAmTOR-WT or a mock transfection. The images show indeed transfected mTOR was able to enter the cells as endogenous mTOR is not seen.

The polymerized actin, a structural protein, was dyed red with Phalloidin-TRITC containing a Rhodamine tag. The DNA was stained blue with a DAPI dye in order to visualize the nucleus of the cell. The transfected HA-mTOR fluoresced green after it was incubated with conjugate an anti-HA FITC antibody. No mTOR is seen within the nucleus as this would appear as a yellow or orange color on the images.

V. CONCLUSIONS

1. Previous studies have lacked a reliable means of overexpressing mTOR in mammalian cells.
2. We have developed four phCMV2-HA-tagged mTOR plasmids: Wild Type, D2357E (Kinase Dead), R2109A (PA Binding Deficient) and S2035T (Rapamycin Resistant). Each one has 12,832 base pairs, and all were verified by restriction enzyme digestions and direct sequencing.
3. Plasmid DNA was overexpressed in COS-7 cells and the mTOR protein of 289 kDa was found in Western Blots developed with anti-HA or anti-mTOR. The overexpressed protein showed a four fold increase over the endogenous mTOR.
4. Kinase activity of the overexpressed protein was measured by phosphorylation of 4E-BP1 and S6K. Lysates of cells transfected with phCMV2-HAmTOR-WT had a 13 fold increase in 4E-BP1 phosphorylation over the mock transfected cells. The Kinase Dead mutant had only a 4 fold increase in kinase activity over the mock. The R2109A and S2035T mutants had a 22 fold and 40 fold increase, respectively, over the mock transfections.
5. mTOR gene expression was elevated over that of the mock transfections as detected by QRT-PCR. Cells transfected with the phCMV2-HAmTOR-WT plasmid DNA had a 170 fold increase in mTOR gene expression over mock transfected cells. The Kinase Dead mutant showed a similar 160 fold increase. However, gene expression of PLD2 was not effected by the over expression of mTOR.

6. Subcellular localization by immunoflourescence indicated that mTOR is concentrated in perinuclear space and none was observed in the nucleus or near the plasma membrane . We hypothesize that mTOR is concentrated in endosomal formations near the nucleus for use in translation regulation.
7. This study provides important molecular biology tools for this lab's continued investigation into the crosstalk between mTOR, S6K, PLD1 and PLD2.

VI. DISCUSSION

The results presented in this thesis fall within the overall study of four signal transduction molecules: mTOR, S6K, PLD1 and PLD2 and their interaction in a living cell. The work to generate and characterize an HA-tagged mTOR construct has provided the lab with another method of investigating these important pathways. Previously studies have focused on work with siRNA technology and a new electroporation method to deliver DNA to the cell nucleus. Tabatabaian, M.S., was successful in using these technologies to show that cells transfected with si-mTOR and si-S6k often had a PLD2 gene expression of several hundred times the basal rate. The new HA-tagged mTOR plasmid constructs allow for mTOR overexpression and the subsequent study of the effect of mTOR overexpression on S6K and PLD which was lacking in the previous study.

The first two aims of this thesis were accomplished through the preparation of the HA-tagged plasmid, phCMV2-HA-mTOR and subsequent point mutations of the parental plasmid to obtain the mutated HA-tagged plasmids. These four plasmids were characterized through restriction enzyme digestions and were sequenced by Cleveland Genomics. They were transfected into mammalian cells with a high efficiency, and cell lysates from those tranfections supplied the raw material for the remainder of the experiments in this thesis.

Protein expression of the HA-tagged mTOR was accomplished by transfecting the mTOR plasmids into mammalian COS-7 cells. COS-7 cells were chosen because of their ease of transfection and ability to produce large amounts of protein. Lysates were obtained, SDS-PAGE gels run and the proteins were transferred to a PVDF

membrane. Western Blotting with anti-HA and anti-mTOR was able to detect the expression of mTOR. We concluded that 2 μg of plasmid DNA was adequate to transfect one well of a six well plate of COS-7 cells at 70% confluency. Using a greater quantity of plasmid for transfection seemed to negatively affect the cells, resulting in more cell death and greater morphology changes before the lysates were harvested at 48 hours after transfection.

During protein expression experiments, we experienced a variability in the amount of total protein that each six well produced. This variability may have been due to the cell harvesting techniques, effectiveness of the lysis buffer or, simply a result of the variability that is inevitably expected in dynamic biological systems. To prevent this variability and to increase the confidence in the protein differences between samples, larger wells or multiple wells for each condition should be used, and the lysates combined. This provides for a larger amount of protein to work with and reduces the variability associated with any live cell experiment.

Various mTOR kinase assays were attempted to show the activity of the WT plasmid compared to the mutated plasmids. We were able to show through the phosphorylation of 4E-BP1, that the overexpressed plasmids increased the phosphorylation of the downstream target compared to a mock transfected lysate. The data shows a 13 fold increase in 4E-BP1 phosphorylation with phCMV2-HAmTOR-WT transfected lysates versus the mock transfected lysates. Additionally, the Kinase Dead plasmid, phCMV2-HA-mTOR-D2357E, had only a four fold increase in phosphorylation over the mock transfections. This is directly in line with the approximately 60% reduction in kinase activity published by Park, *et. al.*[41].

mTOR kinase assay data is scarce in the published literature, but those authors that do publish results often report variability in kinase activity, similar to what we experienced. It is thought that the variability is a result of the many protein to protein interactions that regulate the activity of mTOR[10]. The loss of one or more of these associated proteins during the lysate isolation process may effect the ability of mTOR to remain as an active kinase for an *in vitro* assay.

There are several pieces of evidence that support the missing protein theory. The first is that mTOR contains HEAT repeats, described in the literature review of this thesis. These HEAT repeats are known to be protein to protein interaction domains. These HEAT domains may form an extended superhelical structure, creating multiple large interfaces for proteins to interact[98]. Second, in gel filtration chromatography, mTOR migrates at a disproportionately large apparent molecular weight of 1.5 to 2.0 mDa[10]. While this phenomenon was not observed during our experiments, this data suggests a close association between mTOR and other protein.

mTOR is known to be sensitive to several standard lysate treatment solutions. Non-ionic detergents such as Triton X-100 and NP40 should not be used because they inactivate mTOR[99]. Cell lysis buffers for this thesis included Tween-20, which does not cause the same dissociation as the non-ionic detergents. Also, mTOR is sensitive to phosphate containing buffers and therefore PBS should not be used[99]. This sensitivity was not understood until just a few years ago, and much of the literature published before 2003 report using PBS in their kinase assays[83]. mTOR also requires Mn^{2+} for activity, which was included in our kinase assay buffers.

The [^{32}P]γ–ATP kinase assay was the only assay that we used that produced repeatable mTOR kinase activity data. We showed the ability of mTOR to phosphorylate 4E-BP1 and analyzed the data using Fuji ImageGauge V.4.0. Our kinase dead mutant, phCMV2-HAmTOR-D2357E, showed less than half the activity of the phCMV2-HAmTOR-WT plasmid. The two other mutants, R2109A and S2035T showed a higher kinase activity than the WT plasmid. The [^{32}P]γ–ATP kinase assay using p70 S6K as a substrate did not provide the same results. We hypothesize that the autophosphorlyation capabilities of p70 S6K inhibited our ability to discern what effects mTOR had on this downstream molecule. Interestingly, when p70 S6K was heat inactivated in an effort to prohibit its autophosphorylation capabilities, no mTOR kinase activity was observed.

Futher studies on the intricate interactions between mTOR and its associated proteins are needed in order to study kinase activity. Too little is known even about the structure of mTOR to assert that each of its domains is fully understood. These domains play an important role in protein to protein interactions which may modify the activity of mTOR. Studies need to focus on associated mTOR proteins as important modulators of mTOR activity such that a reliable kinase activity assay can be developed without concern of loss of activity due to disruption of these proteins.

Real time PCR has proven itself as a reliable tool for investigating gene expression at the earliest detectable time in the cell; cDNA expression. Our experiments showed that each of the HA-tagged mTOR plasmids were able to increase the amount of mTOR cDNA being transcribed in the transfected cells.

Gene folds of phCMV2-HAmTOR-WT transfected cells increased 170 fold over that of the mock transfected cells. Similarly the Kinase Dead D2357E plasmid had a gene fold of 160 times the mock. For this experiment we expected a similar increase in gene expression with each of the plasmids. Although the D2357E mutant has a reduced kinase activity, the cDNA copies of the gene are still made at an increased rate over the mock transfections. The pCMV6-XL4-mTOR plasmid obtained from OriGene had a gene fold increase of 210 times the mock transfection. When a Myc-PLD2 plasmid was used to overexpress PLD2, no change in mTOR gene expression was detected.

Our data showed no significant change in PLD1, PLD2 or S6K expression with the overexpression of mTOR using the HA-tagged plasmids. This lab has previously shown that mRNA expression of PLD2, mTOR and S6K are coordinately regulated. In her thesis, Tabatabaian, M.S., showed that transfecting dHL-60 cells with si-mTOR and si-S6k caused PLD 2 gene expression to rise dramatically[96]. The data that we have does not show the opposite to be true. The overexpression of mTOR using HA-tagged mTOR constructs does not seem to increase PLD2 gene expression. However, more studies need to be completed to confirm this hypothesis. Studies should include rapamycin and wortmanin, known inhibitors of mTOR. Additionally experiments adding growth factors to attempt to upregulate mTOR should be attempted.

Finally, fluorescence images were obtained of COS-7 cells transfected with HA-mTOR. These images provided confirmation that mTOR is a cytosolic protein, localized very near the nucleus. These findings agree with Liu *et al.* who published

findings stating that mTOR had unusual endoplasmic reticulum and Golgi apparatus targeting sequences in its HEAT domain[100]. The location of the transfected mTOR may be due to the fact that mTOR is shuttled in and out of the nucleus in order to interact with S6K[101]. However, no mTOR was observed within the nucleus. This may be explained by the fact that there was no mTOR in the nucleus, the anti-HA antibody was unable to penetrate the nucleus, or the mTOR was not yet transported to the nucleus. Experiments to follow the movement of mTOR throughout the life cycle of the cell would provide additional evidence to support the theory that mTOR is shuttled to and from the nucleus.

The importance of understanding the interactions between these molecules can not be underestimated. In this thesis we have established that mTOR plays the roles of both the receptor of cellular signals and as an initiator of cellular pathways. An understanding of mTOR's pathways and, those effected by the crosstalk between the molecules, is vital to the development of drug treatments to manipulate those pathways.

VII. SIGNIFICANCE OF THIS STUDY

mTOR is thought to be a master regulator of the cell. Understanding how this protein kinase is regulated in healthy cells and how it becomes dysregulated in diseased cells is important to our understanding of many different diseases. This study produced four HA-tagged mTOR expression plasmids that were effectively transfected in mammalian cells. These constructs provide the lab with the molecular tools to study the crosstalk between mTOR and various other molecules. The plasmids are available in purified form for the lab and glycerol DH5α stocks exist so the plasmid can be easily replenished. Each of these plasmids went through extensive testing including restriction enzyme digestions and sequencing by a third party.

Western Blotting showed that the HA-mTOR plasmid DNA could be overexpressed in mammalian cells, and detected with both anti-mTOR and anti-HA antibodies. Kinase assays showed the transfected mTOR was active, and the kinase dead mutant showed an expectedly decreased phosphorylation ability. Cells transfected with these plasmids also showed an increase in mTOR gene expression as detected by Real-Time PCR. The HA-mTOR protein was visualized by immunoflourescence microscopy, which confirmed its perinuclear location.

The results of this study complete the next step in the investigation between the crosstalk of these signaling molecules. Gene expression studies should be continued to further verify the effect of mTOR overexpression on PLD1, PLD2 and S6K.

VIII. REFERENCES

1. Vézina C, Kudelski A, Sehgal SN. Rapamycin (AY-22,989), a new antifungal antibiotic. I. taxonomy of the producing streptomycete and isolation of the active principle. *J Antibiot (Tokyo)*. 1975;28:721-726.

2. Bradley D. Piecing together the easter island molecule. *New Sci*. 1993;139:18.

3. Schmelzle T, Hall MN. TOR, a central controller of cell growth. *Cell*. 2000;103:253.

4. Douros J, Suffness M. New antitumor substances of natural origin. *Cancer Treat Rev*. 1981;8:63-87.

5. Houchens DP, Ovejera AA, Riblet SM, Slagel DE. Human brain tumor xenografts in nude mice as a chemotherapy model. *Eur J Cancer Clin Oncol*. 1983;19:799-805.

6. Heitman J, Morra NR. Targets for cell cycle arrest by the immunosuppressant rapamycin in yeast. *Science*. 1991;253:905.

7. Panwalkar A, Verstovsek S, Giles FJ. Mammalian target of rapamycin inhibition as therapy for hematologic malignancies. *Cancer*. 2004;100:657-666.

8. Crespo JL, Hall MN. Elucidating TOR signaling and rapamycin action: Lessons from saccharomyces cerevisiae. *Microbiology & Molecular Biology Reviews*. 2002;66:579.

9. Abraham RT. Identification of TOR signaling complexes: More TORC for the cell growth engine. *Cell*. 2002;111:9.

10. Kim D, Sarbassov DD, Ali SM, et al. mTOR interacts with raptor to form a nutrient-sensitive complex that signals to the cell growth machinery. *Cell*. 2002/7/26;110:163-175.

11. Dennis PB, Jaeschke A, Saitoh M, Fowler B, Kozma SC, Thomas G. Mammalian TOR: A homeostatic ATP sensor. *Science*. 2001;294:1102.

12. Jacinto E, Hall MN. Tor signalling in bugs, brain and brawn. *Nature Reviews Molecular Cell Biology*. 2003;4:117.

13. Martin DE, Hall MN. The expanding TOR signaling network. *Curr Opin Cell Biol*. 2005;17:158-166.

14. Hosoi H, Dilling MB, Shikata T, et al. Rapamycin causes poorly reversible inhibition of mTOR and induces p53-independent apoptosis in human rhabdomyosarcoma cells. *Cancer Res*. 1999;59:886-894.

15. Gingras AC, Raught B, Sonenberg N. Regulation of translation initiation by FRAP/mTOR. *Genes Dev*. 2001;15:807-826.

16. Easton JB, Houghton PJ. mTOR and cancer therapy. *Oncogene*. 2006;25:6436-6446.

17. Liu L, Li F, Cardelli JA, Martin KA, Blenis J, Huang S. Rapamycin inhibits cell motility by suppression of mTOR-mediated S6K1 and 4E-BP1 pathways. *Oncogene*. 2006;25:7029-7040.

18. Huang S, Houghton PJ. Targeting mTOR signaling for cancer therapy. *Current Opinion in Pharmacology*. 2003;3:371.

19. Inoki K. Dysregulation of the TSC-mTOR pathway in human disease. *Nature genetics.* 2005;37:19.

20. Hentges KE, Sirry B, Gingeras A, et al. FRAP/mTOR is required for proliferation and patterning during embryonic development in the mouse. *Proc Natl Acad Sci U S A*. 2001;98:1-1.

21. Hentges K, Thompson K, Peterson A. The flat-top gene is required for the expansion and regionalization of the telencephalic primordium. *Development*. 1999;126:1601-1609.

22. Oldham S, Montagne J, Radimerski T, Thomas G, Hafen E. Genetic and biochemical characterization of dTOR, the drosophila homolog of the target of rapamycin. *Genes Dev*. 2000;14:2689-2694.

23. Keith CT, Schreiber SL. PIK-related kinases: DNA repair, recombination, and cell cycle checkpoints. *Science*. 1995;270:50.

24. Hara K, Yonezawa K, Kozlowski MT, et al. Regulation of eIF-4E BP1 phosphorylation by mTOR. *J Biol Chem*. 1997;272:26457-26463.

25. Chan S. Targeting the mammalian target of rapamycin (mTOR): A new approach to treating cancer. *Br J Cancer*. 2004;91:1420-1424.

26. Sarkaria JN, Tibbetts RS, Busby EC, Kennedy AP, Hill DE, Abraham RT. Inhibition of phosphoinositide 3-kinase related kinases by the radiosensitizing agent wortmannin. *Cancer Res*. 1998;58:4375-4382.

27. Bjornsti M, Houghton PJ. The TOR pathway: A target for cancer therapy. *Nat Rev Cancer*. 2004;4:335-348.

28. Vilella-Bach M, Nuzzi P, Fang Y, Chen J. The FKBP12-rapamycin-binding domain is required for FKBP12-rapamycin-associated protein kinase activity and G1 progression. *J Biol Chem*. 1999;274:4266-4272.

29. Dennis PB, Thomas G. Quick guide: Target of rapamycin. *Current Biology*. 2002;12:R269.

30. Chiu MI, Katz H, Berlin V. RAPT1, a mammalian homolog of yeast tor, interacts with the FKBP12/rapamycin complex. *Proc Natl Acad Sci U S A.* 1994;91:12574-12578.

31. Chen J, Fang Y. A novel pathway regulating the mammalian target of rapamycin (mTOR) signaling. *Biochem Pharmacol.* 2002;64:1071.

32. Chen J, Zheng XF, Brown EJ, Schreiber SL. Identification of an 11-kDa FKBP12-rapamycin-binding domain within the 289-kDa FKBP12-rapamycin-associated protein and characterization of a critical serine residue. *Proc Natl Acad Sci U S A.* 1995;92:4947-4951.

33. Burnett PE, Barrow RK, Cohen NA, Snyder SH, Sabatini DM. RAFT1 phosphorylation of the translational regulators p70 S6 kinase and 4E-BP1. *Proc Natl Acad Sci U S A*. 1998;95:1432.

34. Zheng XF, Florentino D, Chen J, Crabtree GR, Schreiber SL. TOR kinase domains are required for two distinct functions, only one of which is inhibited by rapamycin. *Cell*. 1995;82:121-130.

35. Takahashi T, Hara K, Inoue H, et al. Carboxyl-terminal region conserved among phosphoinositide-kinase-related kinases is indispensable for mTOR function in vivo andin vitro. *Genes to Cells.* 2000;5:765.

36. Kunz J, Henriquez R, Schneider U, Deuter-Reinhard M, Movva NR, Hall MN. Target of rapamycin in yeast, TOR2, is an essential phosphatidylinositol kinase homolog required for G1 progression. *Cell.* 1993;73:585-596.

37. Brown EJ, Beal PA. Control of p70 S6 kinase by kinase activity of FRAP in vivo. *Nature*. 1995;377:441.

38. Sabatini DM, Barrow RK, Blackshaw S, et al. Interaction of Raft1 with gephyrin required for rapamycin-sensitive signaling. *Science*. 1999;284:1161.

39. Kim JE, Chen J. Cytoplasmic-nuclear shuttling of FKBP12-rapamycin-associated protein is involved in rapamycin-sensitive signaling and translation initiation. *Proc Natl Acad Sci U S A*. 2000;97:14340-14345.

40. Christophe D, Christophe-Hobertus C, Pichon B. Nuclear targeting of proteins: How many different signals? *Cell Signal*. 2000;12:337-341.

41. Park I, Bachmann R, Shirazi H, Chen J. Regulation of ribosomal S6 kinase 2 by mammalian target of rapamycin. *J Biol Chem*. 2002;277:31423-31429.

42. Dos D. Sarbassov, Ali SM, Kim D, et al. Rictor, a novel binding partner of mTOR, defines a rapamycin-insensitive and raptor-independent pathway that regulates the cytoskeleton. *Current Biology*. 2004;14:1296-1302.

43. Hara K, Maruki Y, Xiaomeng Long, et al. Raptor, a binding partner of target of rapamycin (TOR), mediates TOR action. *Cell*. 2002;110:177.

44. Sarbassov DD, Guertin DA, Ali SM, Sabatini DM. Phosphorylation and regulation of Akt/PKB by the rictor-mTOR complex. *Science*. 2005;307:1098-1101.

45. Laura R. Pearce, Xu Huang, Jerome Boudeau, et al. Identification of protor as a novel rictor-binding component of mTOR complex-2. *Biochem J.* 2007;405:513-522.

46. Peterson RT, Beal PA, Comb MJ, Schreiber SL. FKBP12-rapamycin-associated protein (FRAP) autophosphorylates at serine 2481 under translationally repressive conditions. *J Biol Chem*. 2000;275:7416-7423.

47. Mayer C, Grummt I. Ribosome biogenesis and cell growth: MTOR coordinates transcription by all three classes of nuclear RNA polymerases. *Oncogene*. 2006;25:6384-6391.

48. Guertin DA, Sabatini DM. Defining the role of mTOR in cancer. *Cancer Cell*. 2007;12:9-22.

49. Wullschleger S, Loewith R, Hall MN. TOR signaling in growth and metabolism. *Cell*. 2006;124:471-484.

50. Guertin DA, Sabatini DM. An expanding role for mTOR in cancer. *Trends Mol Med*. 2005;11:353-361.

51. Dennis PB, Fumagalli S, Thomas G. Target of rapamycin (TOR): Balancing the opposing forces of protein synthesis and degradation. *Curr Opin Genet Dev*. 1999;9:49-54.

52. Chiang GG, Abraham RT. Phosphorylation of mammalian target of rapamycin (mTOR) at ser-2448 is mediated by p70S6 kinase. *J Biol Chem*. 2005;280:25485-25490.

53. Foster DA. Regulation of mTOR by phosphatidic acid? *Cancer Res*. 2007;67:1-4.

54. Huang S, Bjornsti M, Houghton PJ. Rapamycins: Mechanism of action and cellular resistance. *Cancer Biol Ther*. 2003;2:222.

55. Downward J. Mechanisms and consequences of activation of protein kinase B/Akt. *Curr Opin Cell Biol.* 1998;10:262-267.

56. Podsypanina K, Lee RT, Politis C, et al. An inhibitor of mTOR reduces neoplasia and normalizes p70/S6 kinase activity in pten+/- mice. *Proc Natl Acad Sci U S A.* 2001;98:10320-10325.

57. Besson A, Robbins SM, Wee Yong V. PTEN/MMAC1/TEP1 in signal transduction and tumorigenesis. *European Journal of Biochemistry*. 1999;263:605.

58. Potter CJ, Pedraza LG, Xu T. Akt regulates growth by directly phosphorylating Tsc2. *Nat Cell Biol*. 2002;4:658.

59. Gao X, Zhang Y, Arrazola P, et al. Tsc tumour suppressor proteins antagonize amino-acid mTOR signalling. *Nat Cell Biol*. 2002;4:699.

60. Abraham RT. TOR signaling: An odyssey from cellular stress to the cell growth machinery. *Current Biology*. 2005;15:R139-R141.

61. Long X, Lin Y, Ortiz-Vega S, Yonezawa K, Avruch J. Rheb binds and regulates the mTOR kinase. *Current Biology*. 2005;15:702-713.

62. Sancak Y, Thoreen CC, Peterson TR, et al. PRAS40 is an insulin-regulated inhibitor of the mTORC1 protein kinase. *Mol Cell.* 2007;25:903-915.

63. Yan L, Findlay GM, Jones R, Procter J, Cao Y, Lamb RF. Hyperactivation of mammalian target of rapamycin (mTOR) signaling by a gain-of-function mutant of the rheb GTPase. *J Biol Chem*. 2006;281:19793-19797.

64. Hsu Y, Chern JJ, Cai Y, Liu M, Choi K. Drosophila TCTP is essential for growth and proliferation through regulation of dRheb GTPase. *Nature*. 2007;445:785-788.

65. Fang Y, Vilella-Bach M, Bachmann R, Flanigan A, Chen J. Phosphatidic acid-mediated mitogenic activation of mTOR signaling. *Science*. 2001;294:1942-1945.

66. Lehman N, Di Fulvio M, McCray N, Campos I, Tabatabaian F, Gomez-Cambronero J. Phagocyte cell migration is mediated by phospholipases PLD1 and PLD2. *Blood*. 2006;108:3564-3572.

67. Avila-Flores A, Santos T, Rincon E, Merida I. Modulation of the mammalian target of rapamycin pathway by diacylglycerol kinase-produced phosphatidic acid. *J Biol Chem*. 2005;280:10091-10099.

68. Brose N, Betz A, Wegmeyer H. Divergent and convergent signaling by the diacylglycerol second messenger pathway in mammals. *Curr Opin Neurobiol*. 2004;14:328-340.

69. Yang SF, Freer S, Benson AA. Transphosphatidylation by phospholipase D. *J Biol Chem*. 1967;242:477-484.

70. Buckland AG, Wilton DC. Anionic phospholipids, interfacial binding and the regulation of cell functions. *Biochim Biophys Acta*. 2000;1483:199-216.

71. Yimin F, In-Hyun P, Ai-Luen W, et al. PLD1 regulates mTOR signaling and mediates Cdc42 activation of S6K1. *Current Biology*. 2003;13:2037-2044.

72. Sarbassov DD, Ali SM, Sabatini DM. Growing roles for the mTOR pathway. *Curr Opin Cell Biol.* 2005;17:596-603.

73. Fukami K, Takenawa T. Phosphatidic acid that accumulates in platelet-derived growth factor-stimulated Balb/c 3T3 cells is a potential mitogenic signal. *J Biol Chem*. 1992;267:10988-10993.

74. Ha SH, Kim D, Kim I, et al. PLD2 forms a functional complex with mTOR/raptor to transduce mitogenic signals. *Cell Signal*. 2006;18:2283-2291.

75. Corradetti MN, Guan K-. Upstream of the mammalian target of rapamycin: Do all roads pass through mTOR? *Oncogene*. 2006;25:6347-6360.

76. Arsham AM, Howell JJ, Simon MC. A novel hypoxia-inducible factor-independent hypoxic response regulating mammalian target of rapamycin and its targets. *J Biol Chem*. 2003;278:29655-29660.

77. Findlay GM, Yan L, Procter J, Mieulet V, Lamb RF. A MAP4 kinase related to Ste20 is a nutrient-sensitive regulator of mTOR signalling. *Biochem J*. 2007;403:13-20.

78. Brugarolas J, Kui Lei, Hurley RL, et al. Regulation of mTOR function in response to hypoxia by REDD1 and the TSC1/TSC2 tumor suppressor complex. *Genes Dev*. 2004;18:2893-2904.

79. Avruch J, Belham C, Weng Q, Hara K, Yonezawa K. The p70 S6 kinase integrates nutrient and growth signals to control translational capacity. *Prog Mol Subcell Biol.* 2001;26:115-154.

80. Meyuhas O. Synthesis of the translational apparatus is regulated at the translational level. *European Journal of Biochemistry*. 2000;267:6321-6330.

81. Lehman N, Ledford B, Di Fulvio M, Frondorf K, McPhail LC, Gomez-Cambronero J. Phospholipase D2-derived phosphatidic acid binds to and activates ribosomal p70 S6 kinase independently of mTOR. *FASEB J.* 2007.

82. Martin KA, Blenis J. Coordinate regulation of translation by the PI 3-kinase and mTOR pathways. *Adv Cancer Res*. 2002;86:1-39.

83. Fingar DC, Blenis J. Target of rapamycin (TOR): An integrator of nutrient and growth factor signals and coordinator of cell growth and cell cycle progression. *Oncogene*. 2004;23:3151-3171.

84. Alessi DR, Kozlowski MT, Weng QP, Morrice N, Avruch J. 3-phosphoinositide-dependent protein kinase 1 (PDK1) phosphorylates and activates the p70 S6 kinase in vivo and in vitro. *Curr Biol.* 1998;8:69-81.

85. Pearson RB, Dennis PB, Han JW, et al. The principal target of rapamycin-induced p70s6k inactivation is a novel phosphorylation site within a conserved hydrophobic domain. *EMBO J.* 1995;14:5279-5287.

86. Isotani S, Hara K, Tokunaga C, Inoue H, Avruch J, Yonezawa K. Immunopurified mammalian target of rapamycin phosphorylates and activates p70 S6 kinase alpha in vitro. *J Biol Chem*. 1999;274:34493-34498.

87. Hannan KM, Brandenburger Y, Jenkins A, et al. MTOR-dependent regulation of ribosomal gene transcription requires S6K1 and is mediated by phosphorylation of the carboxy-terminal activation domain of the nucleolar transcription factor UBF. *Molecular & Cellular Biology*. 2003;23:8862-8877.

88. Hardwick JS, Kuruvilla FG. Rapamycin-modulated transcription defines the subset of nutrient-sensitive signaling pathways.. *Proc Natl Acad Sci U S A.* 1999;96:14866.

89. Cardenas ME, Cutler NS, Lorenz MC, Di Como CJ, Heitman J. The TOR signaling cascade regulates gene expression in response to nutrients. *Genes Dev*. 1999;13:3271-3279.

90. Reinhard C, Fernandez A, Lamb NJ, Thomas G. Nuclear localization of p85s6k: Functional requirement for entry into S phase. *EMBO J*. 1994;13:1557-1565.

91. Brunn GJ, Hudson CC, Sekuli, Aleksandar, *et al.* Phosphorylation of the translational repressor PHAS-I by the mammalian target of rapamycin. *Science*. 1997;277:99-101.

92. Hay N, Sonenberg N. Upstream and downstream of mTOR. *Genes Dev*. 2004;18:1926-1945.

93. Fingar DC, Richardson CJ, Tee AR, Cheatham L, Tsou C, Blenis J. MTOR controls cell cycle progression through its cell growth effectors S6K1 and 4E-BP1/Eukaryotic translation initiation factor 4E. *Molecular & Cellular Biology*. 2004;24:200-216.

94. Schalm SS, Fingar DC, Sabatini DM, Blenis J. TOS motif-mediated raptor binding regulates 4E-BP1 multisite phosphorylation and function. *Current Biology*. 2003;13:797.

95. Kin Man Choi, McMahon LP, Lawrence Jr. JC. Two motifs in the translational repressor PHAS-I required for efficient phosphorylation by mammalian target of rapamycin and for recognition by raptor. *J Biol Chem*. 2003;278:19667.

96. Tabatabaian F. *The measurement of endogenous mRNA expression of PLD isoforms in HL-60 cells using QRT-PCR and the impact of these isoforms on gene expression of mTOR and S6K*. [Masters]. Wright State University; 2006.

97. Livak KJ, Schmittgen TD. Analysis of relative gene expression data using real-time quantitative PCR and the $2^{(-\delta\delta C_T)}$ method. *Methods*. 2001;25:402-408.

98. Perry J, Kleckner N. The ATRs, ATMs, and TORs are giant HEAT repeat proteins. *Cell*. 2003;112:151.

99. EMD Biosciences I. K-LISA mTOR activity kit. *User Protocol CBA055*. 2006;Revision 31.

100. Liu X, Zheng XFS. Endoplasmic reticulum and golgi localization sequences for mammalian target of rapamycin. *Mol Biol Cell*. 2007;18:1073-1082.

101. Li W, Petrimpol M, Molle KD, Hall MN, Battegay EJ, Humar R. Hypoxia-induced endothelial proliferation requires both mTORC1 and mTORC2. *Circ Res*. 2007;100:79-87.